# INVESTIGATING ENDO-EXO SELECTIVITY IN DIELS-ALDER REACTIONS

TAMMY LYNN GOSSE WELSHMAN


CENTRE FOR NFLD. STUDIES
MEMORIAL UNIVERSITY
OF NEWFOUNDLAND

# Investigating Endo-Exo Selectivity in Diels-Alder Reactions

by

**Tammy Lynn Gosse Welshman**

B.Sc.(Honours, Chemistry)

A thesis submitted to the
School of Graduate Studies
in partial fulfilment of the
requirements for the degree of

Doctor of Philosophy

Department of Chemistry
Memorial University of Newfoundland
St. John's, Newfoundland
January 25, 2010

## Abstract

An important goal for synthetic organic chemists is the synthesis of the desired isomer of a target chemical compound exclusively and in high yield. The value and beauty of the Diels-Alder cycloaddition lies in its capacity for *selectivity*; that is, the isolation of a single stereoisomer in good yield is possible in many cases. A chemist's knowledge of the typical stereochemical outcomes of a variety of Diels-Alder reactions may be used to predict the product distribution for their system of interest. There are three types of selectivity generally observed in these cycloadditions; the reasons for the selectivity we see are not always clear. Endo-exo selectivity is the main focus of this thesis.

In Chapter 2, the Diels-Alder reaction of 3,3-disubstituted cyclopropene with butadiene was determined to be exo selective for all of the substituents examined, as was predicted from a previous study of a 3-substituted cyclopropene / butadiene system. The addition of a second substituent at the C3-position resulted in a greater stabilization of the cyclopropene ring when compared to the 3-substituted cyclopropenes; this result can be attributed to the anomeric effect. The activation barriers for the 3,3-disubstituted cyclopropene / butadiene system were below those of the syn 3-substituted system (for both endo and exo addition), mostly due to the substantial relief of ring strain in the 3,3-disubstituted cyclopropene / butadiene transition state structures.

Long-range and short-range substituent effects on the reactivity of cyclopentene dienophiles were considered in Chapter 3. Disubstitution at C4 (a long-range effect) had essentially no impact on the stabilization of the cyclopentene dienophiles, while

disubstitution at C1 and C2 (the reaction center) resulted in significant changes in the lengths of the C1=C2 bonds. The Diels-Alder reactions of the various 4,4- and 1,2-disubstituted dienophiles with both butadiene and cyclopentadiene were examined and the most significant selectivities were observed for the 4,4-disubstituted cyclopentene / butadiene system (exo selective) and the 1,2-disubstituted cyclopentene / cyclopentadiene system (endo selective). Secondary orbital interactions are not possible in the transition state structures of these cyclopentene Diels-Alder systems and thus cannot play a role in determining endo-exo selectivity. The observed selectivities can be rationalized qualitatively by examining the favourable and unfavourable interactions between the diene and dienophile in the transition state structures.

The investigation of the Diels-Alder reactions involving cyclopentadiene and its substituted analogs in Chapter 4 involved two main objectives: the examination of the endo-exo and facial selectivities for a large number of diene / dienophile combinations, as well as the in-depth analysis of the potential energy curve of the endo dimerization of cyclopentadiene. Endo addition was preferred for all of these cycloadditions, which is the most commonly observed preference. However, a characterization of the reaction coordinate revealed an occurrence considered to be rather atypical for Diels-Alder reactions: the existence of the bispericyclic transition state, first discussed in a 2001 communication by Caramella et al. This transition state leads to a lower energy Cope transition state later on the reaction coordinate. Vibrational frequency data along the curve were examined and product distribution was discussed. In the case of the Diels-Alder reactions of

cyclopentadiene and its derivatives, the wealth of p-orbitals available for favourable secondary orbital interactions are likely the major contributing factor in the determination of the endo selectivity observed.

## Acknowledgments

I extend my heartfelt thanks to everyone who has contributed directly or indirectly to the completion of this work.

First, I am deeply grateful to my supervisor, Dr. Raymond Poirier, for his patience, guidance, and support during my time as a Ph.D. candidate at Memorial University, and his continued encouragement after I departed Newfoundland for Winnipeg, Manitoba. We had a lot of "heated" discussions but also a lot of laughs, and my time in the Poirier group was the absolute best. Thank you for being a true mentor and a wonderful friend.

I wish to thank the Poirier group, past and present, with special thanks reserved for Dr. James Xidos, for "showing me the ropes" and continuing to be an unlimited source of knowledge, advice, and helpful discussion. I cherish our friendship deeply and I've enjoyed my teaching experience at the University of Manitoba even more with you as a fellow instructor!!

I want to say a big thank you to my supervisory committee members, Dr. Yuming Zhao and Dr. Paul Mezey, for reading this thesis and for their helpful comments and suggestions. Thank you to Dr. Jean Burnell, a former supervisory committee member and contributor to the research in Chapter 4 of this thesis. I also wish to acknowledge Mr. Fred Perry and Mr. Mark Staveley for their help with the computing resources at MUN.

I am grateful to the faculty, staff, and students of the Chemistry Department that made my stay at the university such a pleasant experience. In addition, I greatly appreciate the monetary support from the Department of Chemistry, from Memorial University, as well as

from the Natural Sciences and Engineering Research Council of Canada (NSERC).

I wish to thank my family and friends for their ongoing support and encouragement, especially through the many rough spots. I am deeply indebted to my parents, Baxter and Ivy Gosse. Your love and guidance through the years have led me to this place, and you've held my hand every step of the way. This thesis would not have been possible without you.

Finally, I am forever grateful for my best friend and devoted husband, David Welshman, who's unending patience and moral support have been invaluable in the duration of this degree. You've helped me keep my feet on the ground and encouraged me to keep going during the frustrating times. Having you by my side has made this entire process of research and writing much more bearable. Our new baby son, Cole, has made me remember that it's important to take things one day at a time and to treasure every moment. He is the brightest light in my life.

This thesis is dedicated to:

Baxter and Ivy Gosse

David and Cole Welshman

and in remembrance of:

my grandfather, James Dominie

who was always interested in anything I had to say.

## Table of Contents

## List of Tables

## List of Figures

## List of Abbreviations

| | |
|---|---|
| BPC | bispericyclic |
| DA | Diels-Alder |
| DFT | density functional theory |
| EDG | electron-donating group |
| EWG | electron-withdrawing group |
| FMO | frontier molecular orbital |
| GS | ground state |
| HF | Hartree-Fock |
| HOMO | highest occupied molecular orbital |
| HSAB | hard and soft acid and base |
| IRC | intrinsic reaction coordinate |
| LUMO | lowest unoccupied molecular orbital |
| MO | molecular orbital |
| MP2 | second-order Møller-Plesset |
| RHO | reactive hybrid orbital |
| SCF | self-consistent field |
| SOI | secondary orbital interactions |
| TS | transition state |
| ZPE | zero point energy |

# Chapter 1

## Introduction - Stereoselectivity in the Diels-Alder Reaction

### 1.1. The Diels-Alder Reaction

The field of synthetic organic chemistry boasts a diverse array of both simple and complex chemical reactions. One of the most widely-used and versatile reactions is the Diels-Alder (DA) cycloaddition, recognized by Profs. Otto Diels and Kurt Alder in 1928 (1). The reaction occurs between a molecule with a conjugated π system (the diene) and another with at least one π bond (the dienophile). Proceeding through a cyclic transition state (TS) structure, the cycloaddition involves breaking the three π bonds of the starting materials and simultaneously forming two σ bonds, resulting in a six-membered ring product and the generation of a new π bond. The parent reaction, the cycloaddition of 1,3-butadiene (hereafter referred to as butadiene) and ethene, is depicted in Figure 1.1.

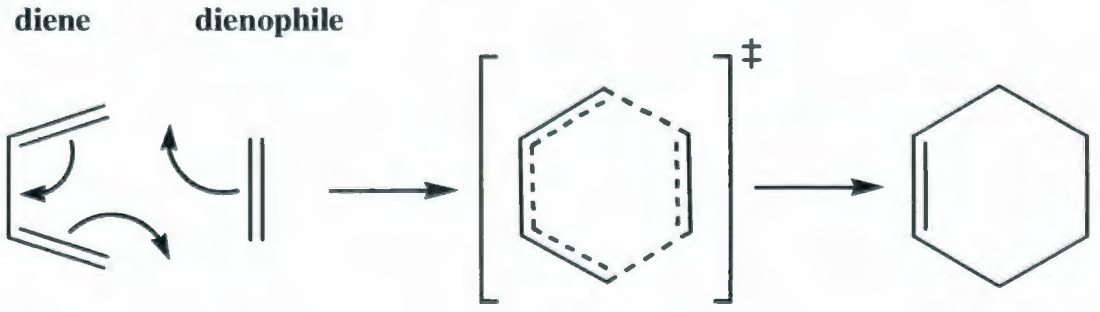


**Figure 1.1.** The DA reaction of butadiene and ethene to form cyclohexene.

The DA cycloaddition is valuable to synthetic chemists for many reasons:

- the formation of a ring and two new σ bonds,
- usually, the use of mild reaction conditions,
- the potential for all four of the new $sp^3$-hybridized atoms in the DA product to be stereogenic centers, and, most importantly,
- the remarkable *selectivity* in product formation.

When multiple products are possible, selectivity is a crucial element for a successful synthesis. For example, Figure 1.2 illustrates a DA reaction that has been used in the synthesis of kempane diterpenes (2). There are eight possible products for this cycloaddition. Incredibly, the reaction produces only a single isomer; that is, 100% of the 80% yield is the product shown.

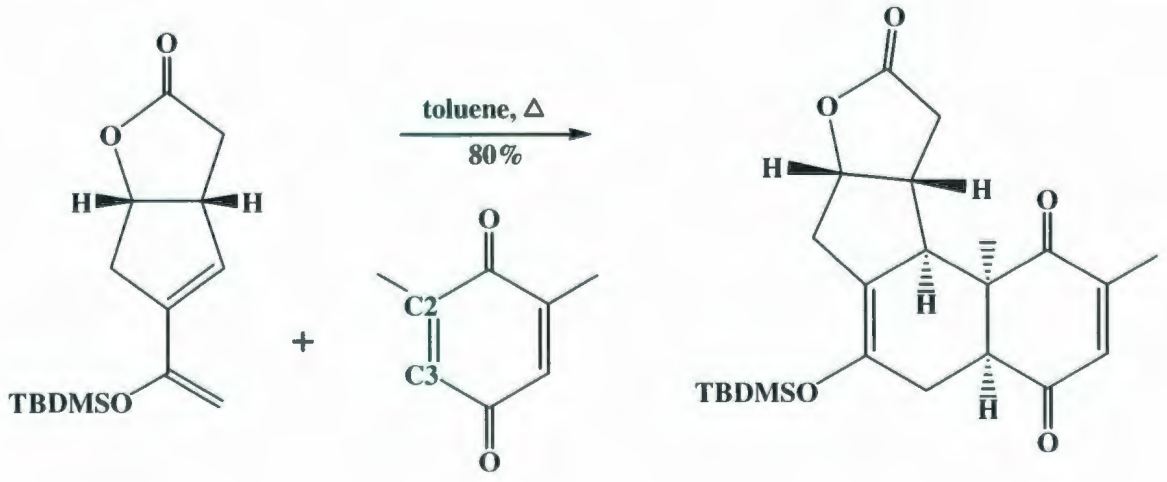


**Figure 1.2.** A step in the synthesis of kempane diterpenes (Burnell et al., 1997). This highly selective DA reaction yields the single product in 80% yield.

If this reaction had produced significant quantities of any of the other seven possible cycloadducts, isolation of the desired isomer would have been an arduous task. The separation of products that are chemically similar or enantiomeric can demand a huge amount of time, effort, and cost. Fortunately, knowledge of substituent effects and the electronic and steric properties of the diene / dienophile often make it possible for researchers to predict the outcome of the reaction and thus modify the reactants accordingly.

It is widely accepted that the mechanism of the DA reaction is concerted (3). However, recent mechanistic studies of these cycloadditions have been fueled by the idea that higher energy stepwise paths are attainable in certain situations. For example, it has been shown that the DA cycloaddition of butadiene and ethene (Figure 1.1) prefers the synchronous concerted mechanism in which both of the σ bonds that close the cyclohexene ring are formed to the same extent in the TS structure. The stepwise mechanism, however, is only 2 - 7 kcal $mol^{-1}$ (8.4 - 29.3 kJ $mol^{-1}$) higher in energy than the concerted path (4).

The parent reaction depicted in Figure 1.1 actually does not work very well and experimental yields are generally low in the absence of optimal reaction conditions (5). Typically, a successful DA cycloaddition requires that the diene and dienophile bear substituents that aid in the redistribution of electronic charge during the reaction. According to Frontier Molecular Orbital (FMO) theory (6), the majority of chemical reactions occur due to an interaction of the outlying frontier MOs, the HOMO and the LUMO (the highest occupied and lowest unoccupied molecular orbitals, respectively). Substitution on the diene and / or dienophile alters the energies of the HOMO and LUMO, thus influencing the

reactivity. Optimal reaction conditions ensure the smallest possible energy gap between the interacting HOMO - LUMO pair. In general, the DA cycloaddition may proceed in two different ways: normal electron demand and inverse electron demand, as shown in Figure 1.3.

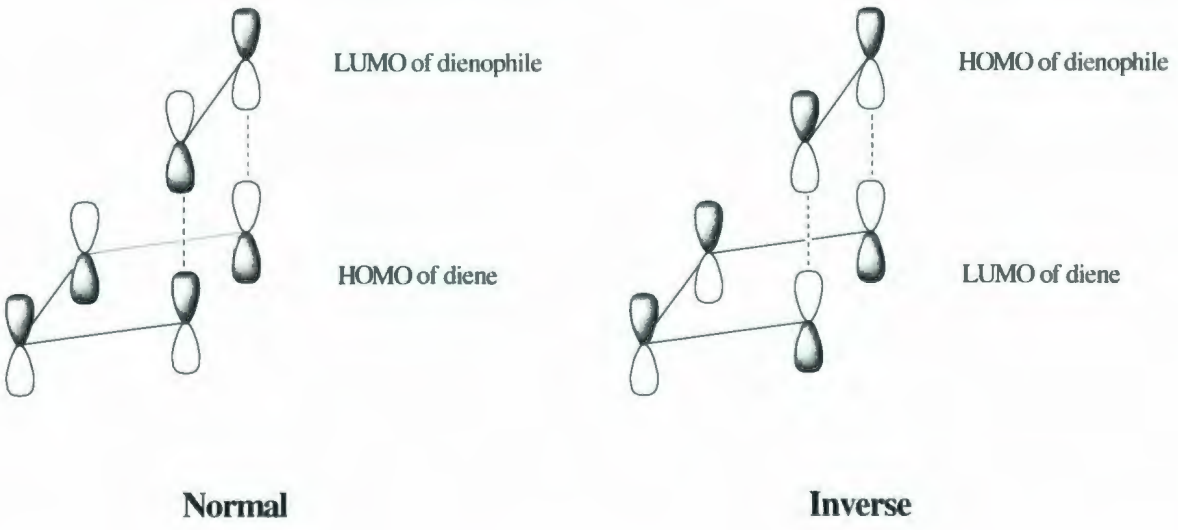


**Figure 1.3.** The FMO interactions of the normal and inverse electron demand DA cycloadditions.

A normal electron demand DA reaction involves the in-phase interaction of the HOMO of the diene and the LUMO of the dienophile; conversely, the LUMO of the diene and the HOMO of the dienophile interact during the inverse electron demand cycloaddition (Figure 1.3). An electron-donating group (EDG) such as hydroxyl (-OH) or amino ($-NH_2$) on the diene increases the energy of the diene's HOMO and the diene is said to become "electron-rich". Conversely, the dienophile becomes "electron-poor" upon the addition of

an electron-withdrawing group (EWG) such as cyano (-C≡N) or fluorine. This substitution results in a lowering of the dienophile's LUMO energy. This particular situation facilitates a normal electron demand DA reaction by decreasing the HOMO-LUMO gap between the diene and dienophile (Figure 1.4).

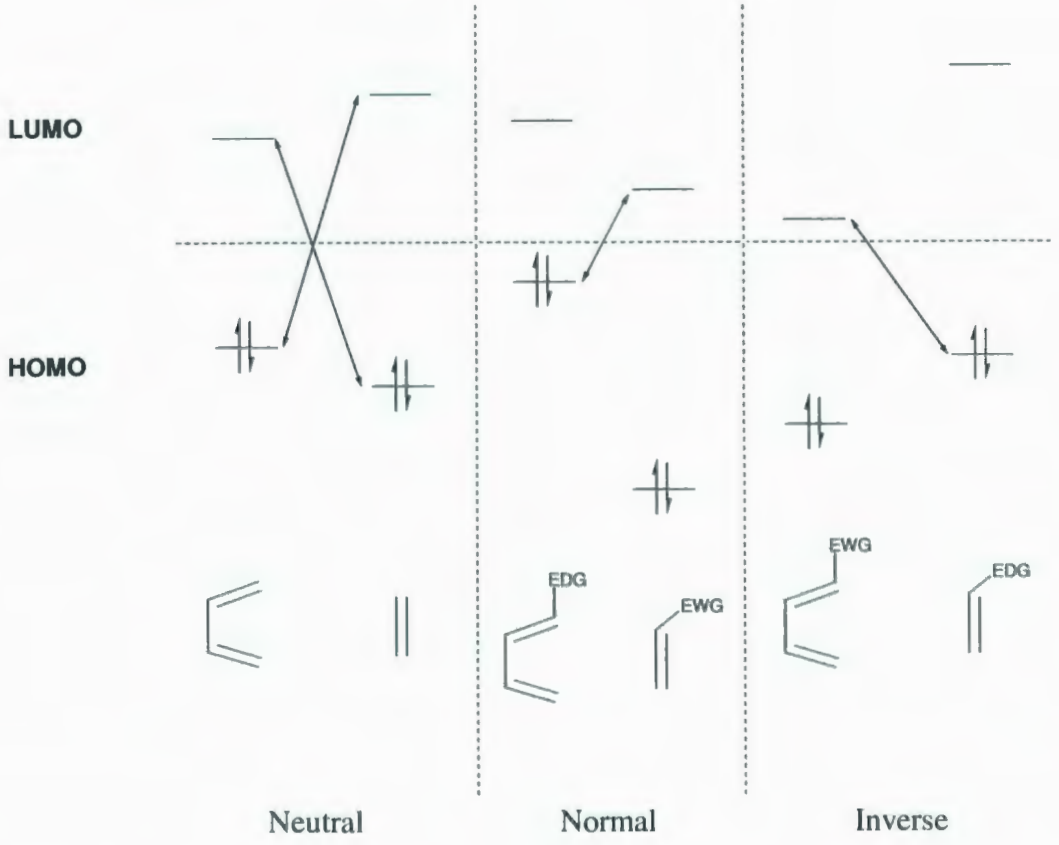


**Figure 1.4.** The FMO depiction of the neutral, normal, and inverse electron demand DA cycloadditions. In the neutral reaction, the mixing of the HOMO (diene) - LUMO (dienophile) is as equally probable as the interaction of the LUMO (diene) - HOMO (dienophile). A substituent (EDG or EWG) on the diene and / or dienophile induces changes in the relative energies of the FMOs, facilitating either normal or inverse electron demand reactions (7).

## 1.2. The Effects of Substitution on Selectivity

Upon substitution, dienes and dienophiles may become electronically and / or sterically altered such that they exhibit distinct preferences for what they can react with. Some reactants may become activated by substitution and hence participate in a DA cycloaddition without effort; this indicates an enhanced reactivity. Other reactants may require more prompting and harsher reaction conditions, while some may not react at all. It is important to point out that the combination of diene / dienophile is the key. The two reactants of the DA pair must complement each other and enable an easy flow of electronic charge from one to the other. Diene / dienophile substitution can introduce a variety of new and different ways that the reactants can approach each other and hence react (reaction *modes*). The likelihood of a reaction mode occurring is reflected in the activation energy barrier, which in turn provides insight into the favourable or unfavourable characteristics of the TS structure itself. It is important to point out that the typical DA cycloaddition is kinetically controlled, so investigations of this reaction (including selectivity studies) require an examination of barrier heights and the TS structures at the peak of those barriers.

A stereoselective reaction is one which has the capacity to form two or more stereoisomeric products but actually yields one product in greater amounts than any of the other stereoisomers. The selectivity may be total and result in a single and exclusive product (as in Figure 1.2), or it may be partial and yield an unequal mixture of different stereoisomers. There are generally three types of selectivity involved in DA cycloadditions: regioselectivity, facial (anti-syn) selectivity, and endo-exo selectivity.

### 1.2.1. Regioselectivity

Regioselectivity is concerned with which "regions" or "ends" of the diene and dienophile will preferentially react with one another. In the reaction depicted in Figure 1.2, the vertical flipping of the dienophile (and thus exchanging the positions of C2 and C3) would result in another possible regioisomeric product in addition to the one shown.

It was previously thought that consideration of the FMOs were sufficient for the determination of regioselectivity (8), however it has been shown in recent years that this simplified method may not be particularly useful for larger systems. The hard and soft acid and base (HSAB) principle (9) has been implemented widely to explain the observed regioselectivities for DA cycloadditions. The global electrophilicity index of Parr et al. (10) was extended by Domingo and co-workers in 2002 to create local or regional electrophilicities; these indices were shown to be useful in the prediction of regioselectivities for polar DA reactions (11). A recent theoretical paper by Hirao and Ohwada (12) proposed that their reactive hybrid orbital (RHO) method provides a superior means to obtaining the correct experimental regioselectivities for a series of DA cycloadditions. The RHO is essentially a single reactive orbital that is localized at the reaction site and, according to the authors, provides a better picture of orbital interactions in the TS structure than the FMOs. In general, it is now apparent that other factors (and particularly, other orbitals) contribute to the regioselectivity observed in DA reactions, and the investigations continue.

### 1.2.2. Facial (anti-syn) Selectivity

Facial selectivity has definitely been one of the hot buttons of controversy through the years. A diene / dienophile can be envisioned as having two sides, or "faces", which may or may not be identical. Facial selectivity, then, refers to the preferential addition of a diene / dienophile to a particular face of its DA partner. The simplest scenario would entail substitution on one face of the diene / dienophile only. In general, anti modes of addition are favoured for these reactions, as the substituent is on the face opposite to the incoming diene / dienophile, thus reducing the possibility of steric interactions (13). However, in some instances, cycloaddition to the same side (syn) as the substituent is overwhelmingly preferred (14). The terms "anti" and "syn" may need to be specifically defined, particularly when both faces of the diene and / or dienophile are substituted. In these cases, one needs to state that the addition is occurring "anti to.." or "syn to.." a specific face of its DA partner. Figure 1.5 illustrates a simple example of these two modes of addition.

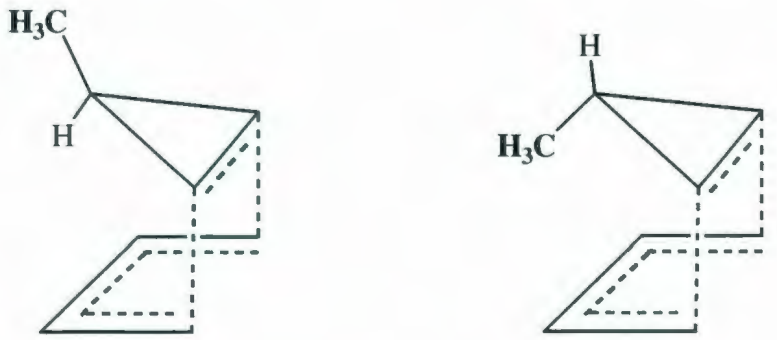


anti syn

**Figure 1.5.** The anti and syn TS structures for the endo DA reaction of butadiene and 3-$CH_3$-cyclopropene. The majority of the hydrogen atoms are omitted for simplicity.

Sometimes, it is the substituent itself that determines the type of facial addition. In these instances, the accurate prediction of the anti-syn selectivity is usually possible. For example, in the case of 1,3-cyclopentadiene (hereafter referred to as cyclopentadiene), the substitution of oxygen (as -OH, -OAc, etc., (15)) or fluorine (16) at the 5-position of the diene typically directs the addition syn to the heteroatom. In contrast, 5-substitution of cyclopentadiene with bromine (17, 18) or iodine (18, 15(d)) results in almost exclusively anti DA products. When benzene oxide is used as the diene (with the oxygen in a position much like that of 5-substituted cyclopentadiene), its DA reaction with dienophiles *N*-phenylmaleimide (19), ethene (20), and ethyne (20) overwhelmingly prefers anti addition. *N*-Phenylmaleimide itself shows mixed preferences in facial selectivity; it has been shown

to prefer either anti or syn addition or, in some cases, no preference at all (21).

A significant number of DA cycloadditions proceed in an unexpected manner and conventional steric hindrance / control arguments can neither predict nor explain the observed facial selectivities. There are also reactions in which the structural characteristics of each face of the diene / dienophile are identical or very similar, so the facial preference for addition, in terms of possible steric problems, is not obvious. Under such circumstances, researchers have put forth a variety of theories and justifications to explain the outcomes of these cycloadditions. Some of these explanations involve hyperconjugation effects (14(a), 15(c), 22), orbital mixing / tilting (23), and electrostatic interactions (24).

At this point, it is sufficient to state that steric hindrance influences the anti-syn selectivity of the majority of DA systems. Also, there is no one theory for explaining those systems which behave in a manner that seems to challenge steric expectations. It is believed that, if steric arguments cannot adequately explain the results of a DA cycloaddition, there are likely many smaller effects that come into play. Undoubtedly, this complicates the picture and can make facial selectivity difficult to predict.

### 1.2.3. Endo-Exo Selectivity

The majority of this work is concerned with endo-exo selectivity, which has received less attention in the literature than the anti-syn selectivity question. There is a reason for this: endo addition dominates in most DA reactions and usually only the endo adduct is formed. Thus, the interest is not typically what *type* of endo-exo selectivity we see, but *why* endo

addition is the preferred mode of cycloaddition.

Endo and exo (from Greek for *within* and *outside*, respectively) addition is best described in terms of the placement of the dienophile relative to the diene in the TS structure. Endo TSs have the bulk of the dienophile positioned in close proximity to the bulk of the diene (above or below), whereas exo TS structures have the bulk of the dienophile "outside" and away from the diene. Figure 1.6 illustrates the difference.

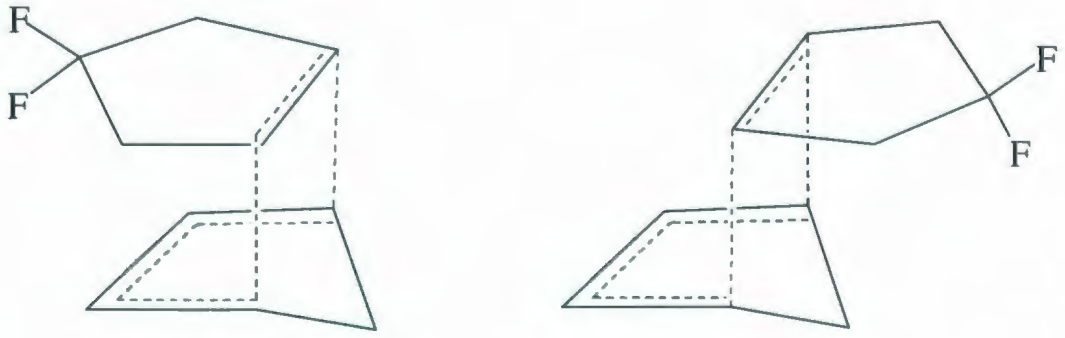


endo exo

**Figure 1.6.** The endo and exo TS structures for the DA reaction of cyclopentadiene and 4,4-difluorocyclopentene. Hydrogen atoms are omitted for simplicity.

A theory to explain the overriding tendency for endo addition in DA reactions was proposed by Alder and Stein in 1937 (25). The so-called "endo rule" states that the endo TS structure is more stable due to the favourable "maximum accumulation of unsaturation".

Woodward and Hoffmann extended this idea in 1965 by using FMO theory; they postulated that the endo preference could be attributed to significant favourable overlap of the secondary orbitals in the endo TS structure (26). The secondary orbitals are the p-orbitals adjacent to the primary reaction centers of the diene and dienophile. Secondary orbital interactions (SOI), then, would involve the overlap of the "in-phase" p-orbitals at these adjacent centers. If SOI are present in the TS structure, endo selectivity would surely predominate, as SOI are not a possibility for exo addition (Figure 1.7).

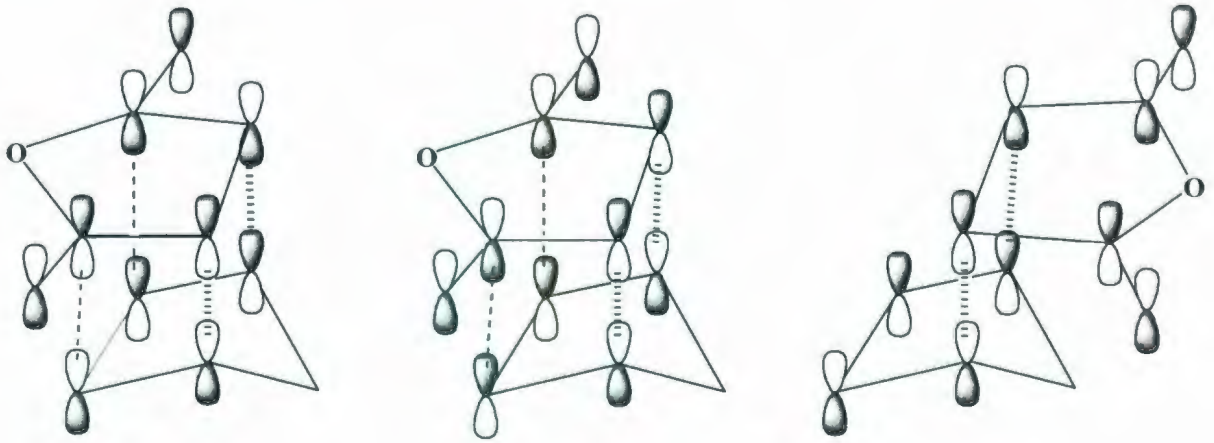


normal ED
**endo**

inverse ED
**endo**

normal ED
**exo**

**Figure 1.7.** Secondary orbital interactions, illustrated in the normal and inverse electron demand endo TS structures of the cyclopentadiene and maleic anhydride DA cycloaddition. The exo TS structure is unable to benefit from SOI due to the "outside" position of the dienophile in relation to the diene. The primary (bonding) interactions are indicated by the hashed lines and the SOI are depicted by thin dashed lines.

Many researchers still maintain that the driving force in the determination of endo-exo selectivity is the existence of stabilizing SOI in the endo TS structure (27). However, it has been proposed in recent years that SOI may not be as significant as once thought, and that numerous other factors play very important roles in endo-exo selectivity. Notably, a paper in 2000 by García, Mayoral, and Salvatella (28) reviewed some of the more common examples used to illustrate SOI, and they concluded that factors such as steric interactions, electrostatic effects, solvent effects, etc., can instead be used to explain the observed endo selectivity. Indeed, for some DA reactions, it is believed that the very atoms that are supposed to participate in these stabilizing interactions are seemingly too far apart in the TS structure (approx. 2.8 Å or more, (29)) or the secondary orbitals are not oriented properly to allow for significant overlap. In addition, not every endo TS structure has secondary orbitals available for favourable SOI, yet endo selectivity may prevail in these cases (30). The importance (or lack thereof) of SOI in stabilizing the endo TS structures of DA reactions is dealt with in greater detail in later chapters.

## 1.3. Computational Methodology

### 1.3.1. Diels-Alder Reactions: Computational Studies

The proliferation of computational studies of the DA cycloaddition in the last couple of decades can be attributed to the dramatic increase of both computing power and the diversity of computer programs available for performing electronic structure calculations. A certain degree of insight can be obtained by viewing the isolated reactants, products, and

TS structures at the atomic level, a view that is not readily available to the experimental chemist performing a DA reaction in a laboratory setting. Computational studies are meant to complement experimental work and vice versa; answers to posed questions and evidence for validating theories can be gleaned from both worlds and united to explain observed outcomes.

The DA cycloaddition, in particular, is a beautiful example of how computational chemistry can be successfully applied to a chemical problem. The TS structure is of particular interest, particularly for selectivity studies; since the reaction is kinetically controlled, this is where the regio- and stereoselectivity is determined. The cycloaddition is concerted, thus the typical reaction path is straightforward and the TS structure is fairly easy to predict and obtain computationally. In addition, the relatively nonpolar nature of the TS permits calculations to be performed in the gas phase. The TS structure differs very little in charge distribution from the diene / dienophile reactants, thus the solvent effect on selectivity is quite small. It is well established that aqueous and polar solvents can affect the activation barriers of DA reactions to varying degrees (14(a), 31), but usually the reaction barriers, and thus endo-exo selectivity, are not changed relative to each other by a significant amount. The omission of solvent effects simplifies the calculations immensely.

The computational study necessarily involves a choice of model, the method and basis set to be employed, and the platform upon which calculations will be done. The rationale for the choice of molecular systems studied in this work varied, but the ultimate goal was to achieve a better understanding of endo-exo selectivity using simple diene / dienophile

combinations. Our research methods included:

- varying the substitution patterns on the dienophile and determining ground state (GS) reactivities,
- examining systems that did not have the typical endo addition preference (such as the 3,3-disubstituted cyclopropene / butadiene system in Chapter 2),
- studying systems in which the selectivity could not be explained by SOI (the aforementioned system in Chapter 2, as well as the disubstituted cyclopentene / butadiene and disubstituted cyclopentene / cyclopentadiene systems in Chapter 3), and,
- investigating a clear case of exclusive endo selectivity and a remarkable example of SOI (the dimerization of 5-substituted cyclopentadienes, Chapter 4).

The Gaussian suite of programs (32) was chosen to perform the calculations. In general, density functional theory (DFT) was used in conjunction with basis sets such as 6-31G(d) or 6-31++G(d).

### 1.3.2. Density Functional Theory

Depending on the objective of the study, the examination of moderately-sized systems generally requires an *ab initio* (first principles) method or DFT. *Ab initio* methods calculate a molecular wavefunction and molecular orbital energies; the properties of the system can be calculated from the optimized wavefunction, $\Psi$. DFT, however, is based on the determination of the molecular electron probability density $\rho$, from which the electronic

energy is obtained.

Unlike the *ab initio* wavefunction $\Psi$, which is not a measurable "observable" feature of atoms and molecules and thus cannot be probed experimentally, the electron density $\rho$ *is* an experimentally observed property. In addition, $\Psi$ is a function of 4N variables: three spatial coordinates and one spin function for each of N electrons. Thus, the complexity of $\Psi$ increases dramatically with the size of the system and the computational effort involved in its determination becomes tremendous. In contrast, $\rho$ remains a function of three spatial coordinates, regardless of system size. Calculations using DFT are also computationally inexpensive and often the results obtained are of the same quality as a second-order Møller-Plesset (MP2) calculation or better.

The type of DFT method is indicated by the definition of the exchange-correlation energy functional, $E_{XC}[\rho(r)]$. $E_{XC}$ can be written as a sum of an exchange energy functional and a correlation energy functional: $E_{XC} = E_X + E_C$. A main focus of the research in DFT is the search for better functionals to represent the exchange-correlation energy. If the exact $E_{XC}$ was known, DFT could provide the exact total energy of the system, including electron correlation. Of the many functionals available today, B3LYP is one of the most reliable and has the added advantage of being around long enough to be widely tested. B3LYP (or Becke3LYP) is a hybrid exchange-correlation three parameter (B3) functional which incorporates the exchange energy functional developed by Becke in 1993 (33) with the gradient-corrected correlation energy functional of Lee, Yang, and Parr (LYP, (34)). It has been well established that DFT calculations (in particular, the B3LYP/6-31G(d) level of

theory) give reasonable activation barriers for pericyclic reactions as well as reliable geometries for GS and TS structures (35). For this reason, it is the main methodology presently used by researchers to study DA reactions and it is implemented in this body of work as well.

While it is recognized that the context in which the term "ground state" is used in this thesis is not entirely appropriate ("equilibrium structure" would be a better choice), we have nonetheless used the term "ground state" to indicate the lowest energy equilibrium structure for a given reactant in the following series of studies. In addition, all energies reported are self-consistent field (SCF) energies and are not corrected for zero point energy (ZPE). The ZPE corrections, if applied, would result in only minor changes, if any, in the reported energies and these differences would not be reflected in the endo-exo selectivity or any other energy analysis to a significant degree.

**References**


(1) Diels, O.; Alder, K. *Justus Liebigs Ann. Chem.* **1928**, *460*, 98.

(2) Liu, C.; Burnell, D. J. *J. Am. Chem. Soc.* **1997**, *119*, 9584.

(3) The mechanism debate is humorously reviewed in: Houk, K. N.; González, J.; Li, Y. *Acc. Chem. Res.* **1995**, *28*, 81.

(4) The experimental estimate as stated in: Doering, W. v. E.; Roth, W. R.; Breuckmann, R.; Figge, L.; Lennartz, T.-W.; Fessner, W.-D.; Prinzbach, H. *Chem. Ber.* **1988**, *121*, 1. Theoretical studies report a variety of barrier differences between the concerted

and stepwise mechanisms, depending on the theory implemented and the inclusion of dynamical correlational energy corrections. See: Goldstein, E.; Beno, B.; Houk, K. N. *J. Am. Chem. Soc.* **1996**, *118*, 6036, and references therein. A more recent paper involving a variety of computational methods: Isobe, H.; Takano, Y.; Kitagawa, Y.; Kawakami, T.; Yamanaka, S.; Yamaguchi, K.; Houk, K. N. *Mol. Phys.* **2002**, *100*, 717. In this publication, for example, barrier differences of 4.5, 4.4, and 4.9 kcal $mol^{-1}$ were obtained for QCISD(T), CCSD(T), and B3LYP, respectively.

(5) Joshel, L. M.; Butz, L. W. *J. Am. Chem. Soc.* **1941**, *63*, 3350.

(6) Fleming, I. *Frontier Orbitals and Organic Chemical Reactions*; Wiley: London, 1976.

(7) Figure 1.3 is a modified version of Figure 11.2 on p. 922 of: Lowry, T. H.; Richardson, K. S. *Mechanism and Theory in Organic Chemistry, 3rd ed.*; HarperCollins: New York, 1987.

(8) For example: (a) Houk, K. N. *Acc. Chem. Res.* **1975**, *8*, 361. (b) Eisenstein, O.; Lefour, J. M.; Anh, N. T.; Hudson, R. F. *Tetrahedron* **1977**, *33*, 523.

(9) (a) Pearson, R. G. *J. Am. Chem. Soc.* **1963**, *85*, 3533. (b) Pearson, R. G. *Chemical Hardness*; Wiley-VCH: Weinheim, Germany, 1997. See also: Ponti, A. *J. Phys. Chem. A* **2000**, *104*, 8843; this is a study of regioselectivity in cycloaddition reactions and introduces DFT-based criteria for selectivity in terms of local softness.

(10) Parr, R. G.; Szentpály, L. v.; Liu, S. *J. Am. Chem. Soc.* **1999**, *121*, 1922.

(11) Domingo, L. R.; Aurell, M. J.; Pérez, P.; Contreras, R. *J. Phys. Chem. A* **2002**, *106*,

6871. See also: Domingo, L. R.; Aurell, M. J.; Pérez, P.; Contreras, R. *Tetrahedron* **2002**, *58*, 4417.

(12) Hirao, H.; Ohwada, T. *J. Phys. Chem. A* **2005**, *109*, 816. The RHO analysis is also applied to electrophilic aromatic substitution reactions in: Hirao, H.; Ohwada, T. *J. Phys. Chem. A* **2003**, *107*, 2875.

(13) Recent articles: (a) Capaccio, C. A. I.; Varela, O. *J. Org. Chem.* **2002**, *67*, 7839. (b) Möhring, D.; Nieger, M.; Lewall, B.; Dötz, K. H. *Eur. J. Org. Chem.* **2005**, 2620. (c) Morrison, C. F.; Vaters, J. P.; Miller, D. O.; Burnell, D. J. *Org. Biomol. Chem.* **2006**, *4*, 1160.

(14) Recent articles: (a) Ohkata, K.; Tamura, Y.; Shetuni, B. B.; Takagi, R.; Miyanaga, W.; Kojima, S.; Paquette, L. A. *J. Am. Chem. Soc.* **2004**, *126*, 16783. (b) Funel, J.-A.; Ricard, L.; Prunet, J. *Chem. Commun.* **2005**, 4833. (c) Takayama, J.; Sugihara, Y.; Takayanagi, T.; Nakayama, J. *Tetrahedron Lett.* **2005**, *46*, 4165.

(15) Some examples are: (a) Winstein, S.; Shatavsky, M.; Norton, C.; Woodward, R. B. *J. Am. Chem. Soc.* **1955**, *77*, 4183. (b) Jones, D. W. *J. Am. Chem. Soc., Chem. Commun.* **1980**, 739. (c) Macaulay, J. B.; Fallis, A. G. *J. Am. Chem. Soc.* **1990**, *112*, 1136. (d) Xidos, J. D.; Poirier, R. A.; Pye, C. C.; Burnell, D. J. *J. Org. Chem.* **1998**, *63*, 105.

(16) McClinton, M. A.; Sik, V. *J. Chem. Soc., Perkin Trans. 1* **1992**, 1891.

(17) (a) Breslow, R.; Hoffman, Jr., J. M.; Perchonock, C. *Tetrahedron Lett.* **1973**, 3723. (b) Franck-Neumann, M.; Sedrati, M. *Tetrahedron Lett.* **1983**, *24*, 1391.

(18) Wellman, M. A.; Burry, L. C.; Letourneau, J. E.; Bridson, J. N.; Miller, D. O.; Burnell, D. J. *J. Org. Chem.* **1997**, *62*, 939.

(19) Gillard, J. R.; Newlands, M. J.; Bridson, J. N.; Burnell, D. J. *Can. J. Chem.* **1991**, *69*, 1337.

(20) Pye, C. C.; Xidos, J. D.; Poirier, R. A.; Burnell, D. J. *J. Phys. Chem. A* **1997**, *101*, 3371.

(21) (a) Krow, G. R.; Carey, J. T.; Zacharias, D. E.; Kraus, E. E. *J. Org. Chem.* **1982**, *47*, 1989. (b) McDougal, P. G.; Rico, J. G.; Derveer, D. V. *J. Org. Chem.* **1986**, *51*, 4492. (c) Reitz, A. B.; Jordan, Jr., A. D.; Maryanoff, B. E. *J. Org. Chem.* **1987**, *52*, 4800. (d) Fisher, M. J.; Overman, L. E. *J. Org. Chem.* **1988**, *53*, 2630. (e) Fisher, M. J.; Hehre, W. J.; Kahn, S. D.; Overman, L. E. *J. Am. Chem. Soc.* **1988**, *110*, 4625.

(22) (a) Coxon, J. M.; McDonald, D. Q. *Tetrahedron* **1992**, *48*, 3353. (b) Cieplak, A. S. *Chem. Rev.* **1999**, *99*, 1265, and references therein. (c) Hou, H.-F.; Peddinti, R. K.; Liao, C.-C. *Org. Lett.* **2002**, *4*, 2477.

(23) Orbital mixing: (a) Inagaki, S.; Fujimoto, H.; Fukui, K. *J. Am. Chem. Soc.* **1976**, *98*, 4054. More recently: (b) Ishida, M.; Sakamoto, M.; Hattori, H.; Shimizu, M.; Inagaki, S. *Tetrahedron Lett.* **2001**, *42*, 3471. (c) Ishida, M.; Hirasawa, S.; Inagaki, S. *Tetrahedron Lett.* **2003**, *44*, 2187. Orbital tilting: (d) Gleiter, R.; Paquette, L. A. *Acc. Chem. Res.* **1983**, *16*, 328.

(24) (a) Kahn, S. D.; Hehre, W. J. *J. Am. Chem. Soc.* **1987**, *109*, 663. More recently: (b) Mehta, G.; Uma, R. *J. Org. Chem.* **2000**, *65*, 1685. (c) Yadav, V. K.; Senthil, G.;

Babu, K. G.; Parvez, M.; Reid, J. L. *J. Org. Chem.* **2002**, *67*, 1109. (d) Bakalova, S. M.; Santos, A. G. *J. Org. Chem.* **2004**, *69*, 8475.

(25) (a) Alder, K.; Stein, G. *Angew. Chem.* **1937**, *50*, 510. Also discussed in: (b) Martin, J. G.; Hill, R. K. *Chem. Rev.* **1961**, *61*, 537.

(26) Hoffmann, R.; Woodward, R. B. *J. Am. Chem. Soc.* **1965**, *87*, 4388.

(27) (a) Arrieta, A.; Cossio, F. P. *J. Org. Chem.* **2001**, *66*, 6178. (b) Quadrelli, P.; Romano, S.; Toma, L.; Caramella, P. *J. Org. Chem.* **2003**, *68*, 6035. (c) Dinadayalane, T. C.; Gayatri, G.; Sastry, G. N.; Leszczynski, J. *J. Phys. Chem. A* **2005**, *109*, 9310. (d) Bansal, R. K.; Gupta, N.; Kumawat, S. K. *Tetrahedron* **2006**, *62*, 1548.

(28) García, J. I.; Mayoral, J. A.; Salvatella, L. *Acc. Chem. Res.* **2000**, *33*, 658.

(29) For example: Calvo-Losada, S.; Suárez, D. *J. Am. Chem. Soc.* **2000**, *122*, 390.

(30) Fox, M. A.; Cardona, R.; Kiwiet, N. J. *J. Org. Chem.* **1987**, *52*, 1469, and references therein.

(31) (a) Rideout, D. C.; Breslow, R. *J. Am. Chem. Soc.* **1980**, *102*, 7817. (b) Kumar, A.; Pawar, S. S. *J. Org. Chem.* **2001**, *66*, 7646. (c) Sections within: Lindström, U. M. *Chem. Rev.* **2002**, *102*, 2751, and references therein. (d) Sarma, D.; Pawar, S. S.; Deshpande, S. S.; Kumar, A. *Tetrahedron Lett.* **2006**, *47*, 3957.

(32) Frisch, M. J.; Trucks, G. W.; Schlegel, H. B.; Scuseria, G. E.; Robb, M. A.; Cheeseman, J. R.; Zakrzewski, V. G.; Montgomery, Jr., J. A.; Stratmann, R. E.; Burant, J. C.; Dapprich, S.; Millam, J. M.; Daniels, A. D.; Kudin, K. N.; Strain, M.

C.; Farkas, O.; Tomasi, J.; Barone, V.; Cossi, M.; Cammi, R.; Mennucci, B.; Pomelli, C.; Adamo, C.; Clifford, S.; Ochterski, J.; Petersson, G. A.; Ayala, P. Y.; Cui, Q.; Morokuma, K.; Rega, N.; Salvador, P.; Dannenberg, J. J.; Malick, D. K.; Rabuck, A. D.; Raghavachari, K.; Foresman, J. B.; Cioslowski, J.; Ortiz, J. V.; Baboul, A. G.; Stefanov, B. B.; Liu, G.; Liashenko, A.; Piskorz, P.; Komaromi, I.; Gomperts, R.; Martin, R. L.; Fox, D. J.; Keith, T.; Al-Laham, M. A.; Peng, C. Y.; Nanayakkara, A.; Challacombe, M.; Gill, P. M. W.; Johnson, B.; Chen, W.; Wong, M. W.; Andres, J. L.; Gonzalez, C.; Head-Gordon, M.; Replogle, E. S.; Pople, J. A. *Gaussian 98*, revision A.11.3; Gaussian, Inc.: Pittsburgh, PA, 2002. (b) Frisch, M. J.; Trucks, G. W.; Schlegel, H. B.; Scuseria, G. E.; Robb, M. A.; Cheeseman, J. R.; Montgomery, Jr., J. A.; Vreven, T.; Kudin, K. N.; Burant, J. C.; Millam, J. M.; Iyengar, S. S.; Tomasi, J.; Barone, V.; Mennucci, B.; Cossi, M.; Scalmani, G.; Rega, N.; Petersson, G. A.; Nakatsuji, H.; Hada, M.; Ehara, M.; Toyota, K.; Fukuda, R.; Hasegawa, J.; Ishida, M.; Nakajima, T.; Honda, Y.; Kitao, O.; Nakai, H.; Klene, M.; Li, X.; Knox, J. E.; Hratchian, H. P.; Cross, J. B.; Adamo, C.; Jaramillo, J.; Gomperts, R.; Stratmann, R. E.; Yazyev, O.; Austin, A. J.; Cammi, R.; Pomelli, C.; Ochterski, J. W.; Ayala, P. Y.; Morokuma, K.; Voth, G. A.; Salvador, P.; Dannenberg, J. J.; Zakrzewski, V. G.; Dapprich, S.; Daniels, A. D.; Strain, M. C.; Farkas, O.; Malick, D. K.; Rabuck, A. D.; Raghavachari, K.; Foresman, J. B.; Ortiz, J. V.; Cui, Q.; Baboul, A. G.; Clifford, S.; Cioslowski, J.; Stefanov, B. B.; Liu, G.; Liashenko, A.; Piskorz, P.; Komaromi, I.; Martin, R. L.; Fox, D. J.; Keith, T.; Al-Laham, M. A.;

Peng, C. Y.; Nanayakkara, A.; Challacombe, M.; Gill, P. M. W.; Johnson, B.; Chen, W.; Wong, M. W.; Gonzalez, C.; Pople, J. A. *Gaussian 03*, revision B.05; Gaussian, Inc.: Pittsburgh, PA, 2003.

(33) Becke, A. D. *J. Chem. Phys.* **1993**, *98*, 5648.

(34) Lee, C.; Yang, W.; Parr, R. G. *Phys. Rev. B* **1988**, *37*, 785.

(35) (a) Wiest, O.; Montiel, D. C.; Houk, K. N. *J. Phys. Chem. A* **1997**, *101*, 8378. (b) Guner, V.; Khuong, K. S.; Leach, A. G.; Lee, P. S.; Bartberger, M. D.; Houk, K. N. *J. Phys. Chem. A* **2003**, *107*, 11445.

# Chapter 2

## Exo Selectivity and the Effect of Disubstitution in the Diels-Alder Reactions of Butadiene with 3,3-Disubstituted Cyclopropenes

### Background and Preamble

Our previous computational examination of the endo-exo and anti-syn selectivities in the 3-substituted cyclopropene / butadiene DA reaction (6) served as a worthy contribution to a debate in the literature regarding the factors that determine endo-exo selectivity for systems with cyclopropene dienophiles. This in-depth study addressed a number of significant issues and described some interesting features of this DA reaction. First, the effect of the 3-substituent on the reactivity of cyclopropene was illustrated by a plot showing the strong correlation between the stabilization upon substitution and the substituent's electronegativity. The stabilization energies ($\Delta E_{isodesmic}$) indicated that 3-substitution results in a stabilization of the cyclopropene ring for almost all substituents considered (an exception was $SiH_3$, which gave a positive $\Delta E_{isodesmic}$), and the degree of stabilization increases with increasing electronegativity. Second, it was shown that the activation energies of the anti additions correlate quite well with the electronegativity of the 3-substituent, while the syn additions show little or no correlation with electronegativity. This was depicted in a plot of the activation energies of all four modes of addition for the 3-substituted cyclopropene / butadiene DA reaction versus electronegativity (Figure 2A).

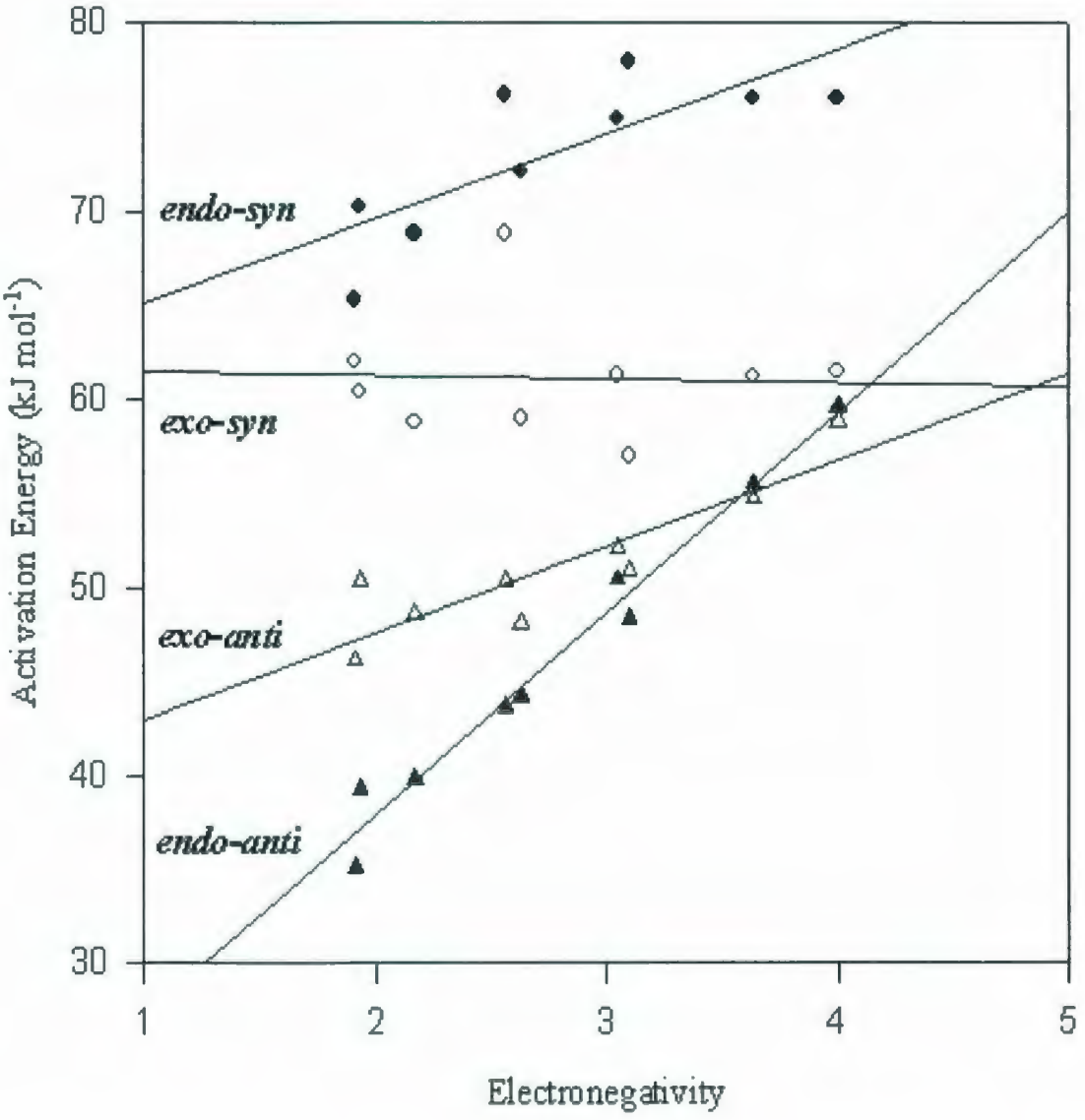


**Figure 2A.** A plot of activation energies (endo-anti (▲), exo-anti (△), endo-syn (●), and exo-syn (○)) versus electronegativity of the substituent atom or group for the DA reaction of 3-substituted cyclopropene with butadiene. Modified version of Figure 5 in: J. D. Xidos et al. *J. Am. Chem. Soc.* **2001**, *123*, 5482.

Figure 2A illustrates the high degree of facial selectivity for this reaction, particularly for the endo cycloadditions. We also noted that, for the syn addition reactions, exo addition is preferred over endo for every substituent examined. This finding was intriguing, and it was predicted that if the question of facial selectivity were removed and the reactions were permitted to proceed via syn addition only, then exo selectivity would prevail. This would be accomplished in the present study by adding a second identical substituent to C3 of cyclopropene, thereby obtaining 3,3-disubstituted cyclopropene and effectively eliminating the issue of anti-syn selectivity in its reaction with butadiene. In addition, we were interested in the effect on the cyclopropene GS reactivity that results from the addition of the second substituent to C3.

The calculations involving the 3-substituted cyclopropene / butadiene reaction were initially performed using the 6-31++G(d) basis set (6). This was deemed necessary at the time in order to adequately describe any stabilizing "H-$\pi$" interactions in the transition state structures that may have been important in deciding the endo-exo selectivity. While it was concluded that these interactions were not energetically significant and thus could not be a determining factor of selectivity, it was decided to continue using this basis set for the present study as well. Therefore, the data for the 3-substituted cyclopropene / butadiene reaction were updated to the B3LYP/6-31++G(d) level of theory to allow for comparison to the present 3,3-disubstituted cyclopropene / butadiene system.

# Exo Selectivity and the Effect of Disubstitution in the Diels-Alder Reactions of Butadiene with 3,3-Disubstituted Cyclopropenes **

**Abstract:** A density functional computational study was performed to accomplish two tasks: to examine the endo-exo selectivity in the Diels-Alder reactions of 3,3-disubstituted cyclopropenes with *s-cis*-butadiene, and to study the effect of disubstitution on the reactivity of the cyclopropene dienophile. Cyclopropene is substituted at C3 with $CH_3$, $SiH_3$, $NH_2$, $PH_2$, OH, SH, F, and Cl; both 3-substituted and 3,3-disubstituted ground states are examined to determine relative reactivities. The exo transition state structures are consistently lower in energy than the endo transition state structures for the 3,3-disubstituted cyclopropene / butadiene system, and surprisingly, both modes of addition have lower activation barriers than the syn 3-substituted cyclopropene / butadiene system. Through a series of isodesmic reactions, we have concluded that there is an additional stabilization in the transition state structures of the 3,3-disubstituted system that can account for the lowering of the activation barriers below that of the 3-substituted cases. This stabilization is a combination of the anomeric effect and the ring relaxation that occurs in the transition state structure.

** This chapter is a modified version of the publication: Gosse, T. L.; Poirier, R. A. *Can. J. Chem.* **2004**, *82*, 1589.

## 2.1. Introduction

It has been demonstrated both experimentally and theoretically that the majority of Diels-Alder (DA) cycloadditions show a preference for the formation of endo products (1, 2). This preponderance for endo selectivity has been shown in a variety of studies involving cyclopropene and its 3-substituted derivatives (3). There have been some specific instances of exo selectivity encountered for this family of cyclic dienophiles with various dienes (4), however this phenomenon is typically not seen and no explanation exists for the exo selectivity.

The endo preference of chemical systems has been explained mainly by the argument of favourable "secondary orbital interactions" (SOI) in the endo geometry, first suggested by Woodward and Hoffmann (5); these interactions are defined as the overlap of the frontier molecular orbitals at the non-reacting $\pi$ centers of the diene and dienophile at the transition state (TS). In the case of the cyclopropene and butadiene endo reaction, this interaction would occur between the syn hydrogen at C3 of cyclopropene and the $\pi$ system of butadiene. While SOI has been the most popular argument discussed in terms of explaining endo selectivity, there are an increasing number of studies providing evidence that lessens its significance. Xidos et al. (6) deduced that these "H-$\pi$" interactions were not energetically significant enough to be a deciding factor of endo-exo selectivity, and Salvatella et al. (7) also disputed the importance of SOI in DA reactions; both groups state that steric interaction arguments may be invoked to explain endo-exo selectivity. A recent paper by Ogawa and Fujimoto (8) employed numerical analysis in the examination of the endo TS of butadiene

and maleic anhydride; they deduced that SOI are much less significant than previously thought.

In recent literature, we have not encountered a theoretical examination of the 3,3-disubstituted cyclopropene and butadiene system, and this is the focus of the present study. An extensive analysis of the facial and endo-exo selectivity of the 3-substituted cyclopropene and butadiene addition reaction (6) suggested that the disubstituted system should show considerable preference for exo addition. Latypova and co-workers (9) examined the DA reactions of 3-methyl-3-cyanocyclopropene with a variety of dienes experimentally, and all cases were shown to be stereospecific with the cyano group in the syn position of the TS; exo selectivity was found for the furan-type dienes. Apeloig et al. (10) determined the stereoselectivity of three different cyclopropene derivatives (none of which were 3,3-disubstituted as in the present case) with a series of substituted dienes by using X-ray and NOE studies; one of the cyclopropene reactants, 1,2,3,3-tetrachlorocyclopropene, was shown to be exo selective when reacted with some 1-substituted-1,3-dienes. This group predicted at that time that 3,3-disubstituted cyclopropenes would yield exo selective products with open-chain dienes. Boger and Brotherton (11) studied the DA reactions of cyclopropenone ketals with electron-rich, electron-poor, and neutral dienes; nearly all of the reactions produced the exo cycloadduct only, and it was concluded that this exo preference was a result of steric factors in the endo TS structure.

Cyclopropene is the simplest cyclic dienophile, and its reactivity can be easily modified by substitution at the C3 position. The cycloaddition reaction of 3,3-disubstituted

cyclopropene to butadiene is an ideal system for studying reactivity and steric effects on the endo-exo selectivity. Herein we examine a series of these reactions, and where applicable, compare the results with those obtained for the previously studied 3-substituted cyclopropene / butadiene system (6).

## 2.2. Computational Methods

Ground state (GS) minima for cyclopropene and its derivatives, disubstituted at C3 by $CH_3$, $SiH_3$, $NH_2$, $PH_2$, OH, SH, F, and Cl, and *s-cis*-butadiene, as well as TS structures for the endo and exo DA cycloadditions were initially obtained using MUNgauss (12) at the HF/6-31++G(d) level of theory. All subsequent calculations were performed with Gaussian 98 (13). The GS and TS structures were further optimized using B3LYP/6-31++G(d). All probable rotational minima were determined for those 3,3-disubstituted cyclopropene GSs with conformational mobility; the GS cyclopropenes reported here refer to the rotational global minimum determined at B3LYP/6-31++G(d), unless otherwise noted. Likewise, all probable rotational minima for the endo and exo TSs with $CH_3$, $SiH_3$, $NH_2$, $PH_2$, OH, and SH, disubstituted at C3 of the dienophile, were obtained. In all cases, the *s-cis*-butadiene with a four-carbon torsion of 31.9° was used as the GS minimum for the diene. Frequency calculations confirmed that all GS minima had no imaginary frequencies and all TS structures had a single imaginary frequency.

All GS and TS structures for the previously studied 3-substituted cyclopropene / butadiene system (6) were updated to the B3LYP/6-31++G(d) level of theory to allow for

comparison to the present 3,3-disubstituted system.

## 2.3. Results and Discussion

### 2.3.1. Ground State Cyclopropenes

The stabilization of the various 3-substituted cyclopropene GSs was studied in a previous examination via an isodesmic reaction, which quantified the effect of substitution at C3 of cyclopropene relative to a similarly substituted methane derivative. These isodesmic energies showed a very good correlation with the electronegativity (14) of the substituent atom or group. The examined substituents, with the exception of $SiH_3$, showed a stabilization of the cyclopropene ring upon substitution and the degree of stabilization increased with increasing electronegativity. This suggested that the stabilization of cyclopropene is strongly influenced by the strength of σ withdrawal by the substituent.

A similar investigation was conducted in the present study for the 3,3-disubstituted cyclopropenes and the results then compared to those obtained for the updated 3-substituted cyclopropenes. Schemes 2.1 and 2.2 show the isodesmic reactions considered here and Table 2.1 includes the isodesmic stabilization energies ($\Delta E^{X}_{stab}$ and $\Delta E^{XX}_{stab}$) for both reactions.

Scheme 2.1


Scheme 2.2

Scheme 2.1 represents the effect (stabilization or destabilization) on the cyclopropene ring that results from the addition of one substituent (X) to C3 of cyclopropene relative to a similarly substituted methane. The X substituents of the methane derivatives all have a staggered conformation. Scheme 2.2 represents the stabilization / destabilization of 3-substituted cyclopropene resulting from the addition of the second X to C3 of 3-substituted cyclopropene relative to a similarly monosubstituted methane derivative.

**Table 2.1.** Energy data (kJ $mol^{-1}$) and GS bond lengths (Å) for 3-substituted and 3,3-disubstituted cyclopropenes at B3LYP/6-31++G(d). Isodesmic energy data for the 3,3-disubstitution of cyclopropane and the results of Scheme 2.5 are also included.

| substituent[a] | GS conformation | | group electronegativity[c] | isodesmic stabilization energies | | | |
|---|---|---|---|---|---|---|---|
| | 3-sub | 3,3-disub[b] | | $\Delta E^{X}_{stab}$ | $\Delta E^{XX}_{stab}$[d] (anom / ring) | $\Delta E_{anom}$[e] | $\Delta\Delta E_{ring}$[f] |
| $SiH_3$ | stag | 1C | 1.91 | 3.1 | 4.7 | -5.7 | 10.4 |
| $PH_2$ | stag | 2B | 2.17 | -10.8 | -5.7 | -4.3 | -1.4 |
| H | - | - | 2.20 | 0 | 0 | 0 | 0 |
| $CH_3$ | stag | 1A | 2.56 | -14.4 | -11.9 | -12.1 | 0.2 |
| SH | gauche | 3A | 2.63 | -23.8 | -14.1 | -10.1 | -4.0 |
| Cl | - | - | 3.05 | -39.5 | -4.0 | 4.3 | -8.3 |
| $NH_2$ | gauche | 2D | 3.10 | -34.2 | -44.8 | -34.2 | -10.6 |
| OH | stag | 3A | 3.64 | -48.5 | -57.7 | -69.5 | 11.8 |
| F | - | - | 4.00 | -57.5 | -43.1 | -39.1 | -4.0 |

**Table 2.1.**, cont.

| substituent[a] | 3-substituted cyclopropene | | 3,3-disubstituted cyclopropene | |
|---|---|---|---|---|
| | C1-C3 C2-C3 | C1=C2 | C1-C3 C2-C3 | C1=C2 |
| $SiH_3$ | 1.528 | 1.292 | 1.546 | 1.289 |
| $PH_2$ | 1.515 | 1.294 | 1.515, 1.518 | 1.295 |
| H | 1.511 | 1.296 | 1.511 | 1.296 |
| $CH_3$ | 1.511 | 1.299 | 1.513 | 1.300 |
| SH | 1.498, 1.494 | 1.298 | 1.488 | 1.301 |
| Cl | 1.471 | 1.306 | 1.456 | 1.310 |
| $NH_2$ | 1.508, 1.490 | 1.306 | 1.493 | 1.313 |
| OH | 1.486 | 1.311 | 1.468 | 1.312 |
| F | 1.466 | 1.309 | 1.445 | 1.321 |

[a] Substituents are placed in order of increasing electronegativity.

[b] Conformations for 3,3-disubstituted cyclopropenes as per Figures 2.1, 2.2, and 2.3.

[c] Group electronegativities as per ref. 14.

[d] Results from Scheme 2.2.

[e] Results from Scheme 2.4.

[f] Calculated as $\Delta E^{XX}_{stab}$ (anom / ring) - $\Delta E_{anom}$ (as per Scheme 2.5).

As depicted in Table 2.1, the addition of the first X to C3 of cyclopropene yields a stabilization of the cyclopropene ring for all substituents examined except $SiH_3$, which is only

slightly destabilized. These results are comparable to the previous energies obtained at the Hartree-Fock (HF) level. The value of $\Delta E^{X}_{stab}$ increases with the electronegativity of X, suggesting a gradual reduction in the reactivity of the dienophile with the increasing electronegativity of the 3-substituent. The energies from Scheme 2.2 indicate a further stabilization upon the addition of the second X to 3-substituted cyclopropene for all substituents examined with the exception of $SiH_3$, which is further destabilized upon substitution.

It is clear that the addition of X to unsubstituted cyclopropene and the addition of the second X to the 3-substituted cyclopropene are not equivalent. Generally, the greatest degree of stabilization (or destabilization) of the cyclopropene ring comes with the addition of the first X substituent. Upon addition of the second X to 3-substituted cyclopropene, we see that the most electronegative groups ($NH_2$, OH, and F) give significantly larger stabilization energies than the other substituents. This can be explained by the occurrence of the anomeric effect (15), which measures the extent to which two substituents bonded to the same $sp^3$-hybridized carbon interact with each other. For $NH_2$, OH, and F, this large stabilizing interaction results from the lone pair of one substituent donating electron density to the $\sigma^*$ system of the other, and vice versa. As a means of expressing this effect quantitatively for the most basic molecular system of disubstituted methane, we considered the isodesmic reaction shown in Scheme 2.3.

Scheme 2.3 $2CH_3X \longrightarrow CH_2X_2 + CH_4$

The result obtained at B3LYP/6-31++G(d) for X = OH ($\Delta E$ = -63.6 kJ $mol^{-1}$) clearly shows a significant anomeric stabilization. The two other electronegative substituents, $NH_2$ ($\Delta E$ = -31.9 kJ $mol^{-1}$) and F ($\Delta E$ = -46.6 kJ $mol^{-1}$) give similar results. The remaining substituents in this study exhibit significantly less stabilization upon disubstitution.

Another substituent worthy of note is Cl, which gives a slightly destabilizing anomeric effect (Scheme 2.3, calculated $\Delta E$ of $CH_2Cl_2$ = 4.9 kJ $mol^{-1}$). As can be seen in Table 2.1, the addition of the second Cl to C3 of 3-Cl-cyclopropene results in little stabilization ($\Delta E^{XX}_{stab}$ = -4.0 kJ $mol^{-1}$) compared to the addition of the first Cl to cyclopropene, which is very stabilizing. This indicates that the second Cl should have very little effect on the stability and reactivity of the dienophile as compared to 3-Cl-cyclopropene.

An examination of the 3,3-disubstituted cyclopropene GS geometries (Table 2.1) reveals trends similar to that of the 3-substituted cyclopropenes as the electronegativity of the substituents increase. Table 2.1 includes the C-C and C=C bonds of both types of dienophiles with the various substituents. The addition of increasingly electronegative substituents results in a longer, and thus more electron-deficient C=C bond, as well as generally shorter C-C bonds of the cyclopropene ring, in comparison to cyclopropene itself. In comparing the 3-substituted to the 3,3-disubstituted cyclopropenes for each substituent, we can see the effect of disubstitution on the molecular geometry. The C=C bonds are generally longer in the 3,3-disubstituted cyclopropenes, and the degree of elongation increases upon the disubstitution of stronger electron-withdrawing groups. An exception is $SiH_3$, which exhibits a further shortening of the C=C bond. This geometric trend supports

the energy data; the cyclopropenes with the longer, more electron-deficient C=C bonds are also the more stable structures. In addition, the C-C bonds get substantially shorter upon disubstitution of electron-withdrawing groups and generally longer for electron-donating groups. In relation to the unsubstituted cyclopropene, we see that 3,3-disubstitution has similar effects on the ring as 3-substitution. The nature of the substituent (electron-withdrawing or -donating) affects the geometries and stabilization energies in a similar way; however, the anomeric effect that results from 3,3-disubstitution can also contribute to the geometry changes in the ring as well as the stabilization energies.

### 2.3.2. Transition State Structures

Because the dienophile in the present DA reaction is disubstituted at the C3 position, we are removing the possibility of anti-syn selectivity and are thus dealing with endo-exo selectivity only. In reference 6, plots of activation energies of the four modes of addition (endo-syn, endo-anti, exo-syn, and exo-anti) of 3-substituted cyclopropene to butadiene versus electronegativity showed that the syn TSs are higher in energy than the anti TSs in all cases. However, in looking solely at the syn additions, we see that additions take place more favourably in the exo geometry than in the endo geometry. This suggested that if the DA reactions could occur via syn addition only, as would be the case with 3,3-disubstituted cyclopropene / butadiene, the exo geometry would be favoured.

**Table 2.2.** Conformations of substituents for endo and exo addition and $\Delta E_{endo\text{-}exo}$ (kJ mol$^{-1}$) for the TS structures of 3,3-disubstituted cyclopropene with butadiene.

| substituent | conformation | | $\Delta E_{endo\text{-}exo}$ |
|---|---|---|---|
| | endo addition | exo addition | |
| $SiH_3$ | 1B | 1C | 2.8 |
| $PH_2$ | 2B | 2B | 10.0 |
| $CH_3$ | 1A | 1A | 7.2 |
| SH | 3B | 3B | 13.0 |
| Cl | - | - | 12.0 |
| $NH_2$ | 2D | 2B | 12.4 |
| OH | 3A | 3A | 14.2 |
| F | - | - | 12.2 |

The TS structures of disubstituted $CH_3$-, $SiH_3$-, F-, and Cl-cyclopropenes with butadiene each have one endo and one exo structure that are first-order saddle points. In the case of the two halogens examined, we see 99.5% exo selectivity with $\Delta E_{endo\text{-}exo}$ = 12.2 and 12.0 kJ mol$^{-1}$ at B3LYP/6-31++G(d) for F and Cl, respectively (Table 2.2). The conformations of the $CH_3$ substituents in the TSs for endo and exo addition are the same (conformation **1A**, Figure 2.1). However, for the $SiH_3$ groups, we see a different conformation preferred for both the endo (staggered, **1B**) and the exo (skewed, **1C**) TS structures. In addition, the $\Delta E_{endo\text{-}exo}$ value for the 3,3-$SiH_3$-cyclopropene / butadiene case is small; the exo addition is favoured by a mere 2.8 kJ mol$^{-1}$ (77.4% exo). The $\Delta E_{endo\text{-}exo}$ when X = $CH_3$ is calculated to be 7.2 kJ mol$^{-1}$ (95.9% exo).

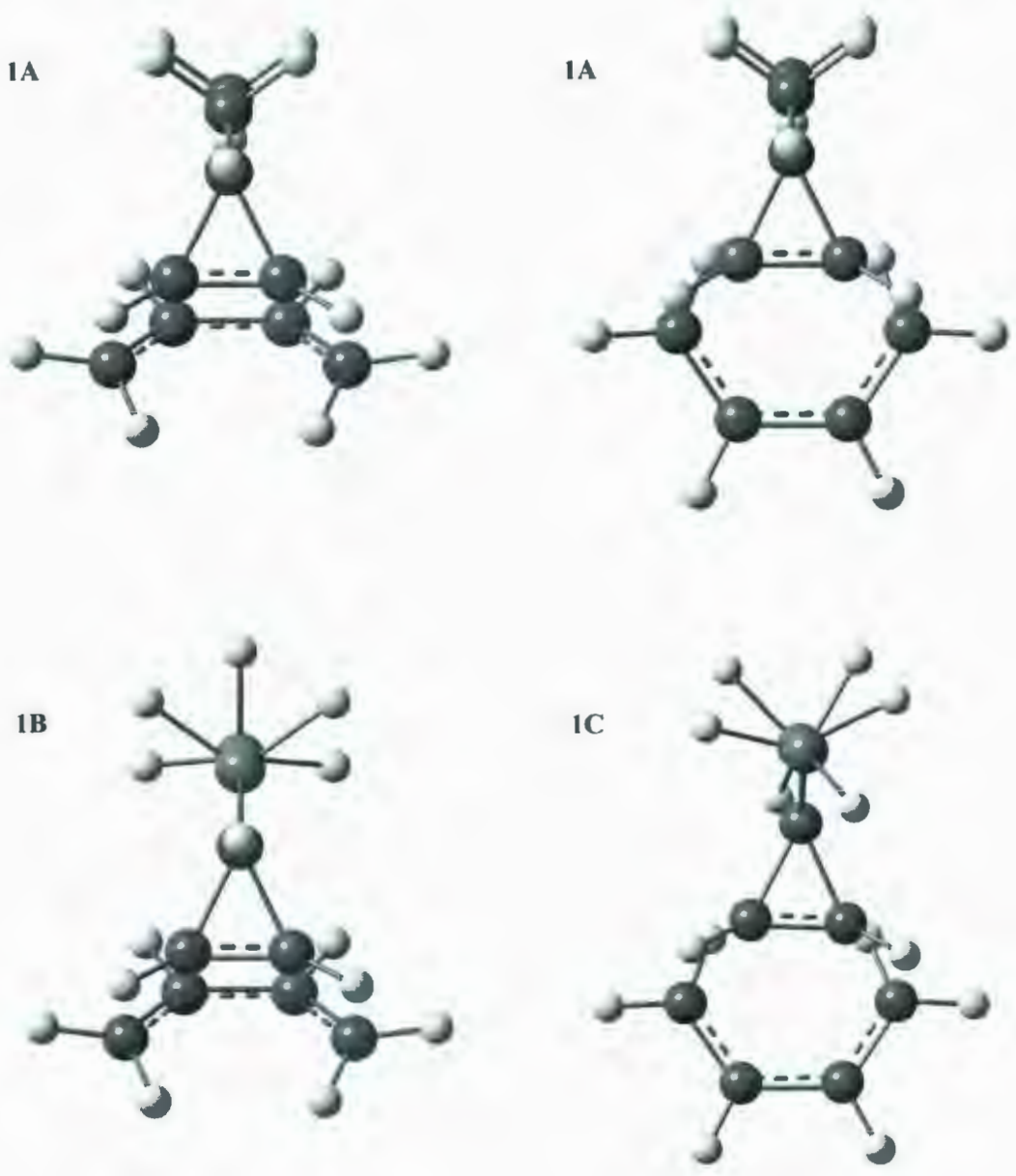


**Figure 2.1.** The TS structures for 3,3-$CH_3$-cyclopropene with butadiene, endo and exo addition (**1A**); 3,3-$SiH_3$-cyclopropene with butadiene, endo addition (**1B**); and 3,3-$SiH_3$-cyclopropene with butadiene, exo addition (**1C**).

The DA reactions of disubstituted $NH_2$-, $PH_2$-, OH-, and SH-cyclopropene with butadiene each have multiple first-order saddle points, owing to the rotational possibilities for these substituents. Figure 2.2 illustrates examples of the four possible conformations for 3,3-$NH_2$- and 3,3-$PH_2$-cyclopropene addition to butadiene, and Table 2.2 lists the lowest energy conformer for each mode. Conformations **2A**, **2B**, and **2D** were identified for 3,3-$NH_2$-cyclopropene / butadiene endo and exo addition; **2C** is a confirmed second-order saddle point for exo addition, but no such conformation was found for endo addition. For the 3,3-$PH_2$-cyclopropene / butadiene cases, conformations **2A**, **2B**, **2C**, and **2D** were found for both endo and exo addition. All, except for **2D** endo addition, which is second-order, are first-order saddle points. The exo geometries are favoured over the endo forms for each conformation. The lowest energy conformation for 3,3-$NH_2$-cyclopropene / butadiene endo addition is **2D**, unlike the other additions for $NH_2$ and $PH_2$, in which **2B** is the preferred conformer.

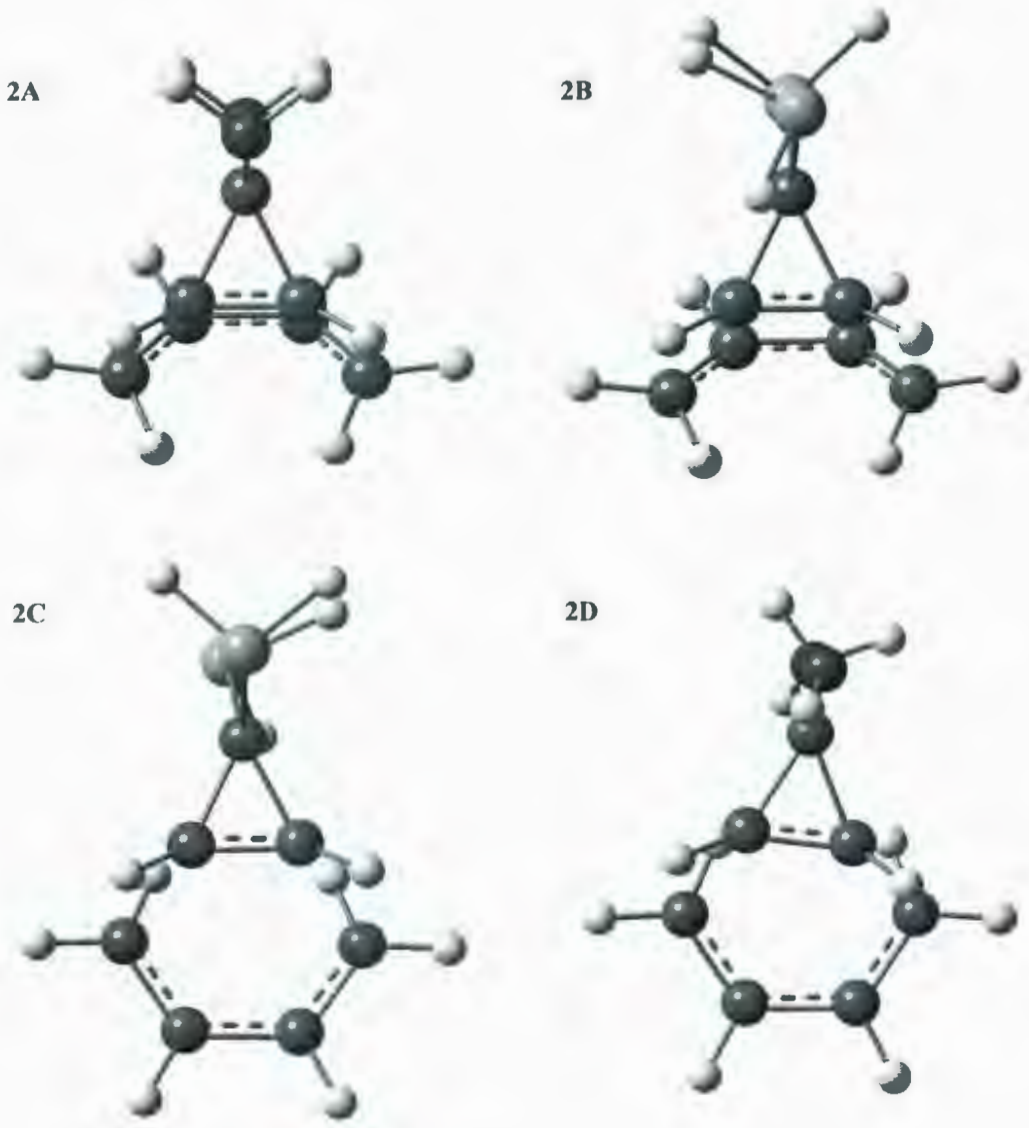


**Figure 2.2.** Examples of TS structures obtained for 3,3-$NH_2$(or $PH_2$)-cyclopropene with butadiene; $NH_2$ endo addition (**2A**), $PH_2$ endo addition (**2B**), $PH_2$ exo addition (**2C**), and $NH_2$ exo addition (**2D**).

For the OH and SH substituents, two different first-order conformations (**3A** and **3B**) were obtained for both endo and exo addition, as illustrated in Figure 2.3. The **3A** and **3B** exo TS structures for both OH and SH are favoured over their endo counterparts. Interestingly, the same conformation (**3A**) is preferred for both endo and exo addition for 3,3-OH-cyclopropene / butadiene, while the **3B** conformation has the lowest energy for both endo and exo addition for 3,3-SH-cyclopropene / butadiene. These reactions exhibit essentially 100% exo selectivity with $\Delta E_{endo\text{-}exo}$ = 14.2 and 13.0 kJ mol$^{-1}$ at B3LYP/6-31++G(d) for OH and SH, respectively (Table 2.2). In both conformers, the H of the syn substituent is pointing away from the π bond (in endo addition) and away from the H's of C1 and C4 of butadiene (in exo addition). The OH and SH substituents in both of their **3A** and **3B** conformations are positioned so as to minimize steric interactions with one another.

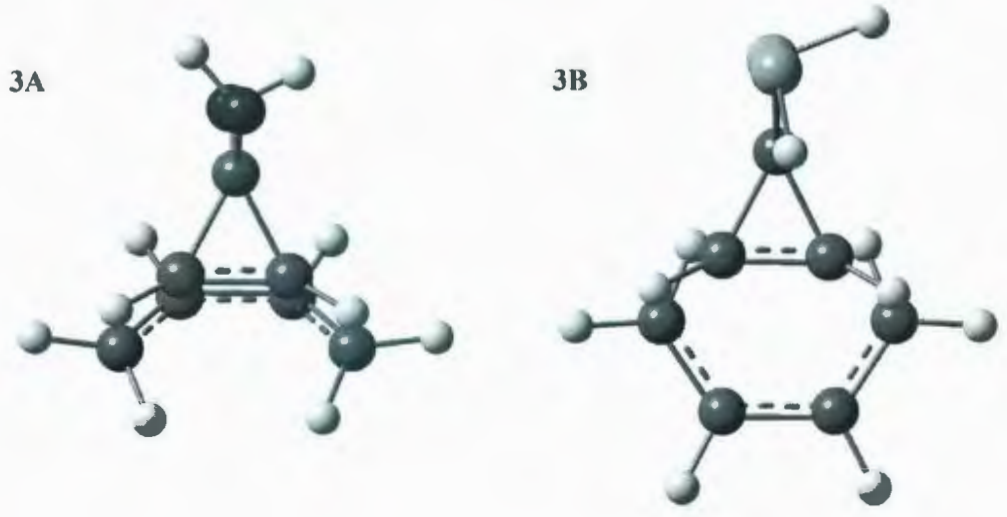


**Figure 2.3.** Examples of TS structures obtained for 3,3-OH(or SH)-cyclopropene with butadiene; OH endo addition (**3A**) and SH exo addition (**3B**).

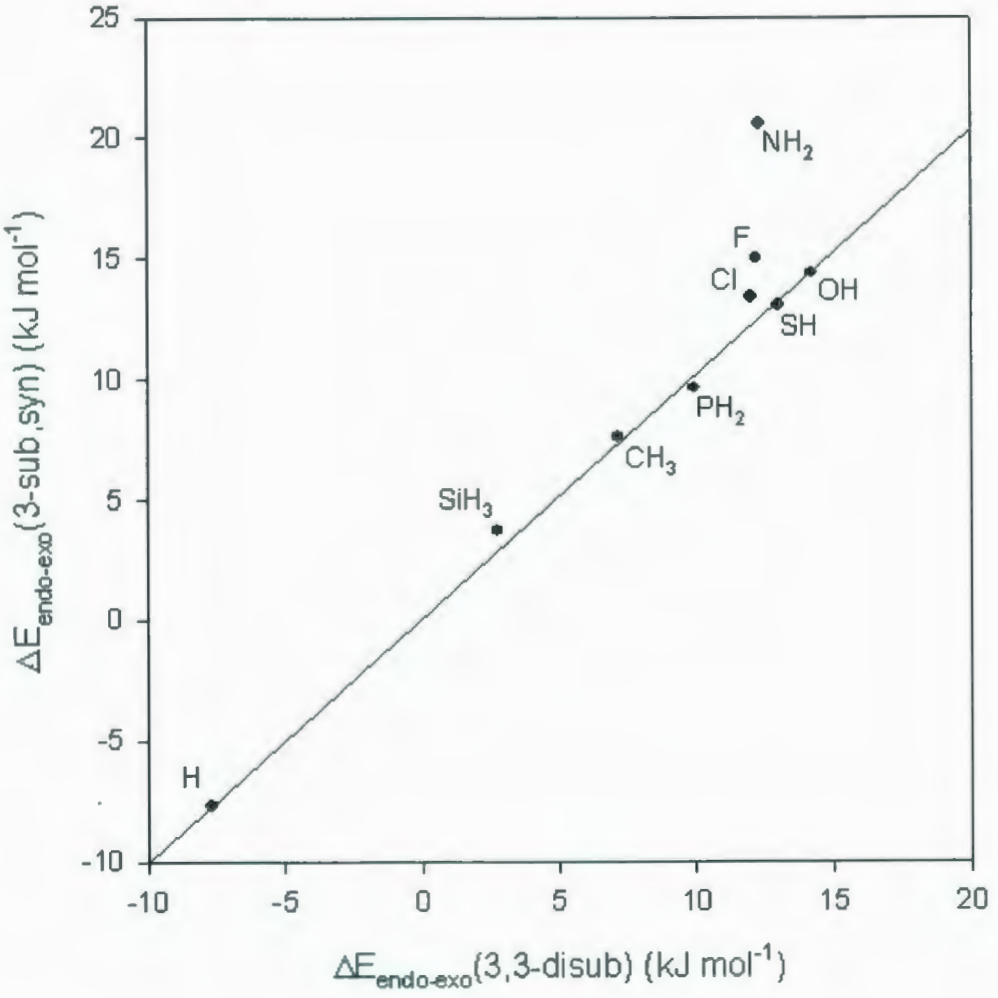


**Figure 2.4.** A plot of $\Delta E_{endo\text{-}exo}$(3-substituted, syn, kJ mol$^{-1}$) versus $\Delta E_{endo\text{-}exo}$(3,3-disubstituted, kJ mol$^{-1}$) at B3LYP/6-31++G(d).

The 3-substituted cyclopropene / butadiene syn TSs from reference 6 were optimized at B3LYP/6-31++G(d) in order to investigate the effects of disubstitution on energies and

structures. Figure 2.4 is a plot of $\Delta E_{endo\text{-}exo}$ of 3-substituted cyclopropene (syn) / butadiene versus $\Delta E_{endo\text{-}exo}$ of 3,3-disubstituted cyclopropene / butadiene, illustrating the effect on the selectivity of adding the second substituent to the anti position of the monosubstituted syn TS. The negative values of $\Delta E$ for cyclopropene are a result of the endo preference in the cyclopropene / butadiene parent system.

**Table 2.3.** A comparison of the calculated endo-exo selectivities of 3-substituted cyclopropene with butadiene (syn, endo and exo addition) and 3,3-disubstituted cyclopropene with butadiene (endo and exo addition). All $(\Delta)\Delta E$'s are in kJ $mol^{-1}$.

| substituent | $\Delta\Delta E^a$ | 3-substituted cyclopropene | | 3,3-disubstituted cyclopropene | |
|---|---|---|---|---|---|
| | | conf change of X from GS to TS / mode of addition | GS $\Delta E_{conf}$ | conf change of X from GS to TS / mode of addition | GS $\Delta E_{conf}$ |
| $SiH_3$ | 0.9 | Yes / endo | 2.6 | Yes / endo | 1.1 |
| $PH_2$ | -0.4 | No | 0 | No | 0 |
| H | 0.0 | No | 0 | No | 0 |
| $CH_3$ | 0.4 | No | 0 | No | 0 |
| SH | 0.0 | No | 0 | Yes / endo, exo | 1.4 |
| Cl | 1.4 | No | 0 | No | 0 |
| $NH_2$ | 8.2 | Yes / exo | 2.2 | Yes / exo | 8.9 |
| OH | 0.2 | Yes / exo | 1.9 | No | 0 |
| F | 2.8 | No | 0 | No | 0 |

[a] Calculated as $\Delta E_{endo\text{-}exo}$(3-substituted, syn) - $\Delta E_{endo\text{-}exo}$(3,3-disubstituted).

As indicated in Table 2.3, most of the differences in $\Delta E_{endo\text{-}exo}$ between the 3-substituted and 3,3-disubstituted cases ($\Delta\Delta E$) are essentially zero. Since the addition of the substituent to the anti position of the syn TS has very little effect on the endo-exo selectivity in general, it may be deduced that the change in the nature of the dienophile (from monosubstituted to disubstituted) does not play as important a role when the steric interactions in the TS are very similar, as is the case here. These similar steric interactions (syn substituent positioned over the diene) translate into very similar selectivities. In addition, it can be stated that, for this system, if there is a substituent *other than H* at the syn position of the TS structure, exo selectivity will prevail regardless of the electron-withdrawing or electron-donating tendency of the substituent.

In Figure 2.4, a substituent worthy of note is $NH_2$ ($\Delta\Delta E$ = 8.2 kJ $mol^{-1}$). An examination of the GS and TS structures revealed that for both the 3-substituted and 3,3-disubstituted $NH_2$ cyclopropene dienophiles, there is a change in conformation of the $NH_2$ substituent(s) from the GS to the *exo* TS structure. The $NH_2$ group of 3-$NH_2$-cyclopropene changes from the preferred gauche conformation in the GS to a staggered conformation in the exo-syn TS structure, with the nitrogen lone pair pointing down toward the C1 and C4 H's of butadiene. Based on computed GS energies, the energy cost of this conformational change ($\Delta E_{conf}$, Table 2.3) is 2.2 kJ $mol^{-1}$. Likewise, we see a change in conformation for the 3,3-$NH_2$-cyclopropene from the **2D** conformation in the GS to **2B** in the exo TS structure. This involves a rotation of the $NH_2$ group syn to the butadiene, which becomes staggered in the exo TS, much like the $NH_2$ group of 3-$NH_2$-cyclopropene in its exo-syn TS structure.

However, we see that there is no conformational change of the anti $NH_2$ substituent from the GS to the exo TS, and it is likely that this introduces steric interactions between the two $NH_2$ groups. The $\Delta E_{conf}$ for the GS 3,3-$NH_2$-cyclopropene is 8.9 kJ $mol^{-1}$; thus the estimated energy cost for the change in conformation for the 3,3-$NH_2$-cyclopropene system is about 6.7 kJ $mol^{-1}$ greater than for the 3-substituted case, which compares favourably with the $\Delta\Delta E$ of 8.2 kJ $mol^{-1}$ for $NH_2$. It is concluded that while the presence of the second substituent at the anti position generally has very little effect on the endo-exo selectivity (Figure 2.4), a *change in conformation* of one or more substituents in the TS can have a significant effect on the selectivity if the conformational change introduces unfavourable steric interactions. In this case, the activation energy required for the exo addition of 3,3-$NH_2$-cyclopropene to butadiene increases due to the energy cost of conformational change, resulting in a smaller $\Delta E_{endo\text{-}exo}$.

### 2.3.3. The Effect of Disubstitution on Activation Energy

Figure 2.5 depicts the plots of activation energies ($\Delta E_{act}$) of the endo and exo modes of addition versus electronegativity for the 3-substituted (syn) and 3,3-disubstituted cyclopropene with butadiene reactions. For both endo and exo addition, the 3,3-disubstituted system has activation energies that are consistently *lower* than those of the 3-substituted system for all substituents examined, with the single exception of $NH_2$ exo addition, where the 3-$NH_2$-cyclopropene / butadiene $\Delta E_{act}$ is lower than that of the 3,3-disubstituted analog ($\Delta\Delta E_{act}$ is approximately 0.5 kJ $mol^{-1}$).

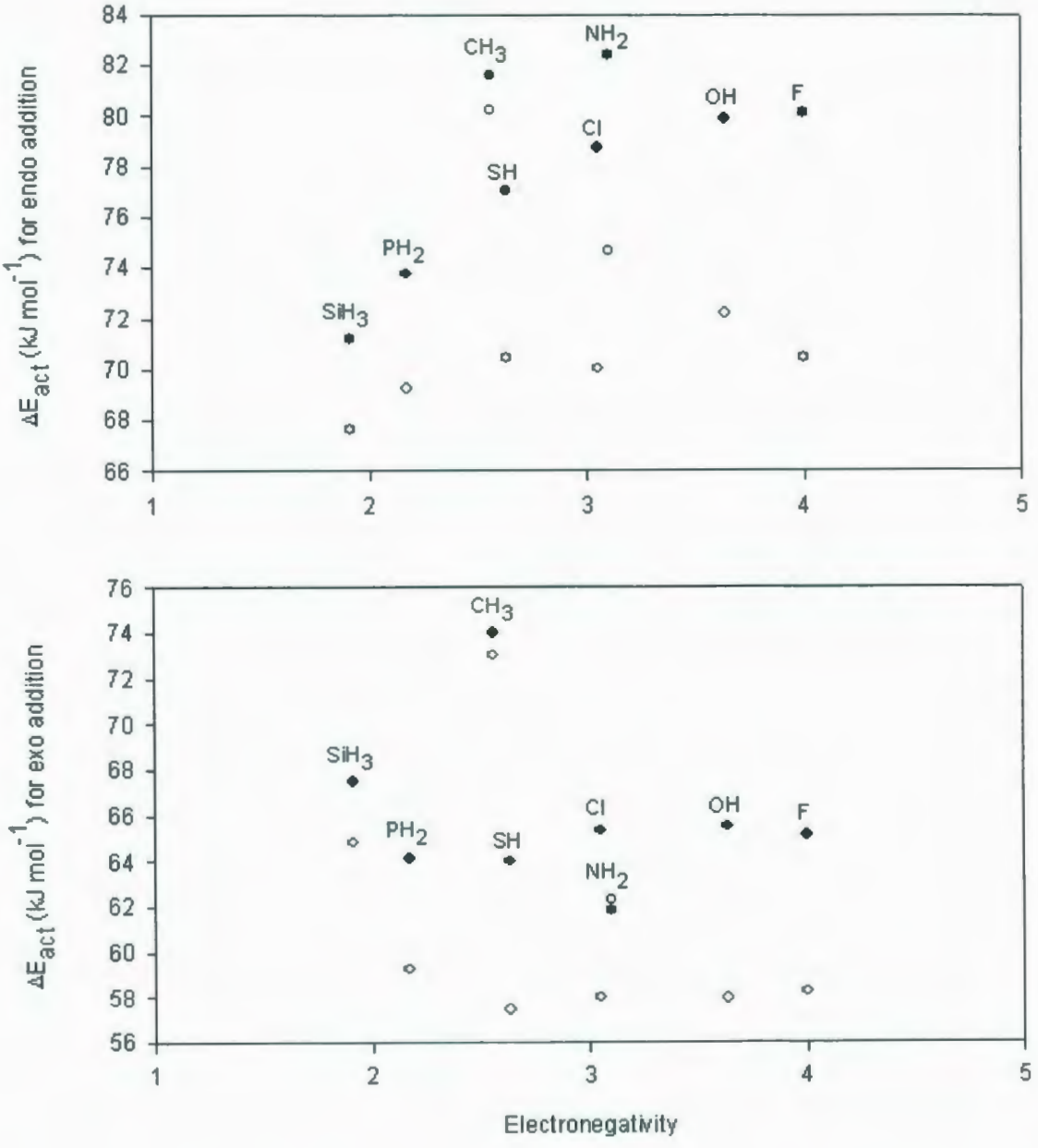


**Figure 2.5.** Plots of $\Delta E_{act}$ for endo (top) and exo (bottom) addition (kJ mol$^{-1}$) versus the electronegativity of the substituent at the B3LYP/6-31++G(d) level of theory. For each plot, $\Delta E_{act}$ for the 3-substituted cyclopropene / butadiene syn additions are represented by (●), and $\Delta E_{act}$ for the 3,3-disubstituted cyclopropene / butadiene additions are represented by (○).

It has been previously established that the 3,3-disubstitution of the cyclopropene GS yields an additional stabilization of the ring and therefore should be less reactive. From this, one would predict an increase in $\Delta E_{act}$ for the 3,3-disubstituted system above that for the 3-substituted case. However, we see that the opposite is true. This implies that there is a significant stabilization component in the TS structure of 3,3-disubstituted cyclopropene / butadiene that enables an overall decrease in the activation barrier for the reaction. In Scheme 2.2, the addition of the second X to the 3-substituted cyclopropene dienophile results in a total stabilization / destabilization that is composed of two effects: the anomeric effect and the overall effect on the cyclopropene ring itself (represented in Table 2.1 as $\Delta E^{XX}_{stab}$ (anom / ring)). Scheme 2.4 illustrates a similar isodesmic reaction using cyclopropane.

Scheme 2.4


The 3-substituted and 3,3-disubstituted cyclopropanes have the same substituent conformations as the corresponding substituted cyclopropenes, with the exception of $SiH_3$; the 3,3-$SiH_3$-cyclopropene has a skewed conformation whereas the 3,3-$SiH_3$-cyclopropane has the substituents in an eclipsed conformation. The cyclopropane isodesmic reaction in Scheme 2.4 (cyclopropane closely resembling the molecule of interest, cyclopropene) is a measure of the anomeric effect only ($\Delta E_{anom}$). Assuming that the anomeric effect is energetically similar in both 3,3-disubstituted cyclopropene and cyclopropane for the same

substituent, the energy difference between these two isodesmic reactions represents the degree to which the ring is affected upon disubstitution (Scheme 2.5), represented as $\Delta\Delta E_{ring}$.

Scheme 2.5


Table 2.1 contains the GS cyclopropene and cyclopropane energy data. The $\Delta E_{anom}$ of Scheme 2.4 compares favourably with the calculated values of the anomeric effect in a system of similarly substituted methanes and thus has no effect on the ring itself. The anomeric effect is stabilizing for all substituents except Cl, which is slightly destabilizing. The values for $\Delta\Delta E_{ring}$ are intended to show the degree of stabilization / destabilization that occurs due to the changes in the ring upon 3,3-disubstitution; these values are supported by noting the *actual* geometric changes that occur in the dienophile upon substitution. Many of the substituents yield small negative values for $\Delta\Delta E_{ring}$ and these correlate well with the degree of elongation that occurs in the C=C bond of the GS cyclopropene upon addition of the second substituent (Table 2.1). The $CH_3$ substituent has almost zero $\Delta\Delta E_{ring}$ and likewise exhibits virtually no change in C=C bond length; on the other hand, the $SiH_3$ group is significantly destabilizing ($\Delta\Delta E_{ring}$ = 10.4 kJ $mol^{-1}$) and thus shows a shortening of the C=C bond. The actual amount of ring stabilization / destabilization, given by $\Delta\Delta E_{ring}$, that results from the 3,3-disubstitution of cyclopropene is substantially less than the stabilization / destabilization observed for the first substitution represented in Scheme 2.1. In other words,

the 3-substituted cyclopropenes exhibit a large stabilization (destabilization for $SiH_3$) as compared to cyclopropene itself; this is evident in both the stabilization energies as well as the geometry changes that occur in the ring (Table 2.1). While the 3,3-disubstituted cyclopropenes show greater stabilities overall (again, greater destabilization for $SiH_3$) as compared to the 3-substituted analogs, the majority of this stability is a consequence of the anomeric effect, not the ring stabilization / destabilization. In some cases, the ring effect upon 3,3-disubstitution is actually destabilizing ($\Delta\Delta E_{ring}$ is positive for $SiH_3$, $CH_3$, and OH).

The question to address now is: what produces the drop in activation energy for the 3,3-disubstituted system below that of the 3-substituted case? It is assumed that the anomeric effect is the same in the GS and TS structures of the 3,3-disubstituted system and therefore remains constant during the DA reaction. As the cyclopropene ring becomes more like cyclopropane during the reaction process, there must be a substantial relief of ring strain in the 3,3-disubstituted cyclopropene / butadiene TS structures. Therefore, the remaining stabilization (after accounting for the anomeric effect) is mostly due to the relaxation of the ring. This further stabilization of the cyclopropene ring produces a drop in the TS energy and an overall lowering of the energy barrier.

As an example and because it deserves comment, the OH substituent has a $\Delta\Delta E_{ring}$ that is destabilizing ($\Delta\Delta E_{ring}$ = 11.8 kJ $mol^{-1}$). Disubstitution with OH has a huge stabilizing anomeric effect (Table 2.1, $\Delta E_{anom}$), and although there is the expected shortening of the C-C bonds of 3,3-OH-cyclopropene upon disubstitution, there is no change in the C=C bond length. Normally, the C=C bond would lengthen in order to relieve bond-bond repulsion that

derives from the increased electron density in the C-C bonds. As a consequence, the 3,3-OH-cyclopropene is destabilized by a high degree of ring strain, which is relieved in the TS structure and corresponds to a large drop in activation energy.

## 2.4. Conclusions

For the DA reactions of 3,3-disubstituted cyclopropene with butadiene, we have shown:

- the important role the second substituent plays in the stability and reactivity of the cyclopropene dienophile. The anomeric effect produces an increased stability upon disubstitution, the consequence of which can be seen in the geometry of the ring.
- the preference for exo addition for all substituents examined.
- the correlation between the endo-exo selectivities of the syn 3-substituted cyclopropene / butadiene system and the 3,3-disubstituted cyclopropene / butadiene system. Conformational changes during the reaction can explain the deviation of the $NH_2$ substituent. It is concluded that for this system, the presence of a substituent *other than H* at the syn position of the TS structure will result in exo selectivity, regardless of the electron-withdrawing or electron-donating nature of the substituent.
- the decrease in the activation barriers of the 3,3-disubstituted cyclopropene / butadiene reactions below those of the syn 3-substituted cyclopropene / butadiene reactions, despite the expectant lower reactivity of the disubstituted dienophiles. Isodesmic reactions using GS cyclopropenes and cyclopropanes indicate that the

anomeric effect accounts for the majority of the stabilization in the 3,3-disubstituted cyclopropenes, and only a small portion can be attributed to ring stabilization / destabilization.

In summary, the effect of 3-substitution of an electron-withdrawing or electron-donating group on cyclopropene can be rationalized based on simple arguments; however, 3,3-disubstitution complicates matters considerably when investigating reactivity in the DA reaction, and at times energies and geometry changes need to be examined on a case-by-case basis.

**Acknowledgments**

We thank the Natural Sciences and Engineering Research Council of Canada for financial support as well as the Memorial University of Newfoundland Advanced Computation and Visualization Centre for computing resources.

**References**

(1) Alder, K.; Stein, G. *Angew. Chem.* **1937**, *50*, 510.

(2) Some recent examples: (a) Avalos, M.; Babiano, R.; Bravo, J. L.; Cintas, P.; Jiménez, J. L.; Palacios, J. C.; Silva, M. A. *J. Org. Chem.* **2000**, *65*, 6613. (b) Ruano, J. L. G.; Alemparte, C.; Castro, A. M. M.; Adams, H.; Ramos, J. H. R. *J. Org. Chem.* **2000**, *65*, 7938. (c) Kong, S.; Evanseck, J. D. *J. Am. Chem. Soc.* **2000**, *122*, 10418. (d) Ge, M.; Stoltz, B. M.; Corey, E. J. *Org. Lett.* **2000**, *2*, 1927. (e) Leach, A. G.;

Houk, K. N. *J. Org. Chem.* **2001**, *66*, 5192. (f) Arrieta, A.; Cossío, F. P. *J. Org. Chem.* **2001**, *66*, 6178. (g) Caramella, P.; Quadrelli, P.; Toma, L. *J. Am. Chem. Soc.* **2002**, *124*, 1130. (h) Quadrelli, P.; Romano, S.; Toma, L.; Caramella, P. *J. Org. Chem.* **2003**, *68*, 6035.

(3) (a) Wiberg, K. B.; Bartley, W. J. *J. Am. Chem. Soc.* **1960**, *82*, 6375. (b) Baldwin, J. E.; Reddy, V. P. *J. Org. Chem.* **1989**, *54*, 5264. (c) Apeloig, Y.; Matzner, E. *J. Am. Chem. Soc.* **1995**, *117*, 5375. (d) Jursic, B. S. *J. Org. Chem.* **1997**, *62*, 3046. (e) Sodupe, M.; Rios, R.; Branchadell, V.; Nicholas, T.; Oliva, A.; Dannenberg, J. J. *J. Am. Chem. Soc.* **1997**, *119*, 4232. (f) Jursic, B. S. *J. Mol. Struct.* **1998**, *454*, 117. (g) Imade, M.; Hirao, H.; Omoto, K.; Fujimoto, H. *J. Org. Chem.* **1999**, *64*, 6697.

(4) (a) Breslow, R.; Oda, M. *J. Am. Chem. Soc.* **1972**, *94*, 4787. (b) Binger, P.; Wedemann, P.; Goddard, R.; Brinker, U. H. *J. Org. Chem.* **1996**, *61*, 6462. (c) Jursic, B. S. *Tetrahedron Lett.* **1997**, *38*, 1305.

(5) Hoffmann, R.; Woodward, R. B. *J. Am. Chem. Soc.* **1965**, *87*, 4388.

(6) Xidos, J. D.; Gosse, T. L.; Burke, E. D.; Poirier, R. A.; Burnell, D. J. *J. Am. Chem. Soc.* **2001**, *123*, 5482.

(7) García, J. I.; Mayoral, J. A.; Salvatella, L. *Acc. Chem. Res.* **2000**, *33*, 658.

(8) Ogawa, A.; Fujimoto, H. *Tetrahedron Lett.* **2002**, *43*, 2055.

(9) Latypova, M. M.; Plemenkov, V. V.; Kalinina, V. N.; Bolesov, I. G. *Zh. Org. Khim.* **1984**, *20*, 542.

(10) Apeloig, Y.; Arad, D.; Kapon, M.; Wallerstein, M. *Tetrahedron Lett.* **1987**, *28*, 5917.

(11) Boger, D. L.; Brotherton, C. E. *Tetrahedron* **1986**, *42*, 2777.

(12) Poirier, R. A. *MUNgauss* (Fortran 90 version); Chemistry Department, Memorial University of Newfoundland, St. John's, Canada. With contributions from: Brooker, M. K.; Bungay, S. D.; El-Sherbiny, A.; Gosse, T. L.; Keefe, D.; Pye, C. C.; Reid, D.; Shaw, M.; Wang, Y.; Xidos, J. D.

(13) Frisch, M. J.; Trucks, G. W.; Schlegel, H. B.; Scuseria, G. E.; Robb, M. A.; Cheeseman, J. R.; Zakrzewski, V. G.; Montgomery, Jr., J. A.; Stratmann, R. E.; Burant, J. C.; Dapprich, S.; Millam, J. M.; Daniels, A. D.; Kudin, K. N.; Strain, M. C.; Farkas, O.; Tomasi, J.; Barone, V.; Cossi, M.; Cammi, R.; Mennucci, B.; Pomelli, C.; Adamo, C.; Clifford, S.; Ochterski, J.; Petersson, G. A.; Ayala, P. Y.; Cui, Q.; Morokuma, K.; Rega, N.; Salvador, P.; Dannenberg, J. J.; Malick, D. K.; Rabuck, A. D.; Raghavachari, K.; Foresman, J. B.; Cioslowski, J.; Ortiz, J. V.; Baboul, A. G.; Stefanov, B. B.; Liu, G.; Liashenko, A.; Piskorz, P.; Komaromi, I.; Gomperts, R.; Martin, R. L.; Fox, D. J.; Keith, T.; Al-Laham, M. A.; Peng, C. Y.; Nanayakkara, A.; Challacombe, M.; Gill, P. M. W.; Johnson, B.; Chen, W.; Wong, M. W.; Andres, J. L.; Gonzalez, C.; Head-Gordon, M.; Replogle, E. S.; Pople, J. A. *Gaussian 98*, revision A.11.3; Gaussian, Inc.: Pittsburgh, PA, 2002.

(14) Boyd, R. J.; Edgecombe, K. E. *J. Am. Chem. Soc.* **1988**, *110*, 4182.

(15) Hehre, W. J.; Radom, L.; Schleyer, P. v.R.; Pople, J. A. *Ab Initio Molecular Orbital Theory*; Wiley-Interscience: New York, 1986.

# Chapter 3

## Disubstituted Cyclopentenes and their Diels-Alder Reactions with Butadiene and Cyclopentadiene : A Study of Reactivity and Endo-Exo Selectivity

### Background and Preamble

To this point, our computational investigations have focused on exploring the effect of substituents on GS reactivities of dienophiles and their corresponding DA endo-exo selectivities. From our research into the DA reactions of 3-substituted cyclopropene with butadiene, we learned that the reactivity of the dienophile could be altered significantly by modifying the X substituent at the C3 position. A variation in GS reactivity was evident in the isodesmic stabilization energies ($\Delta E_{isodesmic}$), which showed an increase in the stability of the cyclopropene dienophile with increasingly electronegative 3-substituents. The substituent effect was also seen in the GS geometries.

Armed with this knowledge, we anticipated that the reactivity of cyclopropene would be affected in a similar, yet enhanced, manner upon disubstitution. That is, the GSs that were stabilized by 3-substitution would be even more stable, and hence less reactive, when disubstituted at C3. While this was indeed the case, the magnitude of stabilization / destabilization that resulted from adding the second X to 3-substituted cyclopropene ($\Delta E^{XX}_{stab}$) did not directly correlate with the electronegativity of the substituent. In addition,

it was seen that the change in stability of the dienophiles upon disubstitution was not reflected in the C=C bond lengths by any appreciable amount. Hence, the addition of the second X appeared to have very little effect on the reactivity of the dienophile in terms of strength of the C=C bond (the "reaction center"). It was concluded that the stabilization (energetically) that we see in the 3,3-disubstituted GSs can be mainly attributed to the anomeric effect, an effect that can stabilize both the GS and TS structures.

In the study that follows, the objective was to investigate the short-range and long-range effects of disubstitution on the reactivity of dienophiles. We selected cyclopentene as the dienophile, which can be disubstituted at the reaction center (positions C1 and C2) and remotely at C4. Disubstitution at these particular sites on the dienophile, as well as the choice of the substituents themselves (C≡CH, $CH_3$, Cl, C≡N, and F), allow for $C_s$ symmetry to be maintained in all GS and TS structures. We investigated both the stabilization / destabilization effects of disubstitution on the cyclopentene dienophile as well as the overall observed reactivity of the DA cycloaddition that the dienophile is involved in. We also expanded our scope by studying the DA reactions of the cyclopentene dienophiles with two different dienes: butadiene and cyclopentadiene. The large assortment of TS structures that resulted from the possible combinations of diene / dienophile permitted an in-depth analysis of endo-exo selectivity and the factors that influence it.

# Disubstituted Cyclopentenes and their Diels-Alder Reactions with Butadiene and Cyclopentadiene : A Study of Reactivity and Endo-Exo Selectivity

**Abstract:** Ground state stabilization energies and endo-exo selectivities are investigated for the Diels-Alder reactions of disubstituted cyclopentenes with *s-cis*-butadiene and cyclopentadiene using the B3LYP/6-31G(d) level of theory. For the purposes of examining both short-range and long-range substituent effects on the dienophile's reactivity, cyclopentene is disubstituted at C1/C2 (1,2-disubstitution, short-range) and C4 (4,4-disubstitution, long-range). It was determined that the remote disubstitution at C4 has a negligible effect on the stabilities of the dienophiles, whereas disubstitution directly at the reaction center (C1/C2) has a much larger impact on the strength of the π bond. Using both energy and geometric data from optimized transition state structures, the calculated endo-exo selectivities, deformation energies, and interaction energies we report are rationalized by identifying important favourable / unfavourable interactions in specific regions of the transition state structures.

## 3.1. Introduction

Chemists often think of reactivity as an important property that is exclusive to ground state (GS) reactants. However, the overall, observed reactivity of the reaction (represented by the activation energy barrier, $\Delta E_{act}$) and the transition state (TS) structure must also be considered (1). As the reactants approach each other during the initial stages of the reaction, the attractive and repulsive interactions that occur between them ultimately balance and the structural form of the TS is determined. The Diels-Alder (DA) reaction is kinetically controlled; this places the TS structure at the center of any discussion of reactivity and selectivity.

The rate at which the DA cycloaddition proceeds depends in part on the relative electron-rich or electron-deficient properties of the reactants. A long and weak $\pi$ bond in a dienophile is usually due to the presence of an electron-withdrawing substituent nearby displacing electron density away from the reaction center. This type of dienophile reacts rapidly with an electron-rich diene in a normal electron demand fashion. The ideal DA partner for a dienophile with a shorter, stronger, more electron-rich $\pi$ bond is an electron-deficient diene (an inverse electron demand DA reaction).

It is clear that substitution can greatly affect the reaction centers of a diene or dienophile by electronically "activating" or "deactivating" the $\pi$ bonds. We view these effects as *stabilization* of the diene / dienophile if the substitution results in a "less reactive" GS structure and *destabilization* if the GS structure becomes less stable, and presumably "more reactive", upon substitution. Dienophiles such as derivatives of ethene (2),

cyclopropene (3), and cyclopentene (4) will have varying degrees of stabilization / destabilization, depending on the number, type, and positions of substituents. While the stabilizing effect of substitution can be difficult to quantify, it is a worthwhile pursuit. The stabilization / destabilization energies of dienes or dienophiles can be compared to gain insight into the reactivities of these structures. Destabilized reactants may react more quickly and easily in a DA cycloaddition, whereas reactants stabilized by substitution may have lower reactivities. The present study will focus on the stabilization energies of disubstituted cyclopentene dienophiles.

The interaction of the reactants is one of the most important determinants of endo-exo selectivity. While the stabilization energy is a property of the GS reactant only, the overall reactivity, or the activation barrier of the reaction, $\Delta E_{act}$, depends on what the particular diene or dienophile is reacting *with*. For this reason, the endo-exo selectivity comes into consideration only when the reactants "see" each other.

Secondary orbital interactions (SOI) (5, 6) continue to be a popular rationalization for the preponderance of endo selectivity in DA cycloadditions. SOI occurs due to a favourable overlap between in-phase p-orbitals of the diene and dienophile that do not participate in the formation of the new σ bonds in the cycloadduct. Such interactions are possible only in the endo TS structure; as such, SOI cannot account for instances of exo selectivity in some DA reactions (7). In addition, SOI may not be a valid justification for endo selectivity seen with cyclopentene dienophiles, as it has been proposed that no secondary orbital stabilization is possible with these dienophiles (4(c)).

In the effort to address the endo-exo selectivity issue, most theories concentrate on the endo TS structure and the region in which the reactants are in closest contact. The other "end" of the TS structure has been largely ignored. In the current study, we consider both areas of the TS structure in our discussion of the interactions between the GS reactants. We have defined the "endo region" and "exo region" as depicted in Figure 3.1. Here, "endo" and "exo" is in reference to the diene; that is, the exo region of a cyclopentadiene TS will refer to the end of the diene that includes the methylene group, regardless of the position of the dienophile.

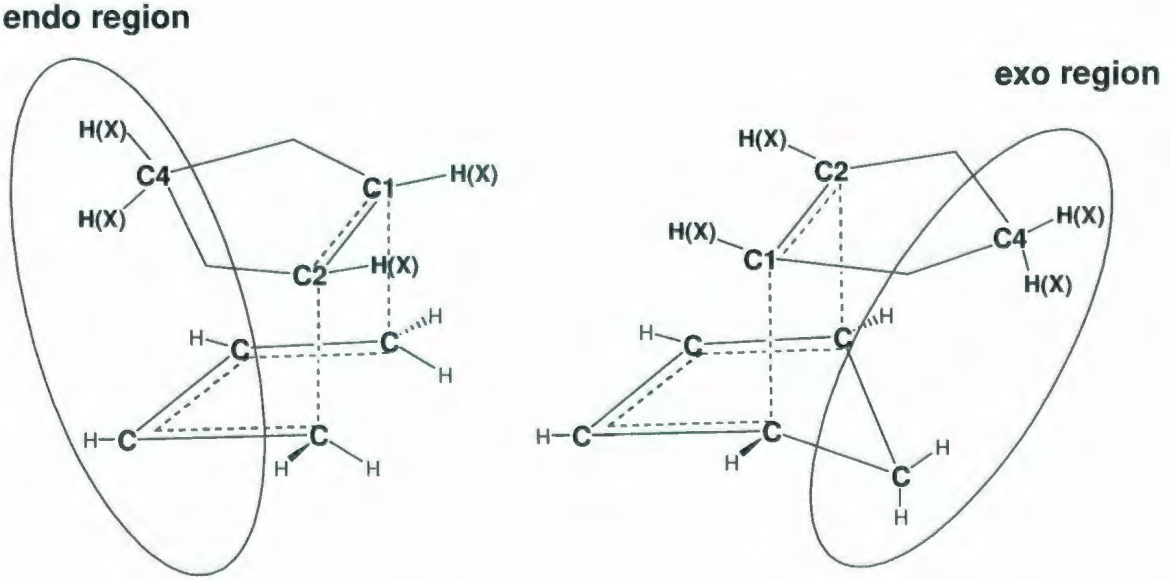


**Figure 3.1.** The "endo region" and "exo region" of the DA TS structure, used to describe important interactions between the GS reactants. The examples show an endo and exo TS with 4,4- or 1,2-disubstituted cyclopentene with either butadiene or cyclopentadiene. Some H's are omitted for clarity.

We present a system in which the endo-exo selectivity differs upon changing the diene and by modifying the dienophile by disubstitution. We will investigate reactivities, both the stabilization / destabilization of the GS dienophiles upon disubstitution, as well as the activation barriers for the various reactions. We will consider the endo-exo selectivities of a selection of disubstituted cyclopentenes in DA cycloadditions with *s-cis*-butadiene (hereafter referred to simply as butadiene) and cyclopentadiene. Substituent effects are introduced by disubstitution at two different locations on the cyclopentene ring; remotely at C4 and locally on the C1 and C2 of the double bond. Finally, we will refer to the regions illustrated in Figure 3.1 to aid in the discussion of the aspects of the TS structures that contribute to the observed endo-exo selectivities.

### 3.2. Computational Methods

All GS and TS structures were optimized at the B3LYP/6-31G(d) level of theory (8, 9) using Gaussian 03 (10). Two different dienes, butadiene and cyclopentadiene, were considered. Cyclopentene was disubstituted at either C4 or C1/C2 with C≡CH, $CH_3$, Cl, C≡N, and F. The endo and exo TS structures for the DA cycloadditions of each dienophile with both dienes were obtained. It was determined that a single GS structure existed for the 4,4-dimethylcyclopentene and the 1,2-dimethylcyclopentene dienophiles. However, for the endo and exo TS structures, there were two possible conformers for $CH_3$ for both modes of disubstitution; only the lowest energy TS structure for each are considered here. Vibrational frequency calculations confirmed that all TS structures had a single imaginary frequency,

corresponding to the formation of the new σ bonds, and all GS structures had no imaginary frequencies.

## 3.3. Results and Discussion

### 3.3.1. Ground State Cyclopentenes

The addition of substituents to various sites of a dienophile is an easy way to modify the strength of the C=C bond and hence the reactivity of the dienophile. The presence of the substituent can affect electron density and the magnitude of the electronic effect on the molecule can be seen both energetically and structurally. It is reasonable to expect that a substituent in close proximity to the reaction center would have a greater influence on the reactivity of the C=C bond. In the present study, we are interested in both the short-range and long-range effects of substituents on the stabilization of the cyclopentene derivatives.

#### 3.3.1.1. 4,4-Disubstitution of Cyclopentene

Table 3.1 shows the changes in the bond lengths of cyclopentene upon disubstitution at C4. A comparison of the bond lengths of cyclopentene itself with those of its 4,4-disubstituted derivatives demonstrates the degree to which the substituent electronic effects extend through the ring system.

**Table 3.1.** GS bond lengths (Å) and $2p_x'$ and $2p_x''$ HOMO coefficients for atoms C1 and C2 for 4,4-disubstituted cyclopentenes, optimized at B3LYP/6-31G(d). Also shown are the isodesmic stabilization energies ($\Delta E^{4,4}_{stab}$, kJ mol$^{-1}$) as calculated per Scheme 3.1. All structures have $C_s$ symmetry.

| substituent | C4-X | C3-C4<br>C5-C4 | C2-C3<br>C1-C5 | C1=C2 | $2p_x'$ for<br>C1/C2 | $2p_x''$ for<br>C1/C2 | $\Delta E^{4,4}_{stab}$ |
|---|---|---|---|---|---|---|---|
| H | 1.096,<br>1.094 | 1.554 | 1.513 | 1.335 | 0.36688 | 0.27072 | 0 |
| C≡CH | 1.474,<br>1.470 | 1.580 | 1.508 | 1.334 | 0.37565 | 0.27324 | -0.4 |
| $CH_3$ | 1.540,<br>1.534 | 1.565 | 1.510 | 1.335 | 0.36841 | 0.27099 | -0.5 |
| Cl | 1.826,<br>1.813 | 1.548 | 1.511 | 1.335 | 0.37917 | 0.27401 | 10.4 |
| C≡N | 1.476,<br>1.472 | 1.579 | 1.509 | 1.333 | 0.37943 | 0.27307 | -1.3 |
| F | 1.376,<br>1.370 | 1.540 | 1.509 | 1.337 | 0.37971 | 0.27566 | 9.2 |

Beginning at the site of disubstitution, we see the C-C bonds of C4 (C3-C4 and C5-C4) change considerably, shortening or lengthening depending on the substituents at C4. There is far less change occurring in the C2-C3 and C1-C5 bonds as we continue toward the

reaction center; upon 4,4-disubstitution, these bonds shorten by 0.002-0.005 Å. More importantly, there is essentially no change in the C1=C2 bond length, regardless of the C4-substitution. The maximum change for the C1=C2 bond length is a mere 0.002 Å. Hence, the geometric data confirms that the electronic influence of the C4-substituents diminishes as the reaction center is approached to the point where there is essentially no change in the double bond. We expect that the C=C bond strength and thus reactivity of these GS dienophiles would closely mirror that of cyclopentene itself.

Further evidence of electronic effects of substitution (or lack thereof) may be observed in the molecular orbital (MO) coefficients. The highest occupied MO (HOMO) of cyclopentene is a π MO that contains contributions from the p-orbitals of the C1 and C2 atoms. The $2p_x'$ and $2p_x''$ HOMO coefficients for C1 and C2 of cyclopentene and its 4,4-disubstituted analogs are listed in Table 3.1. As shown, the MO coefficients for the 4,4-disubstituted cyclopentenes are remarkably similar to those of cyclopentene itself, with no more than a 4% change in the $2p_x'$ coefficients and a mere 2% maximum change in the $2p_x''$ coefficients in any instance. This further confirms that the disubstitution at C4, regardless of the substituent, does not affect the reaction center of the dienophile.

As previously stated, the effect of substitution on a molecule's reactivity in terms of stabilization energy is a quantity that can be difficult to determine. The problem occurs in the definition of the isodesmic reaction to be used, since the resultant stabilization energies may contain the energetic costs of effects other than the particular substituent effect that one is attempting to quantify. Scheme 3.1 illustrates the isodesmic reaction chosen for estimating

the strength of the C1=C2 bond and the stabilization energies for each of the 4,4-disubstituted cyclopentene dienophiles.

Scheme 3.1

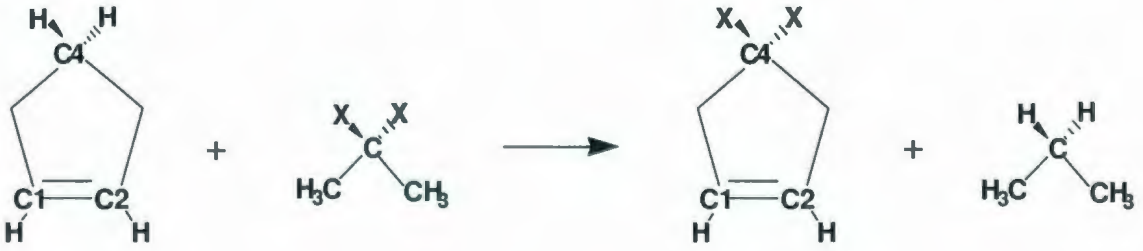


This reaction eliminates the anomeric effect from the resulting energies due to its presence on both sides of the equation in Scheme 3.1; the assumption is that the anomeric effect would be very similar in both the cyclopentene and propane derivatives for a given substituent X. The expectation is that the isodesmic stabilization energies for X ($\Delta E^{4,4}_{stab}$) will not be considerably different from that of cyclopentene itself (X = H) if the GS stability is not affected appreciably by 4,4-disubstitution.

The calculated values of $\Delta E^{4,4}_{stab}$ are presented in Table 3.1. For X = $CH_3$, C≡CH, and C≡N, we see that 4,4-disubstitution of cyclopentene has essentially no effect on the stabilization of the dienophile, as compared to a similarly substituted propane derivative. These substituents give remarkably small values, which is further evidence that these 4,4-disubstituted cyclopentenes have reactivities similar to cyclopentene. However, larger

destabilizing values were calculated for the two other substituents, F and Cl ($\Delta E^{4,4}_{stab}$ = 9.2 and 10.4 kJ $mol^{-1}$ for F and Cl, respectively). It is interesting to note that both halogens have similar destabilizing effects on the cyclopentene ring upon 4,4-disubstitution. The GS geometries indicate that F and Cl are the only substituents that result in a shortening of the C3-C4 and C5-C4 bonds of the ring, shorter than that of even cyclopentene. However, as shown in Table 3.1, there are no further significant changes in the remaining ring bonds upon 4,4-disubstitution, including the C1=C2 reaction center. This indicates that the destabilization that results from the 4,4-disubstitution of F or Cl is not due to any changes in the reaction center, but simply to the introduction of more ring strain.

#### 3.3.1.2. 1,2-Disubstitution of Cyclopentene

Substitution at C1 and C2 of cyclopentene (directly at the reaction center) should, as previously mentioned, have an impact on the stabilization / destabilization and hence reactivity of the dienophile. Table 3.2 outlines the changes in the cyclopentene bond lengths and MO coefficients upon 1,2-disubstitution. The reaction illustrated in Scheme 3.2 is an isogyric reaction, one in which the number of pairs of electrons is conserved. The stabilization energies calculated using this reaction are also shown in Table 3.2.

**Table 3.2.** GS bond lengths (Å) and $2p_x'$ and $2p_x''$ HOMO coefficients for atoms C1 and C2 for 1,2-disubstituted cyclopentenes, optimized at B3LYP/6-31G(d). The isogyric stabilization energies ($\Delta E^{1,2}_{stab}$, kJ mol$^{-1}$), as calculated per Scheme 3.2, are also included. All structures have $C_s$ symmetry.

| substituent | C1-X<br>C2-X | C1=C2 | C2-C3<br>C1-C5 | C3-C4<br>C5-C4 | $2p_x'$ for<br>C1/C2 | $2p_x''$ for<br>C1/C2 | $\Delta E^{1,2}_{stab}$ |
|---|---|---|---|---|---|---|---|
| H | 1.087 | 1.335 | 1.513 | 1.554 | 0.36688 | 0.27072 | 0 |
| C≡CH | 1.416 | 1.361 | 1.521 | 1.547 | 0.28708 | 0.20899 | -70.3 |
| $CH_3$ | 1.500 | 1.344 | 1.518 | 1.547 | 0.36699 | 0.26820 | -42.9 |
| Cl | 1.735 | 1.337 | 1.508 | 1.554 | 0.34025 | 0.24212 | -39.3 |
| C≡N | 1.423 | 1.354 | 1.518 | 1.549 | 0.31311 | 0.22592 | -37.5 |
| F | 1.343 | 1.332 | 1.498 | 1.558 | 0.37762 | 0.23501 | -77.4 |

Beginning near the reaction center, we notice that the C1-X and C2-X substituent bonds are significantly shorter than the C4-X bond lengths of the 4,4-disubstituted cyclopentenes (in Table 3.1). The reaction center itself changes appreciably with the 1,2-disubstitution of $CH_3$, C≡CH, and C≡N; these C1=C2 bonds lengthen, and thus become more electron-deficient. There is very little change in the reaction center with the 1,2-disubstitution by F or Cl, however. When X = F, there is only a slight shortening of C1=C2, but a significant shortening of the neighbouring ring bonds C2-C3 and C1-C5. When X = $CH_3$, C≡CH, and C≡N, we see similar geometric changes with 1,2-disubstitution; a small degree of lengthening in the C2-C3 and C1-C5 bonds, and a minor shortening of the C3-C4

and C5-C4 bonds. The C3-C4 and C5-C4 bonds have a maximum change of only 0.007 Å for the substituents examined here. The electronic influences of the C1/C2 substituents have subsided considerably in the neighbourhood of the remote C4 atom.

The π HOMO coefficients for $2p_x'$ and $2p_x''$ of C1 and C2 of the 1,2-disubstituted cyclopentene dienophiles are shown in Table 3.2. As expected, these MO coefficients now have a very different range of values, with some substituents exhibiting little change from cyclopentene itself (such as X = $CH_3$), and others exhibiting large electronic effects. For instance, both coefficients for C≡CH decrease by about 20% upon 1,2-disubstitution. Thus, it can be stated that 1,2-disubstitution can induce considerable change in the electronic character of the C1=C2 bond (unlike 4,4-disubstitution), but the resulting effect depends on the nature of X.

It was expected that the 1,2-disubstituted cyclopentene stabilization energies, $\Delta E^{1,2}_{stab}$, would reflect a large electronic substituent effect due to the direct substitution at the reaction center. This effect is estimated by the isogyric reaction shown in Scheme 3.2.

Scheme 3.2

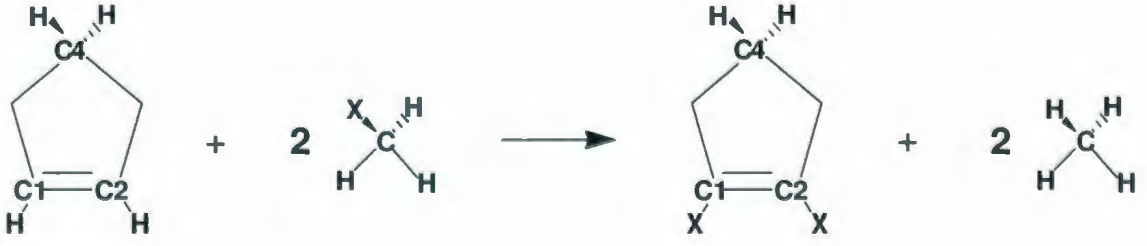

As shown in Table 3.2, the values for $\Delta E^{1,2}_{stab}$ for all X are quite large and negative, corresponding to a very considerable stabilizing effect. While it is believed that the 1,2-disubstitution of cyclopentene should result in an appreciable stabilizing / destabilizing effect, it is recognized that this particular isogyric reaction may not be the best choice to quantify such an effect. As will be seen later, the range of activation energies for the DA reactions involving these dienophiles is typically less than 20 kJ $mol^{-1}$, yet the $\Delta E^{1,2}_{stab}$ values shown in Table 3.2 range from 37.5 - 77.4 kJ $mol^{-1}$. These $\Delta E^{1,2}_{stab}$ values are much too large to be truly reasonable.

The choice of isodesmic or isogyric reaction that yields *only* the quantity of interest is a very difficult one. In cases where the goal is determining energetic effects of substitution, determining the "local" effect may be problematic, as there is a distinct possibility that the reaction being used is measuring additional effects as well. It is very likely that the isogyric reaction in Scheme 3.2 is measuring additional effects (such as ring strain), and the substituents are stabilizing the cyclopentene dienophile in very different ways. This would explain why the stabilization energies and bond lengths cannot be correlated; it is believed that the $\Delta E^{1,2}_{stab}$ values represent more than a measure of the reactivity of the reaction center. Further investigation is necessary here.

### 3.3.2. Transition State Structures

#### 3.3.2.1. 4,4-Disubstituted Cyclopentene with Butadiene or Cyclopentadiene

##### *A. Endo-Exo Selectivities and Energy Data*

Table 3.3 shows that, for the 4,4-disubstituted cyclopentenes with butadiene, the preference is clearly for the exo TS structures ($\Delta E_{endo-exo}$ are all positive), whereas the endo TSs are slightly favoured for those reactions involving cyclopentadiene.

**Table 3.3.** Energy data (kJ $mol^{-1}$) for the endo and exo DA TS structures of 4,4-disubstituted cyclopentenes with butadiene and cyclopentadiene at the B3LYP/6-31G(d) level.

| substituent | $\Delta E_{endo\text{-}exo}$ [a] | $\Delta E_{act}$ | | $\Delta E_{def}$ [b] | | | | $\Delta E_{int}$ [c] | |
|---|---|---|---|---|---|---|---|---|---|
| | | endo | exo | $\Delta E^{diene}_{def}$ endo | $\Delta E^{dph}_{def}$ endo | $\Delta E^{diene}_{def}$ exo | $\Delta E^{dph}_{def}$ exo | endo | exo |
| **butadiene as diene** | | | | | | | | | |
| H | 4.5 | 95.9 | 91.4 | 72.3 | 45.2 | 68.8 | 42.4 | -21.5 | -19.7 |
| C≡CH | 15.2 | 102.6 | 87.4 | 72.7 | 54.1 | 67.3 | 47.3 | -24.2 | -27.2 |
| $CH_3$ | 7.1 | 108.6 | 101.5 | 75.3 | 55.7 | 70.6 | 49.3 | -22.4 | -18.4 |
| Cl | 13.0 | 104.1 | 91.1 | 72.3 | 57.3 | 66.7 | 49.7 | -25.5 | -25.3 |
| C≡N | 6.9 | 94.8 | 87.9 | 72.4 | 54.1 | 68.5 | 48.7 | -31.8 | -29.4 |
| F | 11.1 | 92.8 | 81.8 | 71.4 | 50.3 | 67.1 | 47.6 | -28.9 | -33.0 |
| **cyclopentadiene as diene** | | | | | | | | | |
| H | -8.4 | 99.8 | 108.1 | 73.8 | 44.8 | 75.8 | 49.5 | -18.8 | -17.2 |
| C≡CH | -2.8 | 106.1 | 108.9 | 74.0 | 54.9 | 72.0 | 55.1 | -22.8 | -18.2 |
| $CH_3$ | -4.9 | 107.8 | 112.7 | 71.3 | 56.5 | 74.3 | 55.1 | -20.0 | -16.7 |
| Cl | -7.0 | 96.1 | 103.1 | 66.4 | 54.4 | 69.2 | 54.1 | -24.7 | -20.2 |
| C≡N | -9.5 | 97.0 | 106.5 | 73.4 | 54.8 | 75.4 | 57.4 | -31.3 | -26.3 |
| F | -3.7 | 95.4 | 99.0 | 72.7 | 50.0 | 73.6 | 53.5 | -27.3 | -28.1 |

[a] $\Delta E_{endo\text{-}exo} = \Delta E_{act}$ (endo) - $\Delta E_{act}$ (exo). [b] $\Delta E_{def} = \Delta E$ (TS fragment) - $\Delta E$ (GS). [c] $\Delta E_{int} = \Delta E_{act} - (\Delta E^{diene}_{def} + \Delta E^{dph}_{def})$.

In general, we note that the ranges of $\Delta E_{act}$ for all X for the reaction of 4,4-disubstituted cyclopentene with cyclopentadiene or butadiene are not large; for example, the ranges are only 12.4 and 13.7 kJ $mol^{-1}$ for endo and exo addition with cyclopentadiene, respectively. However, while most of these activation barriers are in fairly close proximity (within 6 - 7 kJ $mol^{-1}$) to those for cyclopentene itself, they do vary, indicating that there are some important interactions occurring in the TS structures. Some of these interactions are favourable, as many of the 4,4-disubstituted cyclopentenes yield lower reaction barriers than that of cyclopentene when reacted with the same diene. If one focuses on a single dienophile and compares its endo or exo $\Delta E_{act}$ for both dienes, we see that, in general, the TS structures involving cyclopentadiene tend to have higher activation barriers than those involving butadiene. It is believed that cyclopentadiene introduces more unfavourable steric interactions in the TS structure than does butadiene, mostly due to the presence of the methylene group (at C5). While higher $\Delta E_{act}$ values might suggest that cyclopentadiene is a "less reactive" diene than butadiene, it is known that, experimentally, cyclopentadiene is actually a more reactive diene in general. The *cisoid* butadiene is used in determining $\Delta E_{act}$ in the present study, whereas the more stable trans isomer would be utilized in experimentally-determined activation barriers. The difference between the two isomers (about 12 kJ $mol^{-1}$) would need to be considered in order to truly compare the two. As such, the barriers for the butadiene cycloadditions are underestimated here as compared to experiment, and should yield higher barriers due to the higher degree of deformation ($\Delta E^{diene}_{def}$) required for butadiene.

Deformation energies are perhaps the most important component of the activation energy barrier, since the GS structure modification can be quite costly. Table 3.3 lists the $\Delta E^{diene}_{def}$ and $\Delta E^{dph}_{def}$ for the endo and exo additions of the 4,4-disubstituted cyclopentenes to both dienes. As is typical for DA cycloadditions, there is significantly more deformation taking place in the dienes of each pair than the dienophiles. This is expected, since three bonds are being modified in the diene during the deformation process and only one in the dienophile. For the reactions involving butadiene, the $\Delta E^{total}_{def}$ (calculated as $\Delta E^{total}_{def} = \Delta E^{diene}_{def} + \Delta E^{dph}_{def}$) required for the exo TS structures are less than what is required for the endo TSs. It is clear that the diene and dienophile require less structural deformation to achieve their exo TS structures, which is understandable considering the lower $\Delta E_{act}$ for the exo additions. For the cyclopentadiene reactions, the $\Delta E^{total}_{def}$ for endo and exo addition are actually quite similar, with the endo TS structures having slightly less $\Delta E^{total}_{def}$ than the exo TSs. The exception is X = C≡CH; the $\Delta\Delta E^{total}_{def}$ for this substituent is only 1.8 kJ $mol^{-1}$. This extremely small difference is not surprising as the endo-exo selectivity is only 2.8 kJ $mol^{-1}$.

Interaction energies are also included in Table 3.3. Clearly, the role of $\Delta E_{int}$ cannot be ignored in a discussion of activation barriers, since it is not a constant value for all X. However, it is difficult to account for the differences (and similarities) we see in the interaction energies. For example, $\Delta E_{endo\text{-}exo}$ = 13.0 kJ $mol^{-1}$ when the 4,4-dichlorocyclopentene dienophile is reacted with butadiene. One would expect that a more negative value, and thus more favourable interaction, would be seen for the exo $\Delta E_{int}$. Yet,

$\Delta E_{int}$ for both endo and exo addition are nearly identical (-25.5 and -25.3 kJ $mol^{-1}$ for endo and exo addition, respectively).

### *B. TS Geometries - Incipient Bonds*

The length of the forming σ bonds in the TS structure is a good indicator of the earliness or lateness of the TS on the reaction coordinate. Table 3.4 shows the incipient bonds for the endo and exo TS structures for the DA reactions of 4,4-disubstituted cyclopentenes with both dienes.

**Table 3.4.** Incipient bond lengths (Å) for the endo and exo DA TS structures of 4,4-disubstituted cyclopentenes with butadiene and cyclopentadiene at the B3LYP/6-31G(d) level.

| substituent | incipient bonds | | | |
|---|---|---|---|---|
| | endo | exo | endo | exo |
| | **butadiene as diene** | | **cyclopentadiene as diene** | |
| H | 2.273 | 2.274 | 2.237 | 2.249 |
| C≡CH | 2.263 | 2.273 | 2.225 | 2.251 |
| $CH_3$ | 2.264 | 2.269 | 2.241 | 2.244 |
| Cl | 2.265 | 2.275 | 2.253 | 2.259 |
| C≡N | 2.263 | 2.278 | 2.226 | 2.238 |
| F | 2.265 | 2.270 | 2.232 | 2.247 |

In Table 3.4, we see that the unsubstituted cyclopentene / butadiene endo TS structure has incipient bonds measuring 2.273 Å. Interestingly, the remaining butadiene endo TSs have incipient bonds that are remarkably similar to each other, ranging from 2.263 - 2.265 Å, in addition to being shorter than the incipient bonds for X = H. Shorter incipient bonds suggest a later TS, as the reactants must approach each other more closely to achieve the TS structure. The incipient bond lengths of the 4,4-disubstituted cyclopentene / butadiene exo TS structures are more varied, but they generally fall within a fairly close range of the cyclopentene / butadiene exo TS. For all of the 4,4-disubstituted cyclopentene dienophiles, the endo TSs with butadiene have shorter incipient bonds than the analogous exo TS structures. The DA reactions involving cyclopentadiene as the diene all have shorter incipient bonds and thus "tighter" TS structures. This suggests that these cyclopentadiene TSs are occurring later on the reaction coordinate than the corresponding TSs involving butadiene.

### *C. Explaining Endo-Exo Selectivity*

The question that naturally arises now is: "what are the most significant factors that contribute to the calculated endo-exo selectivities?" Using Figure 3.1 and the definitions of "endo region" and "exo region" as indicated, we see that the preference for exo selectivity for the 4,4-disubstituted cyclopentene / butadiene TSs can be attributed to the unfavourable eclipsing C-H bonds in the exo region of the endo TS structures. Since the exo region of all of the butadiene endo TSs are virtually identical, the slight differences that we do observe in

the endo $\Delta E_{act}$ can be accounted for by differences in the steric interactions between the syn C4-substituent and butadiene. The 4,4-disubstituted cyclopentene / butadiene exo TSs have no such eclipsing C-H bonds, automatically giving the exo mode of addition an "advantage". Instead, in the exo TS structures, the syn C4-substituent bisects the C1-H and C4-H bonds of butadiene, which is certainly a more favourable situation than the eclipsing bonds of the endo TS structures. In addition to this, in the exo region of the exo TSs, the position of the syn C4-substituent should allow for, in some cases, a strong interaction between it and the H's of C1 and C4 of butadiene. For example, the $\Delta E_{act}$ for the cyclopentene / butadiene exo TS is 91.4 kJ $mol^{-1}$. The 4,4-disubstituted cyclopentene / butadiene exo TSs with X = F and Cl (81.8 and 91.1 kJ $mol^{-1}$, respectively) have lone pairs that can interact favourably with the butadiene H's. Also, the exo TSs with X = C≡CH and C≡N (87.4 and 87.9 kJ $mol^{-1}$, respectively) are positioned in the TS structure in such a way as to allow for a favourable interaction between the electron-dense triple bonds and the butadiene H's. In contrast, the syn $CH_3$ substituent in its C4 position in the exo TS will have an unfavourable H---H interaction between the C1 and C4 H's and the H of the $CH_3$ group that is pointing straight down. This exo region interaction corresponds to the highest butadiene exo activation barrier, $\Delta E_{act}$ = 101.5 kJ $mol^{-1}$. Favourable or unfavourable interactions between X and the exo region of butadiene, if they exist, should appear in the interaction energy, $\Delta E_{int}$. This is evident in some cases; we see a more favourable exo interaction for X = F and C≡CH and a slightly less favourable interaction for X = $CH_3$. However, the exo $\Delta E_{int}$ when X = Cl and C≡N do not follow this trend. This inconsistency means that, at best, one can make this

judgement call on a case-by-case basis only. It is also important to note that favourable or unfavourable interactions might not be reflected in the interaction energies themselves; it is possible that these TS interactions result in geometric changes that get "absorbed" in the deformation energies.

We can address the endo selectivity of the reactions involving cyclopentadiene by first noting the obvious difference between the two dienes - the presence of the methylene group of cyclopentadiene in the exo region. In the 4,4-disubstituted cyclopentene / cyclopentadiene endo TSs, there are no occurrences of C-H bond eclipsing as there are in the analogous butadiene endo TS structures; the methylene group of cyclopentadiene instead bisects the C1-H and C2-H bonds of the dienophile. As well, these endo TS structures have short incipient bond lengths, indicating that the rehybridization of C1 and C2 of the dienophile has progressed further in the endo TSs. The C1 and C2 H's are oriented upwards and away from the methylene group of cyclopentadiene, thereby reducing possible unfavourable steric interactions.

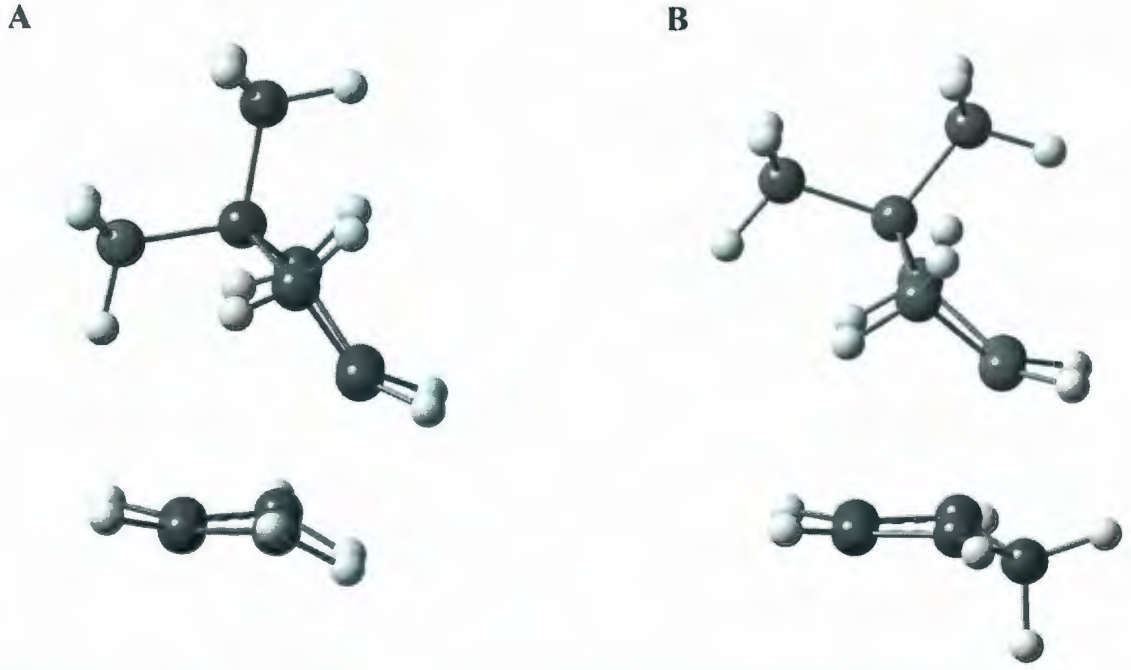


**Figure 3.2.** Example of structural changes in the 4,4-dimethylcyclopentene dienophile when reacted with **A**) butadiene and **B**) cyclopentadiene (endo TS).

Figure 3.2 illustrates a pronounced structural difference that is observed for the butadiene and cyclopentadiene endo TS structures when X = $CH_3$. In the butadiene endo TS structure (Figure 3.2, **A**), C4 is tipped *down* in an envelope conformation, out of the plane of the other four ring carbons, by 7.0°. This brings the syn $CH_3$ substituent in close contact with the endo region of the diene. However, in the cyclopentadiene endo TS structure (Figure 3.2, **B**), C4 is tipped *up* by 18.7°; this allows for a slightly tighter TS (shorter incipient bonds) since the syn $CH_3$ is no longer in a position that may cause unfavourable steric interactions. Interestingly, though, these two TSs have nearly identical $\Delta E_{act}$ (108.6 and

107.8 kJ $mol^{-1}$ for the butadiene and cyclopentadiene endo TSs, respectively).

In general, the cyclopentadiene exo TS structures have the highest energy barriers of the four possible TSs studied here. With the exception of X = F, these TSs also have less favourable interaction energies. An examination of the 4,4-disubstituted cyclopentene / cyclopentadiene exo TS structures shows an obvious steric problem that contributes to the higher activation barriers for this mode of addition. In these structures, the dienophile typically bends up at C4 in an envelope conformation and thus away from the cyclopentadiene. This results in two significant structural changes; one, the C4-substituents are no longer in close contact with the methylene H of the diene and likely do not contribute to unfavourable steric interactions, and two, the downward-facing H's of C3 and C5 of the dienophile are now in very close contact with the methylene H of cyclopentadiene. These interactions between the diene and dienophile are very important as they impose an appreciable steric problem on the TS structure. For example, when X = C≡CH, the distance between the H of C3 (or C5) of the dienophile and the H of C5 (the methylene H) of the diene is only 2.232 Å. For comparison, the incipient bond length for this exo TS is 2.251 Å. When X = Cl, this same H---H distance between the diene and dienophile is 2.214 Å; the incipient bond length is 2.259 Å. When X = F, however, we see that the C4 of the dienophile is tipped down towards the diene, allowing for a favourable interaction between the lone pairs of the syn F substituent and the methylene H of cyclopentadiene; this distance is only 2.443 Å. This H---F interaction actually corresponds to what would be expected for a weak hydrogen bond! Not surprisingly, this cyclopentadiene exo TS has the lowest $\Delta E_{act}$ of the group ($\Delta E_{act}$ = 99.0

kJ $mol^{-1}$), as well as a more stabilizing $\Delta E_{int}$.

### 3.3.2.2. 1,2-Disubstituted Cyclopentene with Butadiene or Cyclopentadiene

#### *A. Endo-Exo Selectivities and Energy Data*

As indicated by Table 3.5, the endo-exo selectivities ($\Delta E_{endo\text{-}exo}$) for the 1,2-disubstituted cyclopentenes with butadiene are small, varied, and do not show an overall specific preference for endo or exo addition (unlike the 4,4-disubstituted TSs discussed previously). However, for those reactions involving the 1,2-disubstituted cyclopentenes with cyclopentadiene, we observe an overall increase in endo selectivity, with some substituents (especially X = C≡CH and Cl) exhibiting 100% endo selectivity.

**Table 3.5.** Energy data (kJ $mol^{-1}$) for the endo and exo DA TS structures of 1,2-disubstituted cyclopentenes with butadiene and cyclopentadiene at the B3LYP/6-31G(d) level.

| substituent | $\Delta E_{endo-exo}$ | $\Delta E_{act}$ | | $\Delta E_{def}$ | | | | $\Delta E_{int}$ | |
|---|---|---|---|---|---|---|---|---|---|
| | | endo | exo | $\Delta E^{diene}_{def}$ endo | $\Delta E^{dph}_{def}$ endo | $\Delta E^{diene}_{def}$ exo | $\Delta E^{dph}_{def}$ exo | endo | exo |
| **butadiene as diene** | | | | | | | | | |
| H | 4.5 | 95.9 | 91.4 | 72.3 | 45.2 | 68.8 | 42.4 | -21.5 | -19.7 |
| C≡CH | -1.6 | 120.5 | 122.1 | 81.5 | 71.3 | 76.0 | 67.9 | -32.4 | -21.9 |
| $CH_3$ | 5.7 | 126.1 | 120.4 | 79.0 | 71.8 | 73.9 | 69.6 | -24.6 | -23.1 |
| Cl | -1.7 | 122.7 | 124.3 | 72.4 | 77.0 | 67.8 | 74.5 | -26.7 | -18.1 |
| C≡N | 4.0 | 99.7 | 95.7 | 77.1 | 67.7 | 71.3 | 63.2 | -45.1 | -38.8 |
| F | -3.1 | 103.0 | 106.1 | 68.0 | 67.0 | 63.5 | 65.0 | -32.0 | -22.4 |
| **cyclopentadiene as diene** | | | | | | | | | |
| H | -8.4 | 99.8 | 108.1 | 73.8 | 44.8 | 75.8 | 49.5 | -18.8 | -17.2 |
| C≡CH | -16.9 | 120.3 | 137.1 | 83.0 | 74.7 | 82.5 | 80.7 | -37.4 | -26.1 |
| $CH_3$ | -4.8 | 134.2 | 139.0 | 83.9 | 76.1 | 84.6 | 79.0 | -25.7 | -24.6 |
| Cl | -14.0 | 122.5 | 136.5 | 73.2 | 79.5 | 72.0 | 86.6 | -30.2 | -22.1 |
| C≡N | -10.9 | 94.9 | 105.7 | 78.7 | 70.8 | 77.9 | 75.6 | -54.6 | -47.7 |
| F | -7.8 | 103.4 | 111.2 | 68.8 | 68.4 | 63.4 | 73.8 | -33.8 | -26.0 |

The endo and exo activation energies ($\Delta E_{act}$) for the 1,2-disubstituted cyclopentenes with either diene show that the majority of the activation barriers have increased considerably when compared to those of the 4,4-disubstituted cyclopentene TSs. The exo TS structures involving cyclopentadiene are particularly noteworthy due to the fact that, for all X, these TSs have the highest $\Delta E_{act}$ of all of the reactions involving the 1,2-disubstituted dienophiles. It is expected that these exo TS structures have significant steric interactions between the diene and dienophile that give rise to these high barriers. Also, for some of the substituents examined here, the $\Delta E_{act}$ for the endo TSs are very similar for both dienes when they are in a TS with the same 1,2-disubstituted dienophile. This implies that, in general, the exo TS structures are being affected to a larger degree by favourable (or unfavourable) interactions.

Table 3.5 shows the deformation energies for the endo and exo additions of the 1,2-disubstituted cyclopentenes to butadiene and cyclopentadiene. We see that the values for $\Delta E^{diene}_{def}$ and $\Delta E^{dph}_{def}$ are generally larger than those calculated for the 4,4-disubstituted TSs; the $\Delta E^{dph}_{def}$, in particular, shows a significant increase, with some dienophiles now requiring as much as 70 kJ $mol^{-1}$ or more energy for the deformation process. The butadiene TSs require comparable total deformation energies for endo and exo, and this coincides with the similar values of $\Delta E_{act}$ for the endo and exo additions and the $\Delta E_{endo-exo}$ selectivities. For the cyclopentadiene TSs, the diene and dienophile reactants require considerably more GS structural deformation than their 4,4-disubstituted counterparts, particularly for the formation of the exo TSs.

### *B. TS Geometries - Incipient Bonds*

**Table 3.6.** Incipient bond lengths (Å) for the endo and exo DA TS structures of 1,2-disubstituted cyclopentenes with butadiene and cyclopentadiene at the B3LYP/6-31G(d) level.

| substituent | incipient bonds | | | |
|---|---|---|---|---|
| | endo | exo | endo | exo |
| | **butadiene as diene** | | **cyclopentadiene as diene** | |
| H | 2.273 | 2.274 | 2.237 | 2.249 |
| C≡CH | 2.246 | 2.260 | 2.207 | 2.229 |
| $CH_3$ | 2.279 | 2.286 | 2.247 | 2.251 |
| Cl | 2.283 | 2.293 | 2.252 | 2.272 |
| C≡N | 2.260 | 2.267 | 2.217 | 2.236 |
| F | 2.279 | 2.300 | 2.250 | 2.276 |

The data in Table 3.6 shows the marked difference between the incipient bond lengths; this variation reflects the impact of the 1,2-disubstitution on the stabilization of the dienophiles and the resulting differences in the geometries of the TS structures. When X = C≡CH, we observed earlier that this 1,2-disubstitution resulted in the smallest π HOMO coefficients and the longest C1=C2 bond in the GS dienophile. The endo and exo TS structures for both dienes with this 1,2-disubstituted dienophile have the shortest incipient bonds and generally high $\Delta E^{total}_{def}$ as compared to the rest of the substituents. This means that the dienophile with the most electron-deficient C1=C2 bond also has the latest TS structures

for both endo and exo addition to both dienes, implying that this dienophile has a relatively low reactivity. Conversely, when X = F, we recall that this 1,2-disubstitution led to a GS dienophile with the shortest C1=C2 bond. The endo and exo TS structures for this dienophile with butadiene and cyclopentadiene have long incipient bonds (the longest for the butadiene and cyclopentadiene exo TSs) and low $\Delta E^{total}_{def}$ as compared to the remaining substituents. This dienophile, relatively more reactive, has an electron-rich C1=C2 bond and leads to a generally earlier TS.

There are also significant differences in the incipient bond lengths between the endo and exo TSs for the same diene / dienophile pair; generally, the exo TSs have longer incipient bonds, suggesting TS formation earlier on the reaction coordinate. We also see that, for all X, the reactions involving cyclopentadiene have substantially shorter incipient bonds and tighter TS structures than the corresponding butadiene TSs. As with the 4,4-disubstituted cases, this indicates that the TSs involving cyclopentadiene are later on the reaction coordinate.

### *C. Explaining Endo-Exo Selectivity*

Figure 3.1 can be employed to help rationalize the observed results shown in Table 3.5. As noted previously, the 1,2-disubstituted cyclopentene / butadiene TSs do not have a significant preference for endo or exo addition. For these particular endo and exo structures, the favourable and / or unfavourable interactions that play an important role in deciding selectivity are likely quite comparable in terms of the degree of structure stabilization /

destabilization. For the 1,2-disubstituted cyclopentene / butadiene TSs, the endo regions of all of the endo TSs are nearly identical, thus the important interactions must reside in the exo regions, where there are again slightly eclipsing bonds. Since the C1-X and C2-X bonds of the dienophile are longer than the typical C-H bond, this bond-eclipsing interaction may not play as large a steric role as what is observed for the 4,4-disubstituted cyclopentene / butadiene endo TSs and, in some cases, may even exhibit a favourable effect. For example, the lone pairs of F and Cl (bonded at C1/C2 of cyclopentene) may induce a small favourable interaction with the C1 and C4 H's of the diene. When X = C≡N, we see a significant $\Delta E_{int}$ for the 1,2-disubstituted cyclopentene / butadiene endo TS structure (-45.1 kJ $mol^{-1}$), indicating a very favourable interaction when the diene / dienophile pair form the TS structure. The 1,2-disubstituted cyclopentene / butadiene exo TSs have a methylene group situated at C4 of the dienophile, and this section of the cyclopentene ring bisects the C1-H and C4-H bonds of butadiene. This $CH_2$ group of the cyclopentene dienophile is tipped down by approximately the same amount for each exo TS (range of 19.2° to 20.1°), and any steric problems here should be minimal, if present at all. The incipient bonds are longer for the exo TSs, thus reducing possible steric interactions in the endo region; in most cases, the X substituents at C1 and C2 are tipped up and away from the π system of the diene. Any favourable or unfavourable interactions in the exo TSs are likely small in magnitude and of minor importance, but at the same time they are comparable to those of the endo TS structures.

An interesting trend is noticed in the 1,2-disubstituted cyclopentene / cyclopentadiene

TS structures. In Table 3.5, we see generally significant values for $\Delta E_{endo\text{-}exo}$, with the endo addition being the preferred mode of addition in every case. The endo region of the 1,2-disubstituted cyclopentene / cyclopentadiene endo TS structure shows a structural feature that is consistent for all X: the methylene of the dienophile is tipped down towards the diene by nearly the same amount (range of 15.5° to 16.6°). This means that the exo region of the cyclopentadiene endo TSs is the most important region to consider, as this is where the TS structural differences lie. The methylene group of cyclopentadiene bisects the C-X bonds of the cyclopentene dienophile. In addition, these endo TSs have incipient bonds that are quite short, suggesting that the rehybridization of the atoms at the reaction center (C1/C2) of the 1,2-disubstituted cyclopentene is more advanced, allowing for the upward movement of the X substituents (and thus away from the $CH_2$ group of cyclopentadiene). When X = $CH_3$, for example, the cyclopentadiene endo TS has one of the longer incipient bond lengths of the group (2.247 Å), which indicates a less advanced rehybridization of the C1 and C2 atoms of the dienophile. The $CH_3$ groups are in close contact with the methylene H of the diene (distance of 2.147 Å), thus causing unfavourable steric interactions and increasing the reaction barrier. The 1,2-dimethylcyclopentene / cyclopentadiene endo TS structure also has one of the smallest, and thus less favourable, interaction energies in the group of substituents examined here. The situation is similar when X = F (an incipient bond length of 2.250 Å); the distance between F and the methylene H of cyclopentadiene (2.470 Å) allows for, in this case, a favourable lone pair---H interaction, again similar to what is expected for a weak hydrogen bond. This stabilization is reflected in the lower $\Delta E_{act}$ for this endo TS.

The occurrence of endo selectivity for the 1,2-disubstituted cyclopentene / cyclopentadiene DA reaction can be viewed in two ways; either the endo TS structures are very stabilized with significant favourable interactions, or the exo TS structures are quite unfavourable with high activation barriers. Since the cyclopentadiene endo TSs are neither particularly favourable nor significantly stabilized, as can be seen from the activation energies, it is believed that the corresponding exo TSs have numerous unfavourable structural characteristics that yield high reaction barriers. In reference to Figure 3.1, the endo region of the exo TS involves the C1-X and C2-X poised above the $\pi$ system of cyclopentadiene. The incipient bonds are substantially shorter for the cyclopentadiene exo TS structures than for the corresponding butadiene exo TSs, but it is thought that, because the "non-bonded" distances are still fairly large, any favourable or unfavourable interactions would still be minimal in the endo region of the cyclopentadiene exo TSs. Conversely, the features of the exo region of the 1,2-disubstituted cyclopentene / cyclopentadiene exo TSs certainly contribute to unfavourable interactions and raise the $\Delta E_{act}$. Here, there are two methylene groups in line with each other and in very close proximity, permitting the direct interaction of two H's. It is interesting to note that we can divide the substituents into two groups; those X substituents that have the lower $\Delta E_{act}$ (X = C≡N, H, and F) and those that have the highest $\Delta E_{act}$ (X = C≡CH, $CH_3$, and Cl). The members of the first group all have H---H distances that are short but comparable (for X = C≡N, H, and F, the distances are 2.002, 2.050, and 2.037 Å, respectively). The members of the latter group have distances that are even shorter (for X = C≡CH, $CH_3$, and Cl, the distances are 1.984, 1.976, and 1.965 Å, respectively).

Clearly, the X substituents that have the highest energy barriers possess methylene groups in their exo TSs that are in the closest steric contact with the methylene of the diene. In general, these unfavourable interactions in the cyclopentadiene exo TSs are sufficient reason for this isomer to have such high activation barriers.

### 3.4. Conclusions

The examination of the 4,4- and 1,2-disubstituted cyclopentene dienophiles and their DA TS structures with butadiene and cyclopentadiene allows for the following conclusions:

- The remote disubstitution at C4 of cyclopentene has essentially no effect on the stabilization and reactivity of the dienophile, and the properties of these GSs tend to be very similar to those for cyclopentene itself.
- The disubstitution at C1 and C2 (directly on the reaction center) has a greater impact on the reactivity of the dienophile, which is reflected in the changes in the C1=C2 bond lengths.
- As shown in Tables 3.3 and 3.5, significant endo-exo selectivities ($\Delta E_{endo\text{-}exo}$) were determined for the 4,4-disubstituted cyclopentene / butadiene system (exo selective) and the 1,2-disubstituted cyclopentene / cyclopentadiene system (endo selective).
- Reactivities of the GSs play a considerable role in the determination of the viabilities of reactions and activation energy barriers (to a degree), but the deciding factor for the absolute observed reactivity, and thus endo-exo selectivity, are the important favourable and unfavourable interactions in the TS structures.

- Our designation of endo and exo regions as depicted in Figure 3.1 serves as a useful tool for analyzing the favourable / unfavourable interactions in the TS structures and for rationalizing the endo-exo selectivities observed in this study.

**Acknowledgments**

We thank the Natural Sciences and Engineering Research Council of Canada (NSERC) for financial support as well as the Memorial University of Newfoundland Advanced Computation and Visualization Centre for computing resources.

**References**

(1) Sections within: Houk, K. N.; Li, Y.; Evanseck, J. D. *Angew. Chem., Int. Ed. Engl.* **1992**, *31*, 682.

(2) Some examples are: (a) Bernardi, F.; Bottoni, A.; Field, M. J.; Guest, M. F.; Hillier, I. H.; Robb, M. A.; Venturini, A. *J. Am. Chem. Soc.* **1988**, *110*, 3050. (b) Houk, K. N.; Loncharich, R. J.; Blake, J. F.; Jorgensen, W. L. *J. Am. Chem. Soc.* **1989**, *111*, 9172. (c) Jorgensen, W. L.; Lim, D.; Blake, J. F. *J. Am. Chem. Soc.* **1993**, *115*, 2936. (d) Xidos, J. D.; Poirier, R. A.; Pye, C. C.; Burnell, D. J. *J. Org. Chem.* **1998**, *63*, 105.

(3) Some examples are: (a) Binger, P.; Wedemann, P.; Goddard, R.; Brinker, U. H. *J. Org. Chem.* **1996**, *61*, 6462. (b) Sodupe, M.; Rios, R.; Branchadell, V.; Nicholas, T.; Oliva, A.; Dannenberg, J. J. *J. Am. Chem. Soc.* **1997**, *119*, 4232. (c) Jursic, B. S. *J.*

*Org. Chem.* **1997**, *62*, 3046. (d) Imade, M.; Hirao, H.; Omoto, K.; Fujimoto, H. *J. Org. Chem.* **1999**, *64*, 6697. (e) Xidos, J. D.; Gosse, T. L.; Burke, E. D.; Poirier, R. A.; Burnell, D. J. *J. Am. Chem. Soc.* **2001**, *123*, 5482. (f) Gosse, T. L.; Poirier, R. A. *Can. J. Chem.* **2004**, *82*, 1589.

(4) Some examples are: (a) Cristol, S. J.; Seifert, W. K.; Soloway, S. B. *J. Am. Chem. Soc.* **1960**, *82*, 2351. (b) Houk, K. N. *Tetrahedron Lett.* **1970**, *30*, 2621. (c) Fox, M. A.; Cardona, R.; Kiwiet, N. J. *J. Org. Chem.* **1987**, *52*, 1469.

(5) (a) Woodward, R. B.; Hoffmann, R. *J. Am. Chem. Soc.* **1965**, *87*, 4388. (b) Woodward, R. B.; Hoffmann, R. *The Conservation of Orbital Symmetry*; Verlag Chemie: Weinheim, 1971.

(6) Some examples are: (a) Apeloig, Y.; Matzner, E. *J. Am. Chem. Soc.* **1995**, *117*, 5375. (b) Jursic, B. S. *Tetrahedron Lett.* **1997**, *38*, 1305. (c) Jursic, B. S. *J. Chem. Soc., Perkin Trans. 2* **1999**, 373. (d) Arrieta, A.; Cossio, F. P. *J. Org. Chem.* **2001**, *66*, 6178.

(7) In addition to refs. 3(e) and 4(c) above, some examples of studies disputing the importance of SOI: (a) García, J. I.; Mayoral, J. A.; Salvatella, L. *Acc. Chem. Res.* **2000**, *33*, 658. (b) Ogawa, A.; Fujimoto, H. *Tetrahedron Lett.* **2002**, *43*, 2055. (c) García, J. I.; Mayoral, J. A.; Salvatella, L. *Eur. J. Org. Chem.* **2005**, 85.

(8) Becke, A. D. *J. Chem. Phys.* **1993**, *98*, 5648.

(9) Lee, C.; Yang, W.; Parr, R. G. *Phys. Rev. B* **1988**, *37*, 785.

(10) Frisch, M. J.; Trucks, G. W.; Schlegel, H. B.; Scuseria, G. E.; Robb, M. A.;

Cheeseman, J. R.; Montgomery, Jr., J. A.; Vreven, T.; Kudin, K. N.; Burant, J. C.; Millam, J. M.; Iyengar, S. S.; Tomasi, J.; Barone, V.; Mennucci, B.; Cossi, M.; Scalmani, G.; Rega, N.; Petersson, G. A.; Nakatsuji, H.; Hada, M.; Ehara, M.; Toyota, K.; Fukuda, R.; Hasegawa, J.; Ishida, M.; Nakajima, T.; Honda, Y.; Kitao, O.; Nakai, H.; Klene, M.; Li, X.; Knox, J. E.; Hratchian, H. P.; Cross, J. B.; Adamo, C.; Jaramillo, J.; Gomperts, R.; Stratmann, R. E.; Yazyev, O.; Austin, A. J.; Cammi, R.; Pomelli, C.; Ochterski, J. W.; Ayala, P. Y.; Morokuma, K.; Voth, G. A.; Salvador, P.; Dannenberg, J. J.; Zakrzewski, V. G.; Dapprich, S.; Daniels, A. D.; Strain, M. C.; Farkas, O.; Malick, D. K.; Rabuck, A. D.; Raghavachari, K.; Foresman, J. B.; Ortiz, J. V.; Cui, Q.; Baboul, A. G.; Clifford, S.; Cioslowski, J.; Stefanov, B. B.; Liu, G.; Liashenko, A.; Piskorz, P.; Komaromi, I.; Martin, R. L.; Fox, D. J.; Keith, T.; Al-Laham, M. A.; Peng, C. Y.; Nanayakkara, A.; Challacombe, M.; Gill, P. M. W.; Johnson, B.; Chen, W.; Wong, M. W.; Gonzalez, C.; Pople, J. A. *Gaussian 03*, revision B.05; Gaussian, Inc.: Pittsburgh, PA, 2003.

# Chapter 4

## The Diels-Alder Reactions and Dimerizations of 5-Substituted Cyclopentadienes : Selectivity and the Reaction Coordinate

**Background and Preamble**

The previously discussed cyclopentene study (Chapter 3) helped us to understand that, in cases where SOI is not a contributing factor to the determination of endo-exo selectivity, it can be difficult to pinpoint exactly what the major determinant actually is. We continue to believe that the explanation is not a simple one, and many factors may contribute to the results we see from our calculations.

The cyclopentadiene dimerization investigation by this group began a number of years ago, before the discovery of the true nature of the dimer TS and the existence of the Cope TS, first discussed by Caramella et al. in 2001. Our goal at the time continued to be the examination of the effect of substituents on the stabilization of reactants, the importance of deformation energies, endo-exo selectivities, non-bonded electrostatic and steric interactions and the resulting effects on molecular structure, etc. In this dimer study, while we strived to reach the same objectives as we usually did, the characterization of the potential energy curve of the endo dimerization was too tempting to ignore. Consequently, a discussion of the results of an intrinsic reaction coordinate calculation and a thoughtful analysis of the distribution of products became part of the research as well.

# The Diels-Alder Reactions and Dimerizations of 5-Substituted Cyclopentadienes : Selectivity and the Reaction Coordinate

**Abstract:** The Diels-Alder reactions of some 5-substituted cyclopentadienes were examined at the HF and B3LYP levels of theory using the 6-31G(d) basis set. Cyclopentadiene is substituted at C5 with $CH_2$-O, Cl, and F. For the cyclodimerization reactions, activation barriers indicate that the endo mode of addition is significantly preferred over the exo mode in every case. Facial selectivities and deformation energies are also presented and discussed, emphasizing the important and sometimes very costly role of reactant deformation. The Diels-Alder reactions of cyclopentadiene with 5-substituted cyclopentadiene (the "mixed pairs", substitution by Cl or F) also exhibited endo selectivity and similar facial selectivities as the dimerization reactions. An intrinsic reaction coordinate calculation of the parent cyclopentadiene endo dimerization at the B3LYP/6-31G(d) level indicates that the potential energy curve proceeds from the higher energy bispericyclic transition state, which incorporates both the [4+2] and [2+4] cycloaddition paths, to the Cope transition state before progressing toward products. We have analyzed the path connecting these two transition states, including the nature of their imaginary frequencies and the distribution of final products.

## 4.1. Introduction

At room temperature, the cyclopentadiene monomer is not stable, and it dimerizes quite rapidly to form dicyclopentadiene. This dimerization yields the endo product exclusively, although it can be prompted to form the exo cycloadduct upon heating (1). A 1992 study by McClinton and Sik (2) confirmed the very rapid dimerization of 5-fluorocyclopentadiene, as well as the tendency for some substituted ethenes to undergo Diels-Alder (DA) cycloadditions with the fluorinated diene to yield only syn addition products. Breslow et al. (3) showed that some 5-halocyclopentadienes (Cl, Br, and I) dimerize faster than cyclopentadiene itself. In addition, a solution of 5-chlorocyclopentadiene and an excess of unsubstituted cyclopentadiene yielded only the dimer with no indication of reaction between the unsubstituted cyclopentadiene and the chloro derivative. It was clear that the presence of halogen enhanced the reactivity of the 5-halocyclopentadienes as both dienes and dienophiles. The halogen-substituted dimer products revealed that the preferential mode of addition was anti/anti; that is, both C5-substituents in the dimer product were located anti to the reacting face. Froese and co-workers (4) studied the cyclodimerization of substituted cyclopentadienes both experimentally and theoretically. Experimental results showed that the oxirane compound (the $CH_2$-O substituent at the C5-position) cyclodimerized to yield the syn/syn and anti/syn products in a 3:1 ratio. Calculations at the HF/6-31G(d) level gave activation barriers for the four different modes of endo addition: approximately 135.6, 147.3, 155.6, and 165.7 kJ $mol^{-1}$ for syn/syn, anti/syn, syn/anti, and anti/anti addition, respectively. Froese et al. noted the high degree of asynchronicity in the incipient bond formation in the

transition state (TS) structures.

For a number of decades, one of most heated debates in the literature involved the mechanism of the DA reaction. While few would argue today that the cycloaddition proceeds in a concerted manner through a single and generally asynchronous TS, researchers still probe this very issue. Mechanistic studies in recent years have considered both the possibility of competing pathways in the DA reaction as well as the feasibility of a diradical or stepwise mechanism. The majority confirm that diradical pathways to reaction are generally higher in energy and therefore less favourable than the concerted paths (5). The intrinsic reaction coordinate (IRC) of a chemical reaction can be determined computationally and has become an important tool in the search for answers to mechanistic questions. An IRC can serve as an illustration of the step-by-step changes in the molecular structure as it progresses through the reaction. For atypical reactions, the IRC calculation can provide a wealth of information that may prove useful in addressing some of the more ambiguous cases.

A communication in 2001 by Caramella et al. (6) was, to our knowledge, the first to identify the existence of the bispericyclic (BPC) TS in the endo dimerization of cyclopentadiene. This group examined the potential energy surface of the cyclopentadiene dimerization at the B3LYP/6-31G(d) level of theory. The endo TS structure (TS **7N**, ref. 6) displayed σ bond formation that was highly asynchronous and almost diradicaloid in nature. This structure had $C_2$ symmetry with one short incipient bond (1.94 Å) and two longer C---C interactions (both 2.90 Å). These structural characteristics, coupled with IRC results, led Caramella and co-workers to conclude that TS **7N** was a BPC TS, the point at which the

[4+2] and [2+4] cycloaddition paths have merged. The product side of the IRC calculation indicated an eventual breaking of the $C_2$ symmetry at a bifurcation point and the divergence of the path in two different directions, leading to the equivalent [4+2] and [2+4] cycloadducts.

According to the authors, at the beginning of the IRC (product side), the path steps toward a lower energy structure called a Cope TS (TS **9**, ref. 6), so-called because of its similarity to the TS of the Cope rearrangement as proposed by Woodward and Katz (7). The IRC calculated by Caramella avoided the Cope TS due to the divergence at the bifurcation point.

This group continued to investigate reactions which involved BPC TS structures and merged reaction paths (8), as did other researchers (9). We will also briefly explore the reaction path of the endo cyclopentadiene dimerization reaction with the aid of an IRC calculation. This part of the investigation is intended to address our curiosity in the interesting (but not unique) BPC TS structure and its path toward products. While the mechanism is still concerted, it is significantly different from what is considered "typical" for a DA reaction and is definitely more complicated.

### 4.2. Computational Methods

The present study focuses on the DA reactions of 5-substituted cyclopentadienes: the dimerization reactions (ie. identical reactants) are discussed first, followed by the DA reactions of 5-substituted cyclopentadienes with cyclopentadiene itself (termed for current

purposes as "mixed pairs"). Both endo-exo and anti-syn addition possibilities were considered for these model systems, and all possible TS structures for the different modes were determined. For each of the endo DA reactions, we have obtained two different first-order saddle points, the BPC TS (which may be referred to in the text as the endo DA TS) and the Cope TS structures. The reaction path of the exo cycloaddition involves a single DA TS only.

The BPC TS and Cope TS structures for the endo additions, the exo TS structures, and the ground state (GS) structures were all obtained at the HF/6-31G(d) and B3LYP/6-31G(d) levels of theory using the Gaussian 03 program (10). In addition, the BPC TS, the Cope TS, and the exo TS structures of the parent cyclopentadiene dimerization reaction were determined at the MP2/6-31G(d) and B3PW91/6-31G(d) levels. Vibrational frequency calculations confirmed that all GS structures had real frequencies and all TS structures had a single imaginary frequency. An IRC calculation was necessary for the exploration of the reaction path of the endo addition reaction; this calculation was performed at the B3LYP/6-31G(d) level for the parent cyclopentadiene endo dimerization. In addition, frequency calculations were performed at various points along the reaction path, also at the B3LYP/6-31G(d) level.

The notation, "diene face/dienophile face", is used throughout the text. For example, in the exo TS structure shown on the right in Figure 4.1, the diene (bottom) is substituted at C5 with Cl, as is the dienophile (top). The designation for this exo TS structure is "anti/anti".

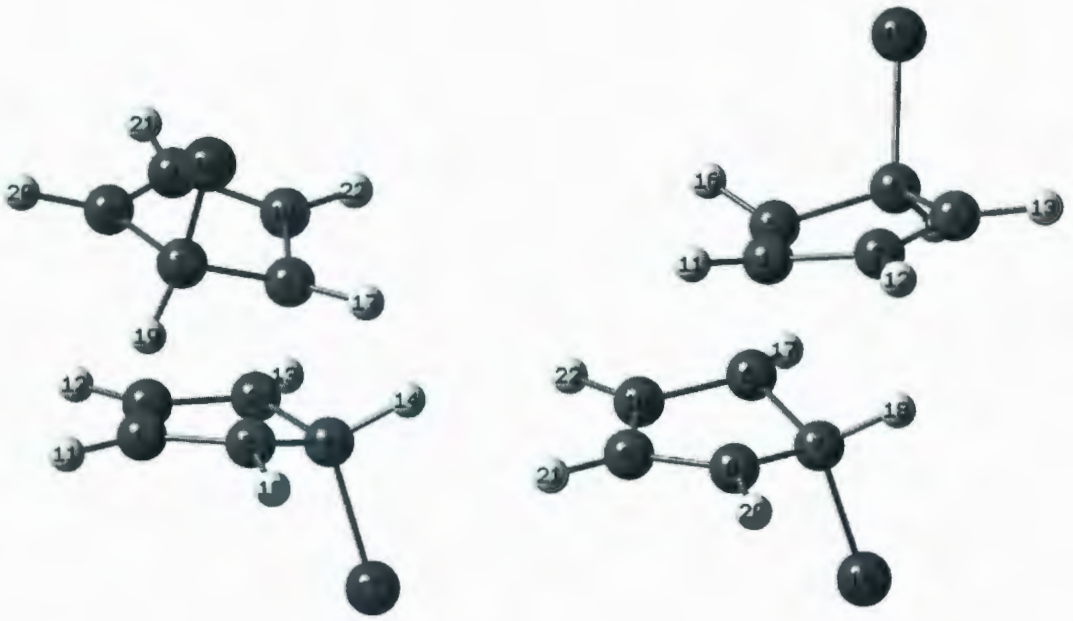

**Figure 4.1.** The numbering scheme for the endo DA TS and the exo DA TS structures, using the optimized geometries of the Cl-substituted cyclopentadiene anti/anti cycloadditions as examples.

## 4.3. Results and Discussion

### 4.3.1. Choice of Theory

Without question, one of the most important decisions to make before commencing a computational investigation of organic reactions is the level of theory and basis set to be used. Many studies of cycloaddition reactions have indicated that the inexpensive B3LYP density functional level of theory coupled with the 6-31G(d) basis set performs very well and provides reliable geometries and energies for reactants, products, and TS structures (11). For

this reason, the discussion will focus on the results obtained at the B3LYP level. All preliminary structures were determined at the HF/6-31G(d) level of theory and these results are included in Tables 4.1, 4.2, 4.3, and 4.4. However, discussion of the HF data will be minimal.

We were inclined to briefly examine the performance of two other methods incorporating electron correlation, in addition to B3LYP. Full geometry optimizations were performed at the MP2 and B3PW91 levels of theory using the same basis set; these theories are considered to be well-tested and reliable and can serve as a basis for comparison to the B3LYP results. The endo activation energies, endo-exo selectivities, and incipient bond lengths of the three TSs (DA endo/exo, Cope) for the parent cyclopentadiene dimerization are given in Table 4.1.

**Table 4.1.** A comparison of the endo activation energies and the endo-exo selectivities ($\Delta E_{act}$ and $\Delta E_{endo\text{-}exo}$ respectively, in kJ $mol^{-1}$) for the cyclopentadiene dimerization reaction at different levels of theory. The incipient bond lengths (Å) of the cyclopentadiene dimer TS structures are also shown.

| level of theory | $\Delta E_{act}$ (endo) | $\Delta E_{endo\text{-}exo}$ [a] | incipient bond lengths | | | | | | | |
|---|---|---|---|---|---|---|---|---|---|---|
| | | | BPC TS (DA endo) | | | Cope TS | | | exo TS | |
| | | | C10-C3 | C6-C5 | C8-C1 | C10-C3 | C6-C5 | C8-C1 | C5-C6 | C1-C8 |
| HF/6-31G(d) | 170.7 | -10.7 | 3.268 | 2.031 | 2.392 | 2.509 | 1.600 | 2.509 | 2.128 | 2.302 |
| MP2/6-31G(d) | 23.5 | -16.0 | 2.804 | 2.093 | 2.804 | 2.490 | 1.610 | 2.490 | 2.170 | 2.426 |
| B3LYP/6-31G(d) | 81.1 | -11.8 | 2.897 | 1.962 | 2.897 | 2.646 | 1.636 | 2.646 | 2.063 | 2.510 |
| B3PW91/6-31G(d) | 68.5 | -11.6 | 2.881 | 2.024 | 2.881 | 2.556 | 1.615 | 2.556 | 2.105 | 2.509 |

[a] The negative signs for the selectivities indicate the degree of endo preference.

Experimentally, the dimerization of cyclopentadiene yields only the endo product with a gas phase reaction barrier of 14.9 - 16.9 kcal $mol^{-1}$ (62.3 - 70.7 kJ $mol^{-1}$) (4). Many ab initio studies on DA reactions have shown that electron correlation is required to obtain activation barriers in close agreement with experiment. In general, calculations at the HF level tend to significantly overestimate activation barriers, whereas MP2 calculations often underestimate them; this is indeed the case for the present study as well (Table 4.1). The two DFT methods, however, reproduce the experimental endo activation barrier quite well (81.1 and 68.5 kJ $mol^{-1}$ for B3LYP/6-31G(d) and B3PW91/6-31G(d), respectively). In addition, Table 4.1 shows that the $\Delta E_{endo\text{-}exo}$ values for the HF and DFT methods do not differ appreciably (10.7, 11.8, and 11.6 kJ $mol^{-1}$ for the HF, B3LYP, and B3PW91 theories, respectively), while the MP2 calculations give a larger $\Delta E_{endo\text{-}exo}$ of 16.0 kJ $mol^{-1}$.

The effect of electron correlation on molecular geometry is clearly seen upon examination of the optimized endo DA TS structures depicted in Figure 4.2. Recall that the endo DA TS for the parent cyclopentadiene dimerization has been proposed to be a "mixture" of the [4+2] and [2+4] reaction paths (6). This implies that the endo DA TS is composed of two reactants that are identical and indistinguishable; in essence, both reactants can serve as either the diene or dienophile and the entire molecular structure has $C_2$ symmetry. This point will be confirmed quantitatively by B3LYP/6-31G(d) deformation energies (shown later in Tables 4.5 and 4.6).

HF

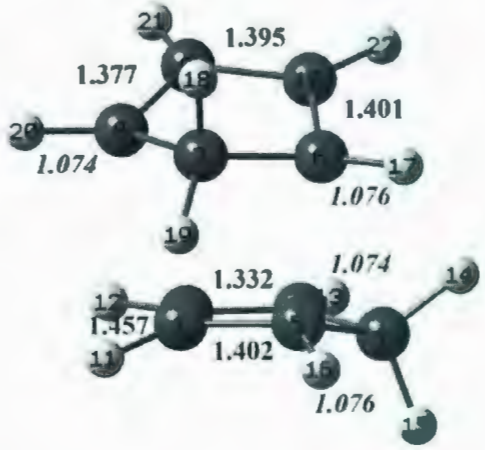


MP2

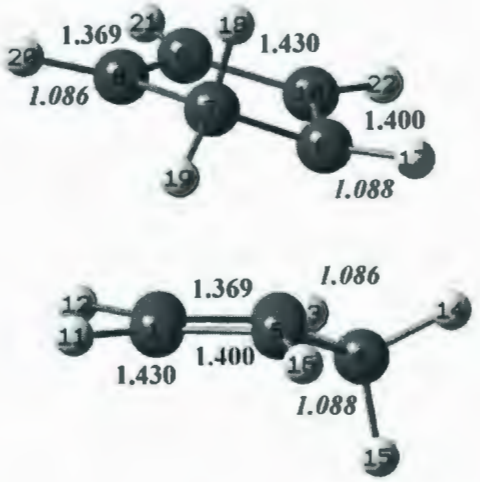


B3LYP

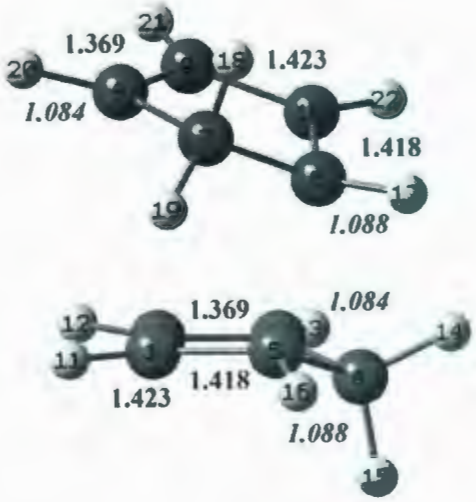


B3PW91

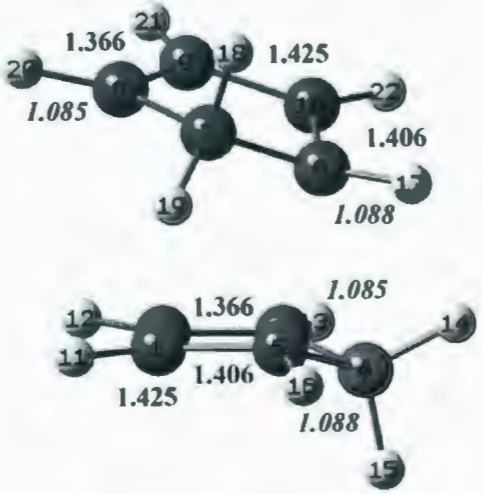


**Figure 4.2.** The optimized DA TS geometries for the cyclopentadiene endo dimerization at four levels of theory: HF, MP2, B3LYP, and B3PW91, all with the 6-31G(d) basis set. Selected C=C, C-C (**bold**) and C-H (***bold italic***) bonds are shown.

Figure 4.2 includes a selection of C=C, C-C, and C-H bonds of the endo DA TS structures for the parent cyclopentadiene dimer, obtained at the HF, MP2, B3LYP, and B3PW91 levels of theory. Table 4.1 contains the incipient bond lengths for these structures. It is evident that the HF method does not optimize to a structure that is $C_2$-symmetric, whereas the three levels incorporating electron correlation do yield the expected $C_2$ geometry. There was an attempt to obtain a $C_2$-symmetric endo DA TS structure for this cyclopentadiene dimer at HF/6-31G(d) using MUNgauss (12) by placing certain geometric constraints on the input structure. The result, interestingly, was a second-order saddle point. The two imaginary frequencies for this structure depict modes similar to what we will encounter later in the examination of the reaction coordinate in section 4.3.4. The imaginary frequency with the largest magnitude closely resembles the imaginary vibrational mode of the B3LYP/6-31G(d) optimized DA endo TS structure: mainly the strong C6---C5 vibration. The other smaller imaginary frequency represents a see-saw motion (alternating C10---C3 and C8---C1 stretches) similar to that of the Cope TS structure. These modes will be covered in more detail later. However, as seen in Table 4.1, the HF calculations do yield the proper $C_2$ symmetry for the lower energy Cope TS for the cyclopentadiene dimerization. It is necessary to point out that not all of the 5-substituted cyclopentadiene dimers studied here have $C_2$ symmetry; for example, the endo DA and Cope TS structures for the anti/syn cyclodimerizations all have $C_1$ symmetry. For those that are $C_2$-symmetric, HF calculations fail to yield the proper $C_2$ structures for the endo DA TSs throughout this study, regardless of substituent. In contrast, this method consistently gives the correct $C_2$-symmetric structures

for the $C_2$ Cope TSs.

Due to the importance of including electron correlation in these calculations and the inability of HF theory to achieve proper symmetry in particular structures, it was decided that the bulk of the discussion would focus on the analysis of the B3LYP data.

### 4.3.2. Diels-Alder Dimerization Reactions of 5-Substituted Cyclopentadienes

#### 4.3.2.1. Endo-Exo and Facial Selectivities

The DA reaction of two identical dienes allows for either of the reactants to act as the diene or the dienophile. Indeed, it is this very feature of the dimerization reaction that makes it interesting to study. Table 4.2 displays the HF/6-31G(d) and B3LYP/6-31G(d) calculated endo-exo selectivities for the 5-substituted cyclopentadiene dimerization reactions. All possible modes of addition were examined. The anti/syn and syn/anti endo DA TS structures are identical for both levels of theory.

**Table 4.2.** HF and B3LYP endo-exo selectivities (kJ $mol^{-1}$) for the dimerization reactions of 5-substituted cyclopentadiene and the DA reactions of 5-substituted cyclopentadiene with cyclopentadiene. Cyclopentadiene is represented in the table as "Cpd".

| 5-substituted Cpd dimers | | | | | |
|---|---|---|---|---|---|
| C5-substituent | level of theory | $\Delta E_{endo\text{-}exo}$ [a] | | | |
| | | anti/anti | anti/syn | syn/anti | syn/syn |
| $CH_2$-O | HF/6-31G(d) | -23.2 | -29.7 | -30.1 | -38.4 |
| | B3LYP/6-31G(d) | -23.9 | -25.2 | -27.7 | -36.1 |
| Cl | HF/6-31G(d) | -20.6 | -21.5 | -47.6 | -53.0 |
| | B3LYP/6-31G(d) | -22.7 | -19.1 | -45.1 | -50.0 |
| F | HF/6-31G(d) | -25.2 | -36.0 | -34.6 | -44.0 |
| | B3LYP/6-31G(d) | -23.8 | -29.0 | -30.8 | -43.3 |
| 5-substituted Cpd/Cpd mixed pairs | | | | | |
| C5-substituent | level of theory | $\Delta E_{endo\text{-}exo}$ [b] | | | |
| | | Cpd/X-Cpd anti | X-Cpd/Cpd anti | Cpd/X-Cpd syn | X-Cpd/Cpd syn |
| Cl | HF/6-31G(d) | -15.8 | -23.0 | -11.2 | -48.9 |
| | B3LYP/6-31G(d) | -15.9 | -18.2 | -12.2 | -44.4 |
| F | HF/6-31G(d) | -16.4 | -27.4 | -18.4 | -33.6 |
| | B3LYP/6-31G(d) | -14.7 | -20.6 | -18.6 | -31.2 |

[a] Anti/syn and syn/anti addition give identical endo TS structures.

[b] Cpd/X-Cpd anti and X-Cpd/Cpd anti give identical endo TS structures, as do Cpd/X-Cpd syn and X-Cpd/Cpd syn.

Because the dimerization reaction usually yields only endo adducts, many theoretical studies concentrate exclusively on the endo cycloaddition. Thus, very little information is available for exo TS structures and hence $\Delta E_{endo\text{-}exo}$ selectivities for these reactions. As expected, the 5-substituted cyclopentadiene dimerization overwhelmingly prefers the endo reaction path for the systems shown here. For the majority of the $\Delta E_{endo\text{-}exo}$ selectivities, the HF/6-31G(d) results are just slightly larger than those at B3LYP/6-31G(d). In all of the B3LYP cases, the largest $\Delta E_{endo\text{-}exo}$ is found for the syn/syn cyclodimerization, and the dimer with Cl at C5 has the largest endo preference, 50.0 kJ $mol^{-1}$. Anti/anti addition, in general, has the smallest $\Delta E_{endo\text{-}exo}$ selectivities; the values for $CH_2$-O, Cl, and F are 23.9, 22.7, and 23.8 kJ $mol^{-1}$ at the B3LYP level, respectively. Another marked difference is observed between anti/syn and syn/anti for the Cl substituent; the endo preference for syn/anti addition is more than twice that of anti/syn, whereas the $\Delta E_{endo\text{-}exo}$ quantities for anti/syn and syn/anti are quite similar for the other substituents. This indicates a relatively large activation barrier for the Cl-cyclopentadiene syn/anti exo dimerization, since the endo DA TSs for anti/syn and syn/anti are identical.

Discussions of facial selectivities have consistently occupied a large share of the research involving DA reactions. Tables 4.3 and 4.4 show the endo and exo (respectively) facial selectivities for the 5-substituted cyclopentadiene dimerization reactions. Again, we see that the HF/6-31G(d) results closely resemble those at the B3LYP level. The $\Delta E$ values displayed in these two tables are relative to the lowest energy endo (Table 4.3) and exo (Table 4.4) TS structures for each substituent.

**Table 4.3.** HF and B3LYP endo facial selectivities (kJ $mol^{-1}$) for the dimerization reactions of 5-substituted cyclopentadiene and the DA reactions of 5-substituted cyclopentadiene with cyclopentadiene.

| 5-substituted Cpd dimers | | | | |
|---|---|---|---|---|
| C5-substituent | level of theory | facial selectivities (endo) | | |
| | | anti/anti | anti/syn or syn/anti | syn/syn |
| $CH_2$-O | HF/6-31G(d) | 30.0 | 12 | 0 |
| | B3LYP/6-31G(d) | 25.9 | 13.3 | 0 |
| Cl | HF/6-31G(d) | 0 | 1.6 | 7.1 |
| | B3LYP/6-31G(d) | 0 | 6.4 | 10.3 |
| F | HF/6-31G(d) | 32.2 | 11 | 0 |
| | B3LYP/6-31G(d) | 33.2 | 16.4 | 0 |
| 5-substituted Cpd/Cpd mixed pairs | | | | |
| C5-substituent | level of theory | facial selectivities (endo) | | |
| | | Cpd/X-Cpd anti or X-Cpd/Cpd anti | Cpd/X-Cpd syn or X-Cpd/Cpd syn | |
| Cl | HF/6-31G(d) | 0 | 7.4 | |
| | B3LYP/6-31G(d) | 0 | 6.3 | |
| F | HF/6-31G(d) | 12.3 | 0 | |
| | B3LYP/6-31G(d) | 15.8 | 0 | |

**Table 4.4.** HF and B3LYP exo facial selectivities (kJ $mol^{-1}$) for the dimerization reactions of 5-substituted cyclopentadiene and the DA reactions of 5-substituted cyclopentadiene with cyclopentadiene.

| 5-substituted Cpd dimers | | | | | |
|---|---|---|---|---|---|
| C5-substituent | level of theory | facial selectivities (exo) | | | |
| | | anti/anti | anti/syn | syn/anti | syn/syn |
| $CH_2$-O | HF/6-31G(d) | 15.0 | 3.3 | 3.7 | 0 |
| | B3LYP/6-31G(d) | 13.8 | 2.5 | 5.0 | 0 |
| Cl | HF/6-31G(d) | 0 | 2.5 | 28.6 | 39.6 |
| | B3LYP/6-31G(d) | 0 | 2.7 | 28.8 | 37.6 |
| F | HF/6-31G(d) | 13.4 | 3.0 | 1.6 | 0 |
| | B3LYP/6-31G(d) | 13.7 | 2.2 | 4.0 | 0 |
| 5-substituted Cpd/Cpd mixed pairs | | | | | |
| C5-substituent | level of theory | facial selectivities (exo) | | | |
| | | Cpd/X-Cpd anti | X-Cpd/Cpd anti | Cpd/X-Cpd syn | X-Cpd/Cpd syn |
| Cl | HF/6-31G(d) | 0 | 7.2 | 2.8 | 40.4 |
| | B3LYP/6-31G(d) | 0 | 2.2 | 2.6 | 34.8 |
| F | HF/6-31G(d) | 10.3 | 21.3 | 0 | 15.2 |
| | B3LYP/6-31G(d) | 12.0 | 17.9 | 0 | 12.6 |

Beginning with the endo dimerization (Table 4.3), we see that syn/syn cyclodimerization is clearly preferred for both $CH_2$-O and F; anti/anti is the least favoured mode of addition. The anti/syn and syn/anti facial selectivities are identical due to their identical endo TS structures and the values fall approximately midway between syn/syn and anti/anti for these two substituents. The Cl substituent, however, exhibits a preference for anti/anti cyclodimerization, though not significantly so. In this case, the least preferred syn/syn addition is higher in relative energy by 10.3 kJ $mol^{-1}$ for B3LYP/6-31G(d).

The facial selectivities shown in Table 4.4 for the 5-substituted cyclopentadiene exo dimerization reaction exhibit preferences similar to those of the endo reaction. Syn/syn addition again yields the favoured TS structure and anti/anti is the least favoured for the $CH_2$-O and F substituents. However, for both $CH_2$-O and F, the degree of anti/anti facial selectivity for exo addition is much smaller than what was calculated for endo addition. Also, the anti/syn and syn/anti facial selectivities are quite small for the exo cyclodimerizations, with one notable exception: the syn/anti addition with Cl as the substituent (facial selectivity of 28.8 kJ $mol^{-1}$ for B3LYP/6-31G(d)). Like the endo facial selectivities for Cl displayed in Table 4.3, we see that the exo dimerization prefers anti/anti addition. As well, the syn/syn exo TS structure is remarkably high in energy relative to the anti/anti exo TS structure. Overall, the most significant facial selectivities for these exo cycloadditions are observed for the Cl substituent. This is quite different than what was seen with the endo facial selectivities, in which the Cl dimers exhibited only minor differences in facial selectivity.

#### 4.3.2.2. Activation and Deformation Energies

Since the focus of this discussion centers on the B3LYP/6-31G(d) results, this level of theory was used to further examine the DA and Cope TSs for the 5-substituted cyclopentadiene dimerization reactions. Table 4.5 features the activation energies ($\Delta E_{act}$) and deformation energies ($\Delta E^{diene}_{def}$ and $\Delta E^{dph}_{def}$ for the diene and dienophile, respectively) calculated at this level of theory.

**Table 4.5.** Activation and deformation energies (kJ $mol^{-1}$) for the Diels-Alder dimerization of 5-substituted cyclopentadiene at the B3LYP/6-31G(d) level of theory.

| C5-substituent | | $\Delta E_{act}$ | | $\Delta E_{def}$ | | | | | |
|---|---|---|---|---|---|---|---|---|---|
| | | endo | exo | $\Delta E^{diene}_{def}$ (endo) | $\Delta E^{dph}_{def}$ (endo) | $\Delta E^{diene}_{def}$ (Cope) | $\Delta E^{dph}_{def}$ (Cope) | $\Delta E^{diene}_{def}$ (exo) | $\Delta E^{dph}_{def}$ (exo) |
| H | - | 81.1 | 92.9 | 52.7 | 52.7 | 126.4 | 126.4 | 66.6 | 44.4 |
| $CH_2$-O | anti/anti | 74.6 | 98.5 | 50.8 | 50.6 | 146.3 | 146.3 | 71.5 | 45.3 |
| | anti/syn | 61.9 | 87.2 | 45.8 | 46.7 | 140.8 | 123.6 | 70.0 | 41.2 |
| | syn/anti | 61.9 | 89.6 | 46.7 | 45.8 | 123.6 | 140.8 | 63.4 | 45.7 |
| | syn/syn | 48.6 | 84.7 | 42.5 | 42.4 | 116.9 | 116.8 | 62.7 | 41.3 |
| Cl | anti/anti | 57.5 | 80.2 | 43.4 | 43.4 | 141.3 | 141.3 | 59.9 | 41.0 |
| | anti/syn | 63.8 | 82.9 | 41.0 | 51.0 | 142.2 | 140.4 | 60.7 | 44.9 |
| | syn/anti | 63.8 | 109.0 | 51.0 | 41.0 | 140.4 | 142.2 | 80.2 | 48.6 |
| | syn/syn | 67.8 | 117.8 | 49.1 | 49.0 | 140.7 | 140.7 | 81.5 | 52.0 |
| F | anti/anti | 55.1 | 78.9 | 42.2 | 42.2 | 159.5 | 159.5 | 60.2 | 38.9 |
| | anti/syn | 38.3 | 67.3 | 37.2 | 34.4 | 153.6 | 129.6 | 60.4 | 34.2 |
| | syn/anti | 38.3 | 69.1 | 34.4 | 37.2 | 129.6 | 153.6 | 54.6 | 42.1 |
| | syn/syn | 21.9 | 65.2 | 30.5 | 30.5 | 121.5 | 121.5 | 54.7 | 36.9 |

Deformation energy represents the amount of energy required to "deform" the reactant diene / dienophile from its GS structure to its form in the TS structure; the TS "fragment" energy is obtained via a single-point energy calculation of the diene / dienophile fragment in the optimized TS structure. The $\Delta E_{def}$ is usually the largest contributor to $\Delta E_{act}$ for a reaction.

The DA endo and Cope TSs for the anti/anti and syn/syn cyclodimerizations contain a pair of reactants that are identical; this means that the $C_2$ symmetry renders the TS fragments indistinguishable. For these two modes of addition, the $C_2$ symmetry of the endo and Cope TS structures is confirmed by the identical calculated $\Delta E^{diene}_{def}$ and $\Delta E^{dph}_{def}$ for each substituent. This somewhat unusual occurrence of diene / dienophile indistinguishability is only possible in cases where the reactants are identical, both are dienes, and there is $C_2$ symmetry at the TS (in this case, the anti/anti and syn/syn addition of two identical 5-substituted cyclopentadienes). The four reactive carbon centers (two for each reactant) must be located in the optimized TS structure such that both [4+2] and [2+4] interactions are possible. This is the essence of the BPC TS, an example of which is depicted in Figure 4.3.

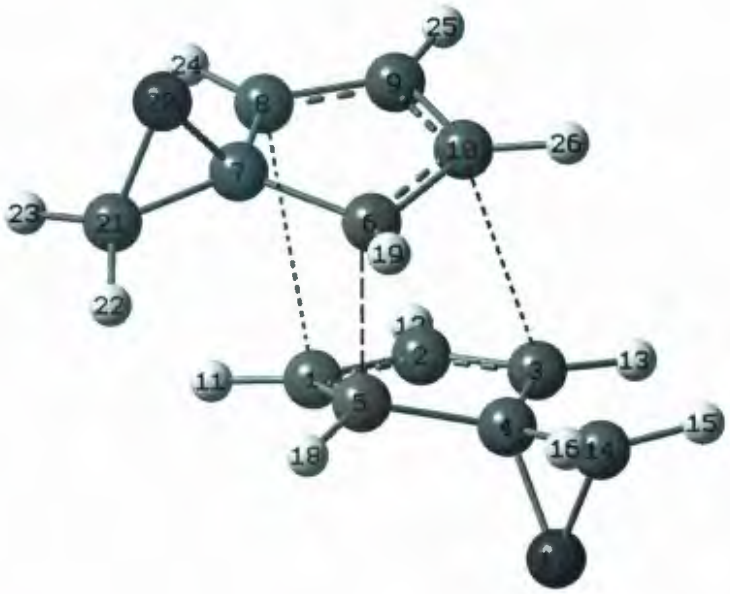


**Figure 4.3.** The BPC TS structure for the $CH_2$-O-substituted endo anti/anti cyclopentadiene cyclodimerization.

Together, the reactant deformation energies ($\Delta E^{diene}_{def} + \Delta E^{dph}_{def}$) for each TS structure yield a total deformation energy ($\Delta E^{total}_{def}$) for that particular cycloaddition, and this quantity is typically larger than $\Delta E_{act}$. The remaining component of the $\Delta E_{act}$ is the interaction energy, $\Delta E_{int}$ (not shown), which has a negative value and indicates a stabilization of the reactant fragments in forming the TS. Interaction energies will not be addressed in the present study.

Table 4.5 shows that the modes of addition with larger $\Delta E_{act}$ have generally larger values for $\Delta E^{diene}_{def}$ and $\Delta E^{dph}_{def}$, as would be expected. The $\Delta E^{total}_{def}$ quantities for the exo dimerizations are all larger than those of the corresponding endo reactions, some significantly

so. We also notice that the diene deformation energies for the exo additions exceed the dienophile deformation energies in all instances studied here, in some cases by as much as 30 kJ $mol^{-1}$. This is not unusual, since more bonds are broken / formed in the diene during the reaction.

The quantities shown in Table 4.5 indicate some noteworthy features of the endo cyclodimerization and the endo and Cope TS structures. First, the parent endo DA TS structure yields the greatest $\Delta E^{total}_{def}$ (105.4 kJ $mol^{-1}$), more than any other endo TS examined here. Since the H atoms at the C5 positions of the reactants are not large nor very sterically-hindering, this would not be an expected outcome. However, it is thought that the relatively short C6-C5 incipient bond length of the parent endo TS structure (1.962 Å) may help to explain the large degree of reactant deformation. Clearly, the large $\Delta E^{total}_{def}$ necessarily leads to a large $\Delta E_{act}$ (81.1 kJ $mol^{-1}$) and thus a higher reaction barrier. It takes more "effort" to reach this TS structure, and the reactant fragments tend to deform to a greater degree and approach each other more closely. The result is a later and "tighter" TS structure with shorter incipient bond lengths. The C6-C5 distance in the other endo TS structures is about 0.05-0.20 Å longer than in the parent cyclopentadiene endo TS structure.

On the opposite end of the scale (refer to Table 4.5), we see that the F-substituted syn/syn endo dimerization has both the lowest $\Delta E_{act}$ and the smallest $\Delta E^{total}_{def}$ of all the reactions studied here, regardless of substituent or mode of addition. As previously mentioned in section 4.3.2.1, this TS structure is definitely the favoured one for F-substituted cyclopentadiene dimerization. The C6-C5 incipient bond length for this structure,

interestingly, is relatively short (2.090 Å, compared to 2.139 Å for anti/syn and 2.165 Å for anti/anti addition). Considering the low activation barrier and the small degree of deformation in the reactant fragments, it is believed that there must be some very favourable interactions occurring in the syn/syn TS structure that override the possible steric problems of bringing two F-substituted dienes so close together in the syn/syn arrangement.

An excellent correlation between activation energy and total deformation energy for both the endo and exo cyclodimerizations demonstrates the integral role of cyclopentadiene deformation in the feasibility of these reactions. Plots of $\Delta E_{act}$ versus $\Delta E^{total}_{def}$ are illustrated in Figure 4.4.

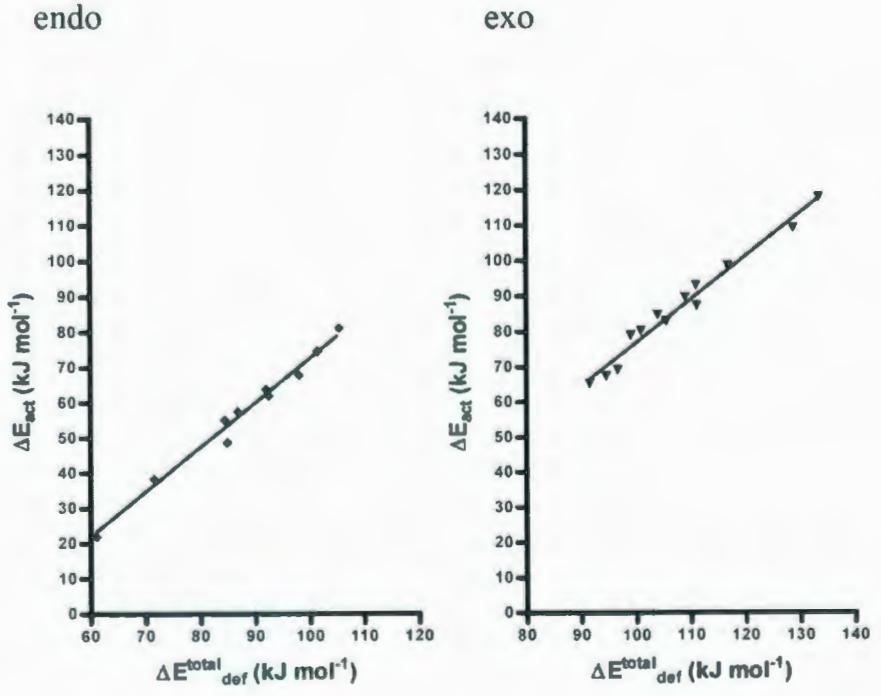


**Figure 4.4.** Plots of $\Delta E_{act}$ versus $\Delta E^{total}_{def}$ (kJ mol$^{-1}$) for the endo and exo cyclodimerization reactions included in Table 4.5.

With $R^2$ values of 0.98 and 0.97 (endo and exo, respectively) and nearly identical slopes, the regression lines clearly display a relationship between increasing activation barrier (and thus decreasing reactivity) and increasing total reactant deformation. In general, one of the reasons for the endo preference in these dimerization reactions is the smaller amount of energy required to deform the diene and dienophile fragments into optimal geometries for the endo TS structure. Since the combined $\Delta E_{def}$ represents the largest percentage of $\Delta E_{act}$, it can be inferred that the relationship depicted in Figure 4.4 demonstrates the importance of the deformation energy in determining the barrier to reaction and thus the degree of endo-exo selectivity.

To this point, the Cope TS has not been addressed to any great degree. The endo-exo selectivity of the cyclodimerization is determined by the $\Delta E_{act}$ of the endo and exo TS structures. Consequently, the Cope TS plays no role in $\Delta E_{endo\text{-}exo}$. It is, however, an integral part of the endo dimerization potential energy curve, and since the endo cycloaddition path is the preferred one, a discussion of the Cope TS is in order. Table 4.5 lists the $\Delta E^{diene}{}_{def}$ and $\Delta E^{dph}{}_{def}$ for the Cope TS structures of the endo reaction paths investigated. The degree of deformation in these structures is substantial, which is expected since the Cope TS is later on the potential energy curve. The total deformation energies ($\Delta E^{total}{}_{def}$) for these structures vary from 233.0 kJ $mol^{-1}$ to 319.0 kJ $mol^{-1}$. The structures themselves, however, do not reveal any significant geometric changes, only that the fragments are now closer together. On average, the distances between C10-C3, C6-C5, and C8-C1 are shorter by approximately 0.4 Å. Figure 4.5 illustrates this progression.

BPC TS

Cope TS

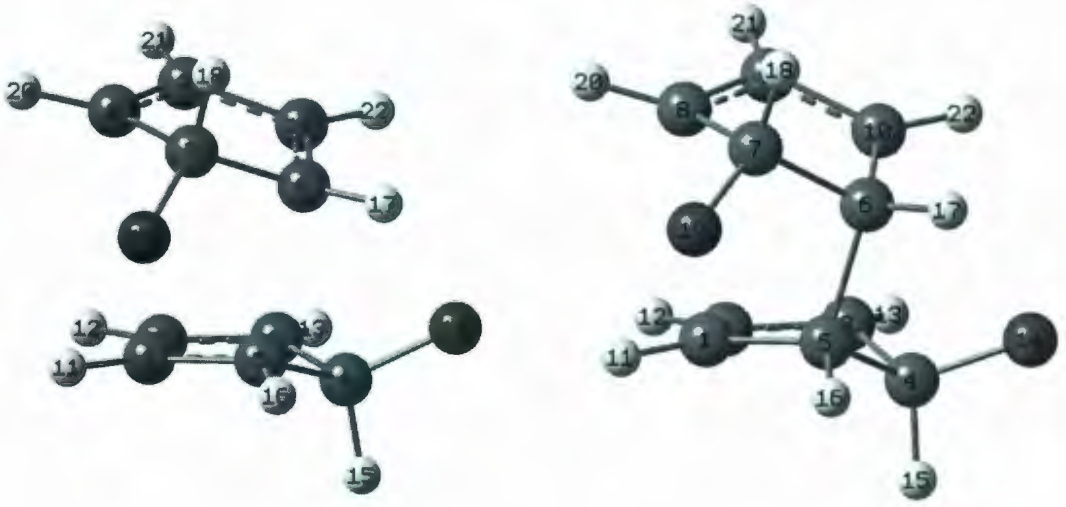

**Figure 4.5.** The BPC TS (or endo DA TS) and the Cope TS structures for the F-substituted cyclopentadiene syn/syn cyclodimerization.

The individual deformation energies highlight some intriguing features of the Cope TS structures. Notably, the cyclic and arguably the most sterically-hindering $CH_2$-O substituent has the smallest deformation energies in the syn/syn Cope TS structures, smaller than even H! In contrast, the F-substituted anti/anti Cope TS has the largest $\Delta E^{total}_{def}$ of any other substituent in any other cycloaddition mode. This is curious because F is not considered to be a sterically-demanding substituent (it is, arguably, "smaller" than H), and the two F's in this particular Cope TS are on opposite sides of the structure (anti/anti).

Hence, one would not expect a large amount of reactant deformation in this case.

It is important to remember that the Cope TS is a component of the potential energy curve of the endo dimerization reaction. As such, it is lower in energy than the DA TS, and has a lower (perhaps significantly so) $\Delta E_{act}$. The incredibly large deformation energies that we see for these Cope TSs is expected because the progression toward products has continued and the reactant fragments are much closer together. More importantly, the C6-C5 incipient bond length has shortened to such a degree that it is within 0.05 Å of forming a C-C $\sigma$ bond. This is depicted in Figure 4.5. Thus, the calculation of the reactant deformation energies involves a "breaking" of that C-C bond, which has an associated bond energy; this translates into large $\Delta E_{def}$. The stabilizing interaction between the reactant fragments has also increased very significantly, and this would be reflected in the comparably large and negative $\Delta E_{int}$ values.

We will revisit the parent cyclopentadiene endo dimerization later in this study, as we probe the endo reaction path in section 4.3.4. We now turn to the second system of interest, the "mixed pairs".

### 4.3.3. Diels-Alder Reactions of Cyclopentadiene with 5-substituted Cyclopentadiene

The analysis and discussion of the dimers in section 4.3.2 emphasizes some of the more interesting details of this DA cycloaddition reaction. For instance, there is $C_2$ symmetry in a few of the DA and Cope TSs, and the equivalence of the two cyclopentadiene reactants at these points on the potential energy curve is additionally verified by identical $\Delta E_{def}$ for each fragment of the TS structures. The "mixed pairs", on the other hand, involve 5-substitution on only one of the cyclopentadiene reactants; in these TS structures, the diene / dienophile roles are unquestionable.

#### 4.3.3.1. Endo-exo and Facial Selectivities

The bottom of Table 4.2 shows the HF/6-31G(d) and B3LYP/6-31G(d) endo-exo selectivities for the DA reaction of 5-substituted cyclopentadiene (Cl or F) with cyclopentadiene. As with the dimers in the previous discussion, all possible modes of addition were investigated. The Cpd/X-Cpd anti and the X-Cpd/Cpd anti endo TS structures are identical for both levels of theory, as are their syn endo counterparts.

The clear preference for the endo TS structures is indicated by the considerable negative values for $\Delta E_{endo\text{-}exo}$. The HF/6-31G(d) results compare well with the DFT values in some cases; others differ by as much as 7 kJ $mol^{-1}$. For the B3LYP/6-31G(d) cases, we see that the magnitudes of $\Delta E_{endo\text{-}exo}$ for the Cl and F mixed pairs are not as large and decisive as those for the Cl and F dimers. Obviously, the presence of the second C5-substituent in the

dimer TS structures affects the reactivity (and the endo-exo selectivity), even if that second Cl or F atom is in an anti position and far removed from the reaction center. The largest selectivities are found for the X-Cpd/Cpd syn cycloaddition (44.4 kJ $mol^{-1}$ and 31.2 kJ $mol^{-1}$ endo preference for Cl and F, respectively). To a much lesser degree, the next largest endo preference for both Cl and F is the X-Cpd/Cpd anti addition reaction, although the first three modes shown in Table 4.2 do not differ appreciably from one another (Cpd/X-Cpd anti, X-Cpd/Cpd anti, and Cpd/X-Cpd syn have an endo-exo selectivity range of about 6 kJ $mol^{-1}$ for both substituents). From the $\Delta E_{endo-exo}$ values shown in Table 4.2, we see that the endo preference is most pronounced in those cases where the C5-substituent is located on the diene. However, since the Cpd/X-Cpd and X-Cpd/Cpd TS structures are identical for both anti and syn endo cycloaddition, it can be stated that this greater endo preference must be due to the relatively higher activation barriers for the X-Cpd/Cpd exo TS structures, particularly in the syn addition case.

The endo and exo facial selectivities for the mixed DA reactions are displayed at the bottom of Tables 4.3 and 4.4, respectively. Due to the equivalency of the Cpd/X-Cpd and X-Cpd/Cpd TS structures for both anti and syn endo cycloaddition, the facial selectivity question reduces to the simple preference between anti and syn (Table 4.3). As only two substituents were examined in this section of the present study, few conclusions can be drawn. However, the results at the HF/6-31G(d) and B3LYP/6-31G(d) levels of theory both show that Cl and F have quite different facial preferences for these reactions. According to the B3LYP/6-31G(d) data, Cl has a moderate preference to be in the anti position (of the

diene or the dienophile, since the two TSs are equivalent), while F has a strong preference to be in the syn position. This is similar to what was observed for the dimerization reactions involving Cl and F.

Table 4.4 presents the four possible modes of exo cycloaddition and their relative facial selectivities. For the Cl substituent, we see that the Cpd/Cl-Cpd anti exo TS, in which the Cl is in the anti position at C5 on the dienophile, is the favoured exo TS structure. The DFT results indicate that the only exo TS that is significantly disfavoured is the Cl-Cpd/Cpd syn TS structure; it is higher in relative energy by 34.8 kJ $mol^{-1}$. This corresponds nicely with the previous observation of the quite large $\Delta E_{endo\text{-}exo}$ value for Cl-Cpd/Cpd syn addition. Since the Cpd/Cl-Cpd syn and Cl-Cpd/Cpd syn endo TS structures are equivalent, the endo-exo selectivity of 44.4 kJ $mol^{-1}$ (refer to Table 4.2) is clearly due to the very high activation barrier (and low reactivity) of the Cl-Cpd/Cpd syn exo TS structure. For the F substituent, the Cpd/F-Cpd syn exo TS structure has the lowest energy of the four possible modes. The B3LYP results show that the Cpd/F-Cpd anti and the F-Cpd/Cpd syn exo TSs are close in relative energy (12.0 and 12.6 kJ $mol^{-1}$, respectively), while the least preferred exo TS in terms of facial selectivity is the F-Cpd/Cpd anti structure (17.9 kJ $mol^{-1}$). While this particular exo TS is the highest in relative energy, this does not translate to the largest $\Delta E_{endo\text{-}exo}$, simply because the F-Cpd/Cpd anti endo TS structure is also relatively high in energy. The largest endo-exo selectivity is observed for the F-Cpd/Cpd syn addition (31.2 kJ $mol^{-1}$, Table 4.2), in which the exo TS energy is moderately high but the endo TS energy is very low. Clearly, the substituents of choice for the present study have very different facial

preferences. In general, Cl prefers to be anti to the incoming diene or dienophile in the TS structure, and F prefers the syn position. These differences are more distinct in the endo TS structures.

#### 4.3.3.2. Activation and Deformation Energies

The $\Delta E_{act}$ and $\Delta E_{def}$ values for the 5-substituted cyclopentadiene / cyclopentadiene DA reactions are presented in Table 4.6. Again, the focus of the analysis remains on the B3LYP/6-31G(d) results, and the table includes the activation energies and fragment deformation energies ($\Delta E^{diene}_{def}$ and $\Delta E^{dph}_{def}$) calculated at this level of theory for all three TS structures.

**Table 4.6.** Activation and deformation energies (kJ $mol^{-1}$) for the Diels-Alder reactions of 5-substituted cyclopentadiene with cyclopentadiene at the B3LYP/6-31G(d) level of theory.

| C5-substituent | | $\Delta E_{act}$ | | $\Delta E_{def}$ | | | | | |
|---|---|---|---|---|---|---|---|---|---|
| | | endo | exo | $\Delta E^{diene}_{def}$ (endo) | $\Delta E^{dph}_{def}$ (endo) | $\Delta E^{diene}_{def}$ (Cope) | $\Delta E^{dph}_{def}$ (Cope) | $\Delta E^{diene}_{def}$ (exo) | $\Delta E^{dph}_{def}$ (exo) |
| Cl | Cpd/X-Cpd anti | 66.7 | 82.6 | 49.2 | 46.1 | 130.0 | 140.9 | 62.8 | 42.9 |
| | X-Cpd/Cpd anti | 66.7 | 84.8 | 46.1 | 49.2 | 140.9 | 130.0 | 63.3 | 42.6 |
| | Cpd/X-Cpd syn | 73.0 | 85.2 | 46.4 | 53.9 | 129.0 | 139.4 | 61.9 | 47.3 |
| | X-Cpd/Cpd syn | 73.0 | 117.4 | 53.9 | 46.4 | 139.4 | 129.0 | 84.0 | 49.3 |
| F | Cpd/X-Cpd anti | 66.1 | 80.8 | 46.5 | 47.1 | 137.0 | 152.5 | 59.1 | 43.3 |
| | X-Cpd/Cpd anti | 66.1 | 86.6 | 47.1 | 46.5 | 152.5 | 137.0 | 66.8 | 40.4 |
| | Cpd/X-Cpd syn | 50.2 | 68.8 | 40.3 | 42.1 | 129.2 | 119.4 | 58.9 | 38.4 |
| | X-Cpd/Cpd syn | 50.2 | 81.4 | 42.1 | 40.3 | 119.4 | 129.2 | 61.6 | 43.7 |

The DA endo and Cope TSs of the mixed pair systems have identical Cpd/X-Cpd and X-Cpd/Cpd endo TS structures for both anti and syn addition. The facial preferences for addition are clearly seen in the values of the endo $\Delta E_{act}$; for instance, the endo activation energy for the equivalent anti pair for the Cl substituent (66.7 kJ $mol^{-1}$) is less than that of the Cl syn pair (73.0 kJ $mol^{-1}$). The opposite holds true for the F substituent; the identical anti pair is approximately 16 kJ $mol^{-1}$ higher in energy than the favoured syn pair. Interestingly, many of the exo TS structures have very similar activation barriers. Of the eight exo TS structures examined here, six of them have $\Delta E_{act}$ values in the range of 80.8 - 86.6 kJ $mol^{-1}$. As suspected, the reaction barrier for Cl-Cpd/Cpd syn exo addition is quite high, thus confirming the conclusion that this particular reaction path is a very unlikely course for this DA cycloaddition.

Overall, we see quite similar values obtained for the $\Delta E^{diene}_{def}$ and $\Delta E^{dph}_{def}$ for each of the endo DA reactions studied here. The endo cycloaddition that has the largest $\Delta E^{total}_{def}$ is the case in which the Cl-cyclopentadiene fragment adds syn to the other cyclopentadiene reactant. Regardless of whether this Cl-substituted fragment is the diene or dienophile (since the resulting TSs are identical), it does have a moderately larger $\Delta E_{def}$ than its cyclopentadiene partner in the TS; there is a difference of 7.5 kJ $mol^{-1}$ between the two fragments. The exo deformation energies for the mixed pairs show a trend similar to that of the dimers: the $\Delta E^{diene}_{def}$ energies exceed the values for $\Delta E^{dph}_{def}$ in every case. The Cl-Cpd/Cpd syn exo TS structure, in particular, owes its significantly high $\Delta E_{act}$ to the large degree of deformation (84.0 kJ $mol^{-1}$) required by the Cl-cyclopentadiene to distort into its

optimal structure for the TS. In contrast, the Cpd/F-Cpd syn exo TS has a relatively small barrier to reaction (68.8 kJ $mol^{-1}$). The smaller $\Delta E^{total}_{def}$ for this cycloaddition is consistent with the lower activation barrier.

It is interesting to note the lack of correlation between the incipient bond length (a measure of the lateness / earliness of a TS) and the magnitude of the activation energies for the mixed pair reactions considered here. For example, the Cl-Cpd/Cpd syn exo TS has a very high activation energy (117.4 kJ $mol^{-1}$), which tends to imply a large deformation in the fragments and a greater effort to reach the TS structure. This might infer that the TS structure must be later and thus "tighter"; we see that the C6-C5 incipient bond length for this structure is 2.093 Å. In comparison, the Cl-Cpd/Cpd anti exo TS has a much smaller activation energy (84.8 kJ $mol^{-1}$), yet the C6-C5 incipient bond is even shorter (2.069 Å). For the F substituent, we can consider three different TS structures: the F-Cpd/Cpd anti endo TS ($\Delta E_{act}$ = 66.1 kJ $mol^{-1}$, C6-C5 length = 2.066 Å), the F-Cpd/Cpd anti exo TS ($\Delta E_{act}$ = 86.6 kJ $mol^{-1}$, C6-C5 length = 2.097 Å), and the Cpd/F-Cpd syn exo TS ($\Delta E_{act}$ = 68.8 kJ $mol^{-1}$, C6-C5 length = 2.088 Å). As shown, there is no clear trend in the magnitudes of the activation energies and the lengths of the incipient bonds. The F-Cpd/Cpd anti exo TS and the Cpd/F-Cpd syn exo TS differ in $\Delta E_{act}$ by 17.8 kJ $mol^{-1}$, yet their C6-C5 incipient bond lengths differ by only 0.009 Å.

The $\Delta E^{diene}_{def}$ and $\Delta E^{dph}_{def}$ for the Cope TS structures associated with the endo 5-substituted cyclopentadiene / cyclopentadiene DA reactions are included in Table 4.6. We observe, much like the dimers considered earlier, remarkably large deformation energies for

both fragments of the Cope TS structures, varying from 119.4 kJ $mol^{-1}$ to 152.5 kJ $mol^{-1}$. The anti and syn cycloadditions involving the F substituent, in particular, reveal some interesting aspects of these structures. The F-cyclopentadiene, as either a diene or dienophile, undergoes a very large degree of deformation ($\Delta E_{def}$ = 152.5 kJ $mol^{-1}$) for the anti Cope TS, and when combined with the $\Delta E_{def}$ of the other cyclopentadiene fragment, the $\Delta E^{total}_{def}$ becomes 289.5 kJ $mol^{-1}$. The C6-C5 incipient bond length of the anti Cope TS is 1.611 Å; thus, this incipient bond has a very high percentage of σ character. In comparison, when the F-cyclopentadiene reacts syn to its partner, the $\Delta E^{total}_{def}$ for the syn Cope TS is 248.6 kJ $mol^{-1}$ and its C6-C5 incipient bond length is 1.626 Å. The C6-C5 incipient bond length in the anti Cope TS is shorter by 0.015 Å, meaning the C6-C5 bond is more "formed" in the anti Cope TS and thus requires more energy to "break" it in the fragmentation of the TS structure; hence the larger $\Delta E^{total}_{def}$. In addition, it is typically the 5-substituted cyclopentadiene fragment that demands the largest degree of deformation, and we see that this is not the case for the F-substituted syn cycloaddition reaction. It is clear that there are stabilizing and destabilizing factors in all of the TS structures in which F is involved (for both the dimers and mixed pairs) that cannot be pinpointed without very detailed examinations. It is sufficient to state here that this highly electronegative substituent plays a more significant role in selectivity than its relatively small size would indicate.

We now turn the focus of the discussion back to the endo dimerization reaction of cyclopentadiene.

### 4.3.4. The Endo Cyclopentadiene Dimerization: The Reaction Coordinate

The examination of the reaction path for the endo cyclopentadiene dimerization was prompted by a number of factors. The existence of the BPC TS as reported by Caramella et al. (6) was intriguing in its own right, but we were also interested in the Cope TS, the lower energy first-order saddle point. At first glance, the structures of these two TSs seem to be almost identical, but upon closer examination, one can see that the Cope TS structure is "tighter"; that is, the fragments have moved closer together. Further examination reveals an even more interesting aspect: the molecular motions attributed to the imaginary vibrational mode of these two TS structures are very different from each other. Caramella explicitly states that the B3LYP/6-31G(d) IRC begins by stepping toward the Cope TS, but *never reaches it.* So the question posed is, what is the relevance of the Cope TS to the dimerization reaction and how is it connected to the BPC TS, if at all? We performed our own IRC calculation at the B3LYP/6-31G(d) level of theory and then analyzed the product side of the reaction coordinate point by point to discern what was happening in the region of the potential energy curve between the BPC TS and the Cope TS.

Since the molecular structures on the path to products are quite similar in appearance, one would expect to see very similar vibrational modes for the structures along the path as well. There are two distinct imaginary vibrational modes, each dominating at different points on the reaction curve. The first, as pointed out by Caramella and his group, is a strong vibration of C6---C5 (as per our numbering scheme; refer to Figure 4.1) and very minute movements of C10---C3 and C8---C1. This symmetric stretch essentially depicts the

formation of the C6-C5 incipient bond. The animation of the other imaginary vibrational mode shows that the C6 and C5 are no longer moving relative to one another; that is, the C6---C5 stretch has disappeared. Instead, the C10---C3 and C8---C1 vibrations now dominate, moving in an alternating "see-saw" motion or asymmetric stretch. The imaginary vibrational mode of the BPC TS (or endo DA TS) is the incipient C6-C5 bond forming motion; this mode embodies the nature of the cyclopentadiene endo dimerization because it incorporates the atomic movements of both the [4+2] and [2+4] reaction paths. The see-saw vibrational mode is the imaginary frequency of the Cope TS. Figure 4.6 illustrates the displacement vectors for these two vibrational modes.

BPC TS

Cope TS

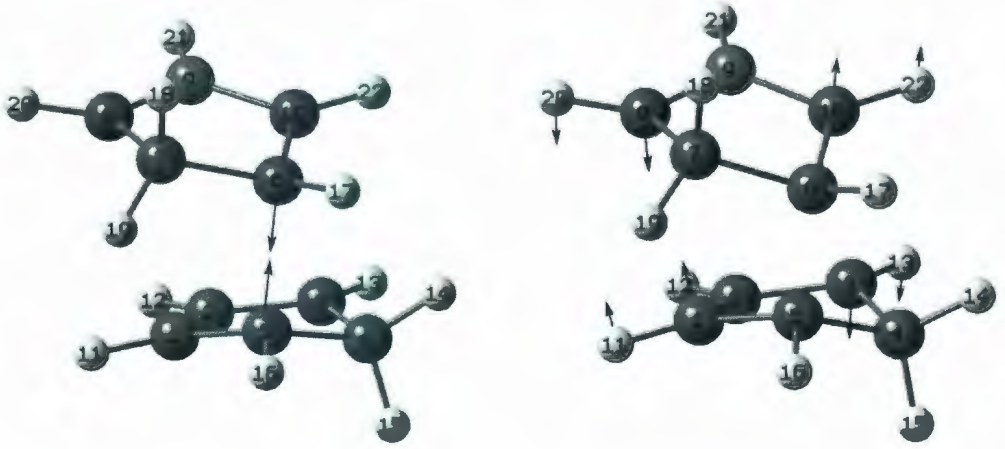

**Figure 4.6.** The BPC TS and the Cope TS structures for the parent cyclopentadiene endo dimerization reaction. The arrows depict the main displacement vectors for the imaginary vibrational modes of each structure.

The potential energy curve obtained from the IRC calculation (representing the path from the BPC TS towards products only) is shown in Figure 4.7. The Opt = CalcAll option was employed so that the analytical Hessian was recalculated for each optimized point along the path. Frequency calculations were performed for a selection of points on the curve; this data, along with the corresponding energies and incipient bond lengths, are presented in Table 4.7.

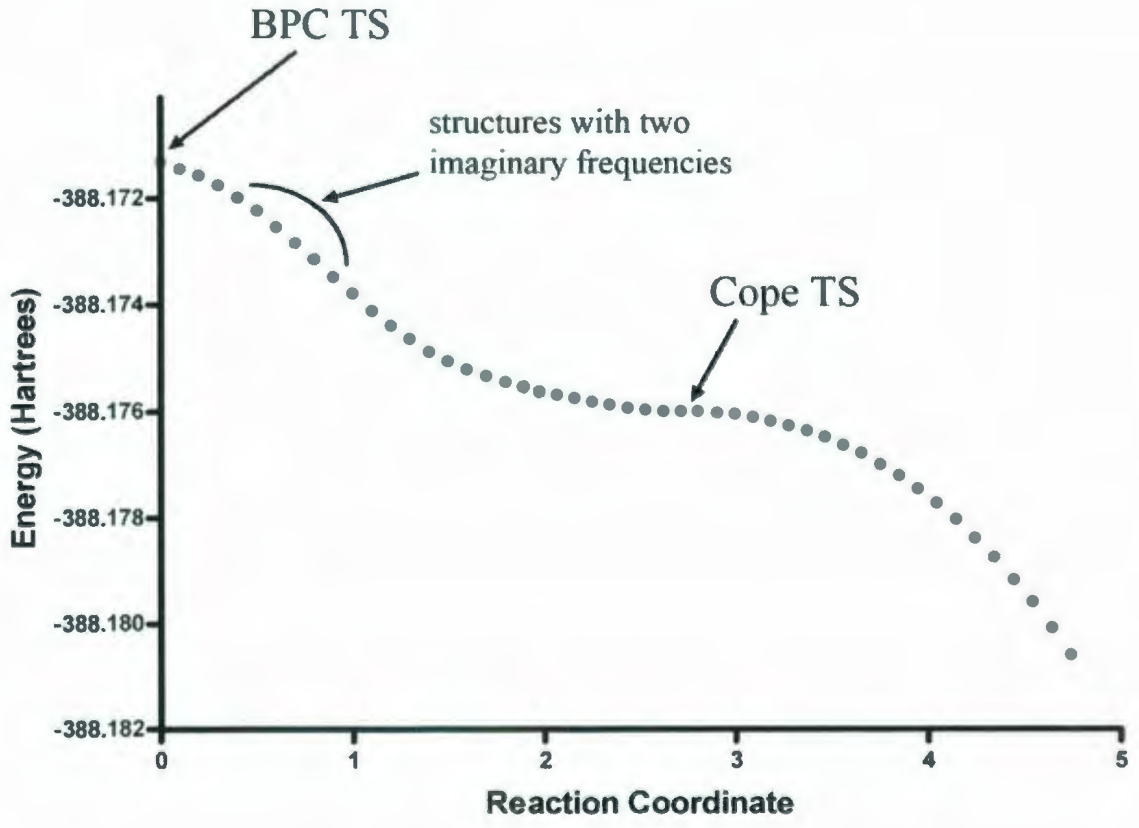


**Figure 4.7.** The reaction path calculated from an IRC calculation at B3LYP/6-31G(d). Only the product side is shown. The BPC TS, the Cope TS, and a region of the curve containing structures with two imaginary frequencies are indicated on the plot.

**Table 4.7.** Reaction coordinate data obtained from IRC and frequency calculations at B3LYP/6-31G(d). Energies (Hartrees), frequencies ($cm^{-1}$), and incipient bond lengths (Å) are shown for structures along the reaction path of the endo dimerization of cyclopentadiene. The shaded area of the table highlights those structures with two imaginary frequencies.

| point on curve | energy | frequencies | | incipient bond lengths | | |
|---|---|---|---|---|---|---|
| | | C6-C5 bonding | see-saw | C10---C3 | C6---C5 | C8---C1 |
| BPC TS | -388.17124190 | 377.3 i | 84.5 | 2.897 | 1.962 | 2.897 |
| 1 | -388.17135994 | 363.6 i | 65.9 | 2.887 | 1.921 | 2.887 |
| 2 | -388.17149307 | 351.0 i | 52.2 | 2.882 | 1.902 | 2.882 |
| 3 | -388.17167431 | 333.4 i | 35.7 | 2.876 | 1.882 | 2.876 |
| 4 | -388.17189693 | 310.2 i | 19.2 i | 2.871 | 1.863 | 2.871 |
| 5 | -388.17215666 | 280.6 i | 45.4 i | 2.866 | 1.843 | 2.866 |
| 6 | -388.17244527 | 242.6 i | 61.8 i | 2.860 | 1.824 | 2.860 |
| 7 | -388.17275106 | 197.0 i | 75.2 i | 2.854 | 1.806 | 2.854 |
| 8 | -388.17306979 | 135.6 i | 86.7 i | 2.848 | 1.787 | 2.848 |
| 9 | -388.17339640 | 38.5 i | 97.3 i | 2.841 | 1.769 | 2.841 |
| 10 | -388.17371827 | 96.7 | 107.2 i | 2.834 | 1.751 | 2.834 |
| 11 | -388.17402651 | 121.7 | 116.6 i | 2.826 | 1.734 | 2.826 |
| 12 | -388.17431201 | 133.1 | 125.6 i | 2.818 | 1.717 | 2.818 |
| 13 | -388.17456808 | 139.3 | 134.4 i | 2.808 | 1.702 | 2.808 |

The BPC TS has a vibrational mode at 377.3 i $cm^{-1}$, representing the C6-C5 bond formation; the animation of the mode at 84.5 $cm^{-1}$ describes the alternating see-saw motion of the C10---C3 and C8---C1 interactions. The recognition of this vibrational mode as similar to the imaginary frequency of the Cope TS prompted us to proceed down the reaction path and pay particular attention to these two low-lying vibrations. The structures at points 1 - 13 on the curve (those following the BPC TS, Table 4.7) show a steady decrease in energy and a continued shortening of the C6-C5, C10-C3, and C8-C1 incipient bond distances, but the $C_2$ symmetry is maintained. As shown in Table 4.7, both the C6-C5 bond formation mode and the see-saw mode are present for the majority of the path to products. The C6-C5 vibrational mode, which is imaginary for the BPC TS, reaches zero and becomes real between points 9 and 10. This is the first inflection point. The see-saw vibrational mode, on the other hand, rapidly approaches zero and becomes imaginary between points 3 and 4 on the curve; this is the second inflection. Thus, there is a section of the reaction path (as indicated in Figure 4.7 and in Table 4.7) in which these two modes of interest are both imaginary. At point 10, the sole imaginary frequency (107.2 i $cm^{-1}$) represents the see-saw vibrational mode. The $C_2$ symmetry is maintained in these structures, as is apparent by the incipient bond distances shown in Table 4.7.

**Table 4.8.** Reaction coordinate data obtained from IRC and frequency calculations at B3LYP/6-31G(d). Energies (Hartrees), frequencies ($cm^{-1}$), and incipient bond lengths (Å) are shown for structures along the reaction path in the vicinity of the Cope TS.

| point on curve | energy | frequency (see-saw) | incipient bond lengths | | |
|---|---|---|---|---|---|
| | | | C10---C3 | C6---C5 | C8---C1 |
| 26 | -388.17589655 | 213.0 i | 2.676 | 1.640 | 2.676 |
| 27 | -388.17592292 | 218.0 i | 2.666 | 1.639 | 2.667 |
| 28 | -388.17593831 | 222.4 i | 2.656 | 1.637 | 2.659 |
| *Optimized* Cope TS here (E = -388.175945015) | | | | | |
| 28 | -388.17594814 | 226.1 i | 2.641 | 1.637 | 2.660 |
| 30 | -388.17596825 | 228.3 i | 2.626 | 1.636 | 2.670 |

The data pertaining to the region of the reaction path just before and immediately after the Cope TS is presented in Table 4.8. By the time the reaction progresses to this extent (points 26 - 30), the vibrational mode associated with the C6-C5 bond formation has completely disappeared and the see-saw vibrational mode is still imaginary. The optimized Cope TS falls neatly between points 28 and 29; a geometry optimization on the structure at point 28 minimized to the Cope TS structure in a single iteration. It should be recalled from a previous discussion that the Cope TS is $C_2$-symmetric; indeed, it appears that the $C_2$ symmetry is retained along the entire path between the BPC TS and the Cope TS. For the IRC presented here, it is at the Cope TS where the symmetry is broken (refer to incipient bond lengths, Table 4.8) and the reaction has "chosen" the path to follow; in this particular

instance, we see the C10---C3 bonding distance shorten and the C8---C1 distance lengthen considerably. Clearly, the resulting cycloadduct here will be from the formation of σ bonds between C6-C5 and C10-C3. Also, the plot illustrated in Figure 4.7 is slightly erroneous in the region immediately following the Cope TS. Obviously, the curve would not continue in the same plane as shown, as this would not serve the definition of a first-order saddle point. The remainder of the path to products must proceed in a plane different than the path prior to the Cope TS, or, by definition, the Cope TS could not be a true TS.

There are a number of issues to address at this point. From our IRC calculation, it appears that the BPC TS and the Cope TS are indeed connected on this dimerization reaction path. This detail alone is intriguing, since there is typically a single TS on the reaction coordinate of a concerted mechanism. However, mathematically, two saddle points on the same curve must connect through a minimum point. This would entail a slight "dip" before the Cope TS and the path through this saddle point would resemble a "shoulder". Note that the energy difference between the BPC TS and the Cope TS for the cyclopentadiene dimerization is only about 12 kJ $mol^{-1}$; thus, we are attempting to characterize a very flat surface with an IRC calculation. Admittedly, it is possible that the B3LYP/6-31G(d) level of theory is not the optimal choice for this particular task, in addition to the likelihood that a finer grid would be required for the integral calculations in order to properly define this very flat surface. One must also consider the possibility of alternate paths that may rival the $C_2$-symmetric reaction path in energy; this could be a description for the results obtained by Caramella's group. In that case, the authors stated that the reaction coordinate encountered

the bifurcation point, and thus broke the symmetry and continued to product formation, *before* reaching the Cope TS. In our study of the reaction path, the loss of symmetry occurred *at* the Cope TS. This would mean the Cope TS is, by definition, the bifurcation point.

Clearly, the potential energy curve of the endo dimerization is more complicated than it appears. However, where the Cope TS does seem to become very important is in the consideration of product distribution. The dimerization reaction is kinetically controlled, so the endo cycloadducts will normally be the only products formed. The endo dimerization can yield two possible products; one from the [2+4] cycloaddition and one from the [4+2] reaction. The Cope TS is the transition structure between these two stereoisomers. In the unsubstituted cyclopentadiene dimerization, as well as the anti/anti and syn/syn 5-substituted cyclopentadiene dimerization, the resulting [2+4] and [4+2] cycloadducts are identical. Regioisomers are also a possibility, and the reaction with the cyclopentadienes in the other orientation will also yield a single product: the enantiomer of the cycloadduct previously mentioned. As there is an equal probability for either regioisomer to form, the product distribution will be a racemic mixture.

The anti/syn and syn/anti dimerizations are a different story altogether. The anti/syn [2+4] product is equivalent to the syn/anti [4+2] product, and the anti/syn [4+2] cycloadduct is identical to the syn/anti [2+4] product. This means that the Cope TS for a mixed face dimerization truly does convert one product to a different product. For example, the Cope TS would serve as the transition between the anti/syn [2+4] and [4+2] cycloadducts. Since the anti/syn [2+4] and syn/anti [4+2] products are the same, one can think of the

rearrangement as being between the [4+2] anti/syn and syn/anti addition products. These dimerization products are not equivalent; they differ in energy by 6.6, 17.1, and 15.1 kJ $mol^{-1}$ for 5-substitution by $CH_2$-O, Cl, and F, respectively. Interestingly, the barrier for the interconversion through the Cope TS is huge, approximately 130 kJ $mol^{-1}$ from the higher energy cycloadduct for all three cases. Comparing this to the typical $\Delta E_{act}$ for the endo dimerization reaction itself (ie. reactants to the BPC TS, approximately 50 - 70 kJ $mol^{-1}$), this reaction is not only remarkably exothermic but highly irreversible; equilibrium is not possible. The high barrier from product to Cope TS prevents any interconversion from occurring. Again, with an equal probability for either cycloadduct to be formed initially (and again considering regioisomers), the result will be a mixture of anti/syn and syn/anti products.

Finally, an overall point to ponder is this: does the nature of the potential energy curve with the existence of the Cope TS play any kind of role in the determination of endo-exo selectivity? It is important to note that the endo-exo selectivity itself is determined from the BPC TS structure at the very top of the energy barrier. The occurrence of the Cope TS *after* the BPC TS on the reaction curve, while very intriguing, does not contribute to the high incidence of endo selectivity for the cyclopentadiene dimerization reaction. However, we believe that the wealth of p-orbitals available for stabilizing secondary orbital interactions (SOI) in the endo TS structure does indeed play a role in the lower activation barriers for the endo cycloadditions.

## 4.4. Conclusions

In this study, we have investigated the DA reactions of some 5-substituted cyclopentadienes. Using $CH_2$-O, Cl, and F as the C5-substituents, we examined the cyclodimerization reaction (in which the reactants are identical) as well as the DA reactions between cyclopentadiene and 5-substituted cyclopentadiene. Our analysis focussed on the energy data obtained from B3LYP/6-31G(d) calculations, including activation energies and deformation energies. We also discussed the very interesting potential energy curve of the endo dimerization reaction and reflected on the nature of the components of the curve and the distribution of products. At this point, we can state that:

- for the cyclodimerizations, activation barriers indicate that the endo mode of addition is significantly preferred over the exo mode in every case.
- the syn/syn cyclodimerizations have the largest endo-exo selectivities and the anti/anti dimerizations have, in general, the smallest values for $\Delta E_{endo\text{-}exo}$.
- some of the DA endo and Cope TS structures in the dimerization reactions are $C_2$-symmetric. This symmetry is confirmed by identical $\Delta E^{diene}_{def}$ and $\Delta E^{dph}_{def}$ values for the fragments. This diene / dienophile indistinguishability is only possible in those cases where the reactants are identical and both are dienes.
- there is an excellent correlation between activation energy and total deformation energy for both the endo and exo cyclodimerizations.
- the Cope TS structures, located later on the potential energy curve, have a substantial degree of deformation (generally in the 150-300 kJ $mol^{-1}$ range). The structures

themselves, however, do not reveal any significant geometric changes from the DA TS structure, only that the fragments are much closer together.

- for both the dimerizations and the mixed pair reactions, the Cl substituent generally exhibits a preference for the anti position while F usually has a strong preference to be in the syn position.
- in the investigation of the potential energy curve of the cyclopentadiene endo dimerization reaction, we see two distinct imaginary vibrational modes, each dominating at different points on the reaction path. The imaginary vibrational mode of the BPC TS is the incipient C6-C5 bond forming motion which incorporates the atomic movements of both the [4+2] and [2+4] reaction paths. The other "see-saw" vibrational mode is the imaginary frequency of the Cope TS.
- the cycloaddition reactions of cyclopentadiene and its derivatives have many p-orbitals available to contribute to favourable and stabilizing SOI, and this very likely plays a role in the significant endo selectivity encountered for these reactions.

**Acknowledgments**

We thank the Natural Sciences and Engineering Research Council of Canada (NSERC) for financial support as well as the Memorial University of Newfoundland Advanced Computation and Visualization Centre for computing resources.

**References**


(1) (a) Herndon, W. C.; Grayson, C. R.; Manion, J. M. *J. Org. Chem.* **1967**, *32*, 526. (b) Lenz, T. G.; Vaughan, J. D. *J. Phys. Chem.* **1989**, *93*, 1592.

(2) McClinton, M. A.; Sik, V. *J. Chem. Soc., Perkin Trans. 1* **1992**, 1891.

(3) (a) Breslow, R.; Hoffman, Jr., J. M. *J. Am. Chem. Soc.* **1972**, *94*, 2110. (b) Breslow, R.; Hoffman, Jr., J. M.; Perchonock, C. *Tetrahedron Lett.* **1973**, *38*, 3723.

(4) Froese, R. D. J.; Organ, M. G.; Goddard, J. D.; Stack, T. D. P.; Frost, B. M. *J. Am. Chem. Soc.* **1995**, *117*, 10931.

(5) For example: (a) Goldstein, E.; Beno, B.; Houk, K. N. *J. Am. Chem. Soc.* **1996**, *118*, 6036. (b) Sakai, S. *J. Phys. Chem. A* **2000**, *104*, 922. (c) Orlova, G.; Goddard, J. D. *J. Org. Chem.* **2001**, *66*, 4026. (d) Sakai, S. *J. Mol. Structure (Theochem)* **2003**, *630*, 177.

(6) Caramella, P.; Quadrelli, P.; Toma, L. *J. Am. Chem. Soc.* **2001**, *124*, 1130.

(7) Woodward, R. B.; Katz, T. J. *Tetrahedron* **1959**, *5*, 70.

(8) (a) Toma, L.; Romano, S.; Quadrelli, P.; Caramella, P. *Tetrahedron Lett.* **2001**, *42*, 5077. (b) Quadrelli, P.; Romano, S.; Toma, L.; Caramella, P. *Tetrahedron Lett.* **2002**, *43*, 8785. (c) Quadrelli, P.; Romano, S.; Toma, L.; Caramella, P. *J. Org. Chem.* **2003**, *68*, 6035.

(9) (a) Zhou, C.; Birney, D. M. *Org. Lett.* **2002**, *4*, 3279. (b) Dinadayalane, T. C.; Sastry, G. N. *Organometallics* **2003**, *22*, 5526. (c) Singleton, D. A.; Hang, C.; Szymanski, M. J.; Meyer, M. P.; Leach, A. G.; Kuwata, K. T.; Chen, J. S.; Greer, A.; Foote, C.

S.; Houk, K. N. *J. Am. Chem. Soc.* **2003**, *125*, 1319. (d) Dinadayalane, T. C.; Gayatri, G.; Sastry, G. N.; Leszczynski, J. *J. Phys. Chem. A* **2005**, *109*, 9310. (e) Lasorne, B.; Dive, G.; Desouter-Lecomte, M. *J. Chem. Phys.* **2005**, *122*, 184304.

(10) Frisch, M. J.; Trucks, G. W.; Schlegel, H. B.; Scuseria, G. E.; Robb, M. A.; Cheeseman, J. R.; Montgomery, Jr., J. A.; Vreven, T.; Kudin, K. N.; Burant, J. C.; Millam, J. M.; Iyengar, S. S.; Tomasi, J.; Barone, V.; Mennucci, B.; Cossi, M.; Scalmani, G.; Rega, N.; Petersson, G. A.; Nakatsuji, H.; Hada, M.; Ehara, M.; Toyota, K.; Fukuda, R.; Hasegawa, J.; Ishida, M.; Nakajima, T.; Honda, Y.; Kitao, O.; Nakai, H.; Klene, M.; Li, X.; Knox, J. E.; Hratchian, H. P.; Cross, J. B.; Adamo, C.; Jaramillo, J.; Gomperts, R.; Stratmann, R. E.; Yazyev, O.; Austin, A. J.; Cammi, R.; Pomelli, C.; Ochterski, J. W.; Ayala, P. Y.; Morokuma, K.; Voth, G. A.; Salvador, P.; Dannenberg, J. J.; Zakrzewski, V. G.; Dapprich, S.; Daniels, A. D.; Strain, M. C.; Farkas, O.; Malick, D. K.; Rabuck, A. D.; Raghavachari, K.; Foresman, J. B.; Ortiz, J. V.; Cui, Q.; Baboul, A. G.; Clifford, S.; Cioslowski, J.; Stefanov, B. B.; Liu, G.; Liashenko, A.; Piskorz, P.; Komaromi, I.; Martin, R. L.; Fox, D. J.; Keith, T.; Al-Laham, M. A.; Peng, C. Y.; Nanayakkara, A.; Challacombe, M.; Gill, P. M. W.; Johnson, B.; Chen, W.; Wong, M. W.; Gonzalez, C.; Pople, J. A. *Gaussian 03*, revision B.05; Gaussian, Inc.: Pittsburgh, PA, 2003.

(11) Guner, V.; Khuong, K. S.; Leach, A. G.; Lee, P. S.; Bartberger, M. D.; Houk, K. N. *J. Phys. Chem. A* **2003**, *107*, 11445.

(12) Poirier, R. A. *MUNgauss* (Fortran 90 version); Chemistry Department, Memorial

University of Newfoundland, St. John's, Canada. Contributions from: Brooker, M. K.; Bungay, S. D.; El-Sherbiny, A.; Gosse, T. L.; Keefe, D.; Pye, C. C.; Reid, D.; Shaw, M.; Wang, Y.; Xidos, J. D.

# Chapter 5

## Conclusions

The series of investigations that comprise this thesis all had a number of common goals. First of all, we believed that a better general understanding of the DA reaction was required, from the preferred modes of addition for various diene / dienophile pairs to the documented theories and explanations pertaining to the behaviour of these reactions. We had a keen interest in the effect of substitution on the dienophile in terms of the stabilization or destabilization of the structure. Since computational studies tend to look for trends in energies and structural characteristics as a way to explain or rationalize results, there was no need to complicate our DA systems; we chose simple dienes, dienophiles, and substituents. We looked at disubstitution at different sites of the dienophile as a means of quantifying the substituent effect on the reactivity of the reaction center, the double bond. The main goal, however, was to pinpoint the determining factor (or factors) in endo-exo selectivity. We calculated activation energies, deformation energies, and interaction energies and made appropriate connections between these data and the structural characteristics of the TS. These characteristics included non-bonded electrostatic and steric interactions as well as bond lengths, bond angles, and incipient bonds. We maintain that the underlying reasons for endo-exo selectivity are complicated and cannot be wholly attributed to a single factor.

The cyclopropene study (Chapter 2) and the cyclopentene study (Chapter 3) both revealed some interesting features involving substitution on the dienophile. Mainly, the location of the substituent(s) dictates the overall electronic effect of the substitution; the

closer the substituents are to the reaction center of the dienophile, the greater the effect. The effect, of course, can be stabilizing or destabilizing. In addition, the degree of substitution (ie. monosubstitution versus disubstitution, Chapter 2) plays an important role in the stability of the reactants; disubstitution tends to amplify the stabilizing or destabilizing effect. Quantifying the energetic effect of substitution can be a daunting task since any choice of isodesmic reaction to be used in the calculation may measure effects beyond the desired ones. This is especially problematic for DA dienophiles, as one is typically dealing with ring structures and possibly substitution on double bonds. However, sometimes simply considering structural changes to the dienophile upon substitution can give some indication of the resulting effect of substitution on the molecule.

The bulk of the discussion for all projects involved the energy and geometric data pertaining to the various TS structures. While knowledge of substituent effects is worthwhile, the real story lies in the structure at the top of the activation barrier, the structure that ultimately determines the viability of the reaction as well as the endo-exo selectivity. It is well known that the DA reaction usually prefers endo addition, and the reasoning for this preference has been SOI. Because of this, some of the systems we chose either preferred exo addition, or, in the case of the cyclopentene dienophile, stabilization by SOI was not possible. These were excellent systems to investigate, as we were required to consider other avenues of reasoning. The dimers and the mixed pairs reactions in Chapter 4 were all endo selective and we concur that SOI likely plays a significant role in these cases.

Activation barriers are composed of deformation energies and energies of interaction.

We tended to see greater deformations in the structures of the dienes than the dienophiles. This made sense because dienes have three bonds that are changing significantly compared to one bond in the dienophiles. It is believed that sometimes the favourable / unfavourable interactions between the diene and dienophile may be amplified or reduced during the deformation process. This can be a reason why the interaction energies often do not clearly relate to what is seen in the TS structure itself since the interactions may have been contended with during the deformation process and are part of the deformation energy. In Chapter 4, we discussed deformation energies at length, especially for the Cope TS structure. Located quite far along on the reaction coordinate, this TS structure had incredibly large total deformation energies, usually in excess of 200 kJ $mol^{-1}$.

Finally, in our quest to rationalize activation barriers and thus endo-exo selectivities, we looked to the TS structure and the interactions between the diene / dienophile pair. Many times, the endo-exo selectivity could be accounted for (in a qualitative way) by favourable or unfavourable interactions between the two reactants. These interactions sometimes took the form of close steric interactions. Steric interactions occurred when bulky substituent groups were in close proximity to some other part of the structure, as well as when short incipient bonds yielded tight TSs and various parts of the TS structure came into close contact. Electrostatic interactions, such as triple bonds or lone pairs on substituents interacting with different parts of the TS structure, could be attractive or repulsive. In order to be able to *predict* the effect of these interactions on endo-exo selectivity, it is essential to quantify the energetic cost of these interactions. Until this can be achieved, it remains

necessary to consider the energy and structural characteristics of the TS structures and make connections between them on a case-by-case basis.